Utilization of a nano-TiO2 modified bilayer coating for paper conservation

Aleksić, Gabriela

University of Zagreb

Faculty of Graphic Arts

Gabriela Aleksić

UTILIZATION OF A NANO-TiO_2 MODIFIED BILAYER COATING FOR PAPER CONSERVATION

DOCTORAL DISSERTATION

Supervisor: Assoc. prof. Tomislav Cigula, PhD

Zagreb, 2024

Sveučilište u Zagrebu

Grafički fakultet

Gabriela Aleksić

UPORABA DVOSLOJNOGA PREMAZA MODIFICIRANOGA NANOČESTICAMA TiO_2 U KONZERVACIJI PAPIRA

DOKTORSKI RAD

Mentor: izv. prof. dr. sc. Tomislav Cigula

Zagreb, 2024.

UDK 655:676.064.1:620.197.6:66:7.025.3

Imenovano Povjerenstvo za ocjenu doktorskoga rada:

1. doc. dr. sc. Marina Vukoje, Sveučilište u Zagrebu Grafički fakultet, predsjednica
2. prof. dr. sc. Branka Lozo, Sveučilište u Zagrebu Grafički fakultet, članica
3. izv. prof. dr. sc. Magdolna Pal, Univerzitet u Novom Sadu Fakultet tehničkih nauka, vanjska članica

Imenovano Povjerenstvo za obranu doktorskoga rada:

1. doc. dr. sc. Marina Vukoje, Sveučilište u Zagrebu Grafički fakultet, predsjednica
2. prof. dr. sc. Branka Lozo, Sveučilište u Zagrebu Grafički fakultet, članica
3. izv. prof. dr. sc. Magdolna Pal, Univerzitet u Novom Sadu Fakultet tehničkih nauka, vanjska članica
4. doc. dr. sc. Katarina Itrić Ivanda, Sveučilište u Zagrebu Grafički fakultet, zamjenska članica
5. prof. dr. sc. Raša Urbas, Univerza v Ljubljani Naravoslovnotehniška fakulteta, zamjenska vanjska članica

Mentor:

izv. prof. dr. sc. Tomislav Cigula, Sveučilište u Zagrebu Grafički fakultet

Datum obrane doktorskoga rada: 20. lipnja 2024.

Mjesto obrane doktorskoga rada: Sveučilište u Zagrebu Grafički fakultet

Povjerenstvo za obranu doktorskoga rada donijelo je sljedeću jednoglasnu odluku:

„Obranila s pohvalom *magna cum laude*“

INFORMATION ABOUT SUPERVISOR

Tomislav Cigula was born on October 24th, 1979. After completing his primary education, he pursued studies at the Graphic School in Zagreb, graduating with a degree in printing. He furthered his education at the University of Zagreb, Faculty of Graphic Arts, earning both his master's and doctoral degrees in technical sciences in 2006 and 2011, respectively. Since then, he has worked at the Department for Printing Plates. In 2017, he was appointed as an assistant professor in the field of graphic technology, and he was subsequently promoted to associate professor in 2022.

His academic journey has been marked by a dedication to research in graphic reproduction processes, where he has contributed to numerous national and international projects. Notably, he has led significant initiatives exploring printing plate properties and overprint coatings. Among his achievements are two completed projects, one of which was a bilateral endeavour with the Faculty of Chemistry and Chemical Engineering at the University of Maribor, Slovenia, and another funded by the Croatian Science Foundation. Currently, he spearheads a national project titled “Improvement of packaging products by application of eco-friendly materials and inclusive design” alongside serving as a partner coordinator for an EU Culture Call project, EPE, in collaboration with ESAD in Valence, France. His scientific profile on the Croatian portal can be found at: https://www.croris.hr/osobe/profil/26671?lang=en

In addition to his academic endeavours, Tomislav has actively collaborated with industry partners, providing technical expertise to projects “Improvement of cardboard packaging production at Alkaloid A.D.” with Grafik.net in 2019 and “Development of the coatings in the packaging industry” with Bakrotisak d.d. in 2021, aimed at enhancing cardboard packaging production and developing coatings for the packaging industry.

His contributions extend beyond academia, as evidenced by his involvement in the Technical Committee HZN/TO 130 at the Croatian Standards Institute, where he was elected committee president in 2023. He has also been a valued member of various committees at the University of Zagreb, Faculty of Graphic Arts, including the Committee for Proposing the Faculty's Research Strategy for 2021-2028.

Beyond his professional commitments, Tomislav is deeply engaged in community service, notably as a resolute member of the volunteer firefighters. In his roles as president of the local voluntary fire brigade, general secretary of the city's firefighter’s association, and a member of the civil defence of the city of Krapina, he demonstrates a commitment to ensuring the safety and well-being of his community.

ACKNOWLEDGEMENTS

I would like to express my heartfelt gratitude and deep appreciation to my research supervisor, Assoc. Prof. Tomislav Cigula, PhD, for his guidance, unwavering support, and patience throughout the completion of this work.

I extend my sincere appreciation to Asst. Prof. Marina Vukoje, PhD, for providing practical tips and helping me with the interpretation of the results obtained from FT-IR measurements.

A special thanks goes to Res. Assoc. Željko Savković, PhD, from the University of Belgrade, Faculty of Biology, and Sr. Res. Assoc. Manuela Zadravec, PhD, from the Croatian Veterinary Institute, for all their help with the fungal assays.

I am also grateful to Mr. Miloš Bokorov from the University of Novi Sad, Faculty of Sciences, University Centre for Electron Microscopy Novi Sad, Asst. Prof. Katarina Itrić, PhD, from the University of Zagreb, Faculty of Graphic Arts, and Asst. Prof. Jelena Lončar, PhD, from the University of Zadar, Department of Ecology, Agronomy, and Aquaculture, for their help concerning my experimental work.

I also thank my dear colleague, Mrs. Sonja Hrelja from the National and University Library in Zagreb, for capturing images from Figure 1.

And last but certainly not least, I would like to extend endless thanks to my family for their patience and support.

Gabriela Aleksić

Zagreb, April 2024

ABSTRACT

This research presents the development of a protective paper coating aimed at minimizing the impact of environmental factors on historic paper in uncontrolled settings. The coating was developed to fulfil a dual purpose: (i) to restore damaged paper's lost mechanical properties, and (ii) to protect historic paper from physical, chemical, and biological causes of deterioration while at the same time preserving its visual appearance, structural integrity, and tactile characteristics. To achieve this, the model paper selected to simulate historic paper was coated in two layers. The bottom layer consisted of starch coating, while the top layer comprised methylcellulose coating incorporating various TiO_2 NP weight concentrations (0.2%, 0.5%, 0.75%, 1%, and 2%). Research covered three main aspects of the conservation process: application, ageing, and reversal. For this purpose, several properties of the samples were evaluated, including surface morphology, film formation, physical characteristics, surface properties, optical properties, mechanical properties, chemical properties, antifungal properties, and coatings' reversibility. Additionally, correlations were established between the coatings' composition and the resulting changes. The findings have confirmed that the thickness and composition of each coating layer influence the model paper's optical and surface properties. At lower TiO_2 weight concentrations, the bilayer coating can slow down the colour change induced by UV exposure. The proposed nano-TiO_2-modified bilayer coatings cannot deactivate the growth of two cellulolytic fungal species (*Aspergillus niger* and *Trichoderma citrinoviride*) on the surface of the coated model paper. The presence of TiO_2 in the top layer of the coating also induces sporulation, which is attributed to the fungal stress response. The bilayer coatings are not entirely reversible.

The findings from this research offer new insights into the behaviour of cellulolytic fungi and their stress-related mechanisms.

KEYWORDS: *historic paper, coatings, biopolymers, TiO_2 nanoparticles, UV radiation, cellulolytic fungi*

PROŠIRENI SAŽETAK

Stari ručno rađeni papir dugovječan je materijal. Unatoč navedenome, prirodni proces starenja staroga papira nije moguće u potpunosti zaustaviti, već samo djelomično usporiti. S druge strane, ubrzano starenje staroga papira posljedica je djelovanja brojnih fizikalnih, kemijskih i bioloških činitelja propadanja kojima je papir izložen tijekom pohrane, izlaganja i sl. Kako bi se umanjio utjecaj činitelja propadanja te produljio vijek trajanja staroga papira, konzervatori-restauratori služe se dvjema metodama: prva uključuje kontrolu okolišnih uvjeta u kojima se pisana građa nalazi (preventivna zaštita), dok druga uključuje direktnu zaštitu materijala od kojih je pisana građa sastavljena (kurativna zaštita).

Kurativna zaštita papirne građe uključuje razne postupke poput čišćenja, spajanja, ojačavanja, neutralizacije, konsolidacije, dimenzioniranja, premazivanja i sl., od kojih je neke moguće provoditi pomoću biopolimernih materijala. Takvi se materijali, ovisno o njihovoj kemijskoj čistoći te fizikalno-kemijskih svojstvima, mogu koristiti kao zaštitni premazi. Zaštitni premazi često sadržavaju dodatne tvari, poput nanočestica, koje su u odnosu na čestice većih dimenzija značajno reaktivnije te stoga mogu povećati stupanj zaštite papira.

Budući da svaka konzervatorsko-restauratorska intervencija može izazvati razne neželjene promjene papirne građe (optičke, kemijske, mehaničke i sl.), ista treba biti izvedena ciljano i minimalistički te s mogućnošću kasnijeg uklanjanja (reverzibilnost). Osim za papir, intervencija treba biti sigurna za konzervatora-restauratora koji izvodi intervenciju, druge djelatnike i okoliš.

Cilj ovoga istraživanja bio je osmisliti nanokompozitni premaz sastavljen od biopolimernih materijala korištenih u konzervaciji-restauraciji papira i nanočestica metalnih oksida, koji će strukturalno ojačati oslabjeli papir te ga zaštititi od djelovanja bioloških, kemijskih i fizikalnih činitelja propadanja. Ujedno navedeni premaz neće značajno utjecati na izgled, strukturalni integritet i taktilna svojstva podloge na koju je nanesen.

Budući da uvođenje novih materijala i postupaka nosi određen rizik i stoga zahtijeva prethodno ispitivanje njihova dugoročnog utjecaja na papir, tijekom istraživanja korišteni su odgovarajući modeli. Kao radna podloga korišten je ručno rađeni japanski papir s visokim udjelom *kozo* vlakana (70%), dok je kao osnovni premaz odabran škrob. Kao vanjski premaz i osnova nanokompozita korištena je metilceluloza, dok je kao aktivna tvar koja će pridonijeti zaštiti papira od UV (engl. Ultraviolet) zračenja i mikroorganizama odabran titanijev dioksid (TiO_2) u različitim masenim koncentracijama (0.2%, 0.5%, 0.75%, 1% i 2%).

Kako bi se ispitao utjecaj premaza i njegovih pojedinačnih dijelova na papir, uzorci su

podvrgnuti ubrzanome starenju (toplinsko starenje i UV starenje) te su ispitana njihova optička, površinska, kemijska i mehanička svojstva prije i nakon navedenih postupaka. Uz navedeno, ispitana je antifungalnost površine premazanoga papira te reverzibilnost premaza.
Rezultati su pokazali kako količina i sastav premaza utječu na optička i površinska svojstva papira. Uz navedeno, premazi koji sadrže nanočestice TiO_2 mogu usporiti promjenu boje papira izloženog UV zračenju, pri čemu niže koncentracije TiO_2 (0.2%, 0.5%) omogućavaju veći stupanj zaštite boje. Antifungalno djelovanje premaza nije potvrđeno. Celulolitičke gljivice reagirale su na prisustvo nanočestica TiO_2 u premazu povećanom sporulacijom kao mehanizmom obrane od stresnih uvjeta. Prisustvo nanočestica TiO_2 u premazu povećava stabilnost papira izloženog toplinskome starenju u odnosu na premazani papir koji ne sadržava nanočestice. Navedeni premazi nisu u potpunosti reverzibilni.
Provedeno istraživanje potvrdilo je ulogu premaza u zaštiti boje papira od djelovanja UV zračenja i povišene temperature te ponudilo uvid u ponašanje celulolitičkih gljivica.

Ključne riječi: *stari papir, premazi, biopolimeri, nanočestice TiO_2, UV zračenje, celulolitičke gljivice*

Contents

1. INTRODUCTION

Cultural heritage as the "physical carrier of information and human thought" [1] encompasses a variety of printed and handcrafted works, including books, documents, artworks, musical notes, letters, photographs, manuscripts, globes, and more. Among these works, which are composed of diverse materials (leather, parchment, wood, metal, textiles, paper, waxes, and inks), paper serves as the dominant medium used for writing, drawing, or printing. Paper, being a composite material, consists of interwoven cellulose fibres alongside various other components, such as lignin, hemicellulose, pectin, fillers, resins, pigments, sizing, dyes, and coatings. Each of these components influences the properties of paper. Considering that cellulose fibres serve as the fundamental component of paper, both the quality and lifespan of paper significantly depend on the stability of cellulose [2–4].

Cellulose-based items experience deterioration due to several causes that may be biological, physical, or chemical in nature. While the damage to any paper item primarily arises from its age and use, the main reasons responsible for paper's deterioration are various internal (endogenous) and external (exogenous) factors [4]. Most internal factors of deterioration are related to the papermaking process. They are associated with the composition of paper, covering aspects such as fibre characteristics, degree of polymerization and crystallinity of cellulose, as well as the presence of fillers, additives, acidic components, functional groups, and metal ion impurities [5,6]. On the other hand, external factors are associated with the paper item's surroundings. These factors include heat, moisture, oxygen, light (electromagnetic radiation), and atmospheric pollutants. The synergistic action of internal and external factors significantly accelerates the rate of chemical reactions, which in turn leads to heightened rates of paper degradation. Therefore, to effectively preserve paper, a comprehensive understanding of paper's structure, composition, production processes, current condition, deterioration factors, and degradation mechanisms is needed. This knowledge aids in selecting the proper materials and methods for preserving paper.

Cellulose commonly degrades due to four main processes: photodegradation, biodeterioration[1], acid hydrolysis, and oxidation [7]. These processes, interrelated in many ways, result in chemical alterations, affecting paper's appearance, tactile properties, and structural integrity. To address these issues and effectively preserve paper, preventive

[1] Within the realm of cultural heritage preservation, "biodeterioration denotes the degradation processes induced by microorganisms (bacteria and fungi) on diverse cultural heritage substrates" [68].

measures and curative treatments are employed by conservators on a daily basis. Protection, as the concluding phase in the curative process, typically involves the application of coatings. Applying coatings is a surface engineering technique for imparting targeted properties to materials, including paper. Coatings used for the preservation of cultural heritage items should improve the functional properties of the materials these items are made of, prolong their lifetime, and preserve their aesthetics, structural integrity, and tactile characteristics. Coatings should also provide protection from environmental factors (temperature, moisture, and light) during storage, exhibitions, or research. To achieve this, coatings are sometimes enhanced with other substances in the form of fillers [8].

In the last decades, titanium dioxide (TiO_2) nanoparticles (NPs) have been extensively researched as fillers for protective coatings in cultural heritage studies [9–12]. The effectiveness of nanoparticles is attributed to their tiny particle size, which leads to an increased surface area-to-volume ratio. This occurrence makes the surface significantly more reactive and prone to transformations [13]. Furthermore, uniform size distribution and particle size are crucial elements in coating applications, as they significantly influence the stability of the entire formulation. Stable coating formulations can enhance the properties of paper in novel ways and, if properly designed, can protect it more efficiently from the influence of environmental factors. Previous research in paper conservation primarily utilized cellulose ethers as the polymer matrix and several types of nanoparticles as fillers [14–17], owing to their ability to be bound through physical interactions [18]. However, only a few of these studies have explored nanocomposite coatings for the protection of paper using titanium dioxide (TiO_2) as a nanofiller [14,19]. Incorporated into a polymeric coating system, TiO_2 can provide several protective features to the coated paper owing to its photocatalytic ability [20]. Nanocomposite coatings that incorporated TiO_2 NPs proved successful in preserving the properties of coated paper from UV radiation, heat, and the activity of microorganisms [14,19]. However, up to now, only a few studies have explored these types of coatings [14,19]. Considering the variations in historic paper's structure, composition, and age, developing different coating formulations is essential for efficiently protecting cellulose-based materials from degradation. Moreover, having a variety of coating formulations expands treatment options, therefore providing greater control over degradation processes. For this reason, it is vital to further explore promising materials such as nano-TiO_2 in paper conservation studies.

To be considered successful, conservation treatment needs to block or slow down degradation processes without negatively affecting the visual, tactile, or structural

characteristics of paper. During the planning of such interventions, the consequences of preparation, treatment, and post-treatment should be considered, and the safety of the historic paper item, conservator-restorer, other people, and environment should be ensured [21]. Accelerated ageing studies on model materials are performed to assess the long-term effects of novel treatments on historic materials. Selected model materials should share similar physicochemical properties with original historic materials, as such materials are expected to degrade (and age) in a similar way. The selection of the proper model is critical. Usually, selecting overly simple materials as models does not capture the complexity of the actual system but can provide a basic understanding of the degradation mechanism in question [22]. Experimental methodology should be structured as a cycle encompassing application, ageing, and removal phases [8]. In the case of polymeric materials, the proposed treatment is expected to endure for the next 20–100 years [8]. Once the properties and current condition of the historic material have been analysed and the risks of the treatment eliminated, conservation-restoration treatment on the actual materials can safely be executed.

1.1. OBJECTIVE AND HYPOTHESES OF RESEARCH

The goal of this research is to define the composition and optimal quantity of a coating incorporating titanium dioxide (TiO_2) nanoparticles and two types of biopolymers utilized in the conservation and restoration of written heritage to provide the model paper with protection against the detrimental effects of electromagnetic radiation and microbial activity.

The hypotheses of this research are as follows:

- The thickness of the coating and its composition affect both the optical and surface properties of paper used in the conservation and restoration of cultural heritage.
- Nanocomposite coatings can protect Japanese paper from deterioration resulting from exposure to electromagnetic radiation.
- The nanocomposite coating composition inhibits the growth rate of target microorganisms.

1.2. METHODOLOGY

The theoretical part of the dissertation will present an analysis of risks and risk routes that threaten historic paper, along with a description of the main concepts related to paper, coatings, nanomaterials, and paper conservation. With this foundation in mind, the following part of the dissertation will explore the design of the protective paper coating. As the introduction of new materials and formulations presents certain risks and therefore requires a preliminary analysis of their long-term influence on historic papers, this research will use models. Models are commonly used in conservation studies for ethical considerations [21,23], for a better understanding of basic degradation mechanisms [22], and to promote the idea of the reproducibility of the obtained results [4].

The methodology will include the following:

1. Assessment of the model paper

The morphological features of the model paper will be observed through optical microscopy and scanning electron microscopy (SEM). Additionally, SEM-EDS will be employed to conduct elemental analysis of the model paper's surface.

2. Assessment of the model paper coated with monolayer coatings

The viscosity and pH value of the monolayer coatings (starch, methylcellulose) will be determined. Subsequently, coatings will be applied to the model paper's surface using different wet film thicknesses.

All samples will undergo accelerated thermal ageing.

The following methods will be used to compare the influence of different wet film thicknesses on the model paper before and after accelerated thermal ageing:

- Evaluation of the film formation properties of the coatings
- Evaluation of the optical properties of the samples (colour, yellowness, opacity, gloss).
- Evaluation of the surface properties of the samples (contact angle, water droplet absorption time).
- Evaluation of the physical characteristics of the samples (thickness, grammage).

- Characterization of the samples and determination of their degradation degree with Fourier transform infrared (FT-IR) spectroscopy.

After the evaluation of individual coating layers, the nano-TiO_2 modified bilayer coatings will be applied to the model paper accordingly.

3. Assessment of the model paper coated with nano-TiO_2 modified bilayer coatings

The homogeneity of the bilayer coatings, the distribution of TiO_2 NPs in the nanocomposite film, and the presence of aggregates will be assessed with scanning electron microscopy (SEM).

The prepared samples will undergo accelerated UV ageing.
The following methods will be used to compare the samples' properties before and after accelerated UV ageing:

- Evaluation of the optical properties of the samples (colour, fluorescence intensity).
- Evaluation of the surface properties of the samples (contact angle, water droplet absorption time, average surface roughness).
- Characterization of the samples and determination of their degradation degree with Fourier transform infrared (FT-IR) spectroscopy.

The prepared samples will also undergo accelerated thermal ageing.
The following methods will be performed to compare the samples' properties before and after thermal ageing:

- Evaluation of the optical properties of the samples (colour, gloss).
- Evaluation of the mechanical properties of the samples (tensile force, bursting strength, stiffness, short-span compression).
- Characterization of the samples and determination of their degradation degree with Fourier transform infrared (FT-IR) spectroscopy.

The antifungal efficacy of the samples will be assessed by inoculating the samples with two strains of cellulolytic fungi, namely *Aspergillus niger* and *Trichoderma citrinoviride*, followed by visual monitoring of their growth.
The reversibility of the coatings will be determined by SEM-EDS analyses.

2. THEORETICAL PART

2.1. POLYMERS

The term “polymer” was coined from two Greek words (*poly* and *meros*), which collectively refer to “many single parts”. Most commonly, polymers are described as “substances composed of macromolecules” [24,25]. These large molecules are formed by linking smaller molecules (monomers) together through covalent bonds. Polymers can be made from one kind of monomer (homopolymers) or from several kinds of monomers (copolymers) [26]. The process of joining monomers is known as polymerization.

The polymer structure consists of multiple repeating units. These units of identical structure can be arranged in linear, branched, crosslinked, or networked forms [2]. Among these structures, the linear form is the simplest one. Among polymers with linear structures, cellulose stands out as the most significant in paper conservation.

Based on their origin, polymers are classified as natural (cellulose, starch, chitosan, pectin, collagen, dried oils, natural rubber), semi-synthetic (cellulose derivatives, cellulose nitrates, cellulose acetates, vulcanized rubber), or synthetic (polyester, polyamide, silicon, polyether, polyurethane) [27]. Polymers and polymer materials have been extensively employed throughout history. Today, they are still indispensable across diverse industries, contributing to food products, construction materials, plastics, rubbers, coatings, adhesives, fibres, pharmaceutical products, agricultural chemicals, and many other products.

In the realm of written cultural heritage, polymers are often found in materials used for artistic or artisan purposes, such as dyes, inks, paper, adhesives, and sizing; furthermore, polymeric materials contribute significantly to active efforts aimed at historic material preservation (e.g., coatings, consolidants, natural and synthetic adhesives, paper, board, Teflon folding tools, and more).

2.1.1. Polymer properties

The main information on polymers is commonly obtained through their characterization. This process involves assessing factors such as nature and configuration of

monomers, degree of polymerization[2], chain characteristics, molecular weight (or mass), crosslinking, crystallinity, glass transition temperature, melting point, copolymer distribution, branching, tacticity[3], nature of end-groups, fracture mechanisms (brittleness[4], ductility[5]), and more [2,28]. These basic characteristics are shared by all types of polymers.

A variety of scientific techniques, often overlapping or complementing one another, can be employed to analyse polymers and polymer materials. Depending on requirements or intended application, the interface, surface, mechanical, chemical, optical, thermal, security, general, production-related, electrical, or economical properties of polymers are investigated.

Polymers experience continuous vibrations caused by the movement of their molecules. This movement is influenced by temperature, molecular structure, and intermolecular interactions [29]. The vibrational behaviour of polymers can be observed through several techniques, including Fourier transform infrared spectroscopy (FT-IR) [30].

Polymers exhibit amorphous or semi-crystalline structures, which significantly influence their behaviour. Polymers with semi-crystalline structures possess greater stiffness, lower solubility, and higher density than polymers with amorphous structures [28]. Due to their higher density, semi-crystalline polymers are also opaque. In contrast, amorphous polymers are transparent and weak, resembling "cooked spaghetti" [31]. Their transparency is attributed to the absence of "crystalline domains that scatter light" [28]. Both amorphous (e.g., PVA) and semi-crystalline (e.g., starch, cellulose) polymers are used in the preservation of historic paper items on a daily basis.

Polymers are usually converted to colloidal systems through synthesis or dispersion [32]. Such systems are heavily influenced by interfaces[6]. The addition of new materials to a colloidal system usually changes the interface.

Across various fields, polymers are used in the form of films. The film-forming process begins as the polymer is dissolved in a solvent or dispersed within a liquid medium. After the solution or dispersion reaches the substrate, it forms a wet film on the surface of the material [33], such as paper. The formation of the dry film depends on the properties of the solution or dispersion and is different for polymer solutions and polymer aqueous dispersions, as explained by Felton [34].

[2] The degree of polymerization relates to the total number of monomers in the polymer.
[3] Tacticity is a property of polymers that refers to the way pendant groups are arranged along the hydrocarbon chain [315].
[4] Brittle materials are stiff and strong but not tough, as they do not deform before breaking.
[5] Ductile materials are strong or not strong, but tough.
[6] An interface is a point where two systems meet and interact.

To improve their innate properties or expand their application, polymers undergo modification or are combined into novel materials. The latter is commonly achieved through copolymerization, blending, or forming composites [2,26].

Ageing causes changes in the behaviour and properties of polymers. These changes are usually caused by factors broadly classified as (i) chemical, (ii) thermal, and (iii) radiative [28]. The ageing process affects the longevity and performance of polymer materials across diverse applications. Preventing ageing is particularly important in cultural heritage settings, where the longevity and availability of heritage materials need to be preserved for future generations.

2.1.2. Polysaccharides

Natural polymers are typically classified into three main categories: (i) proteins and polypeptides; (ii) polynucleotides; and (iii) polysaccharides [26], with polysaccharides being most commonly encountered within the field of paper conservation.

Polysaccharides may come from different sources, some of which include plant cell walls (starch, cellulose, pectin), seeds (guar gum), tubers and roots (konjac mannan), seaweed (alginate, agar, carrageenan), or excreta of trees (gum arabic), animals (chitosan, chitin), and microorganisms (xanthan gum, gellan gum, bacterial cellulose) [35,36].

Polysaccharides consist of many monosaccharide units. These units are joined together by glycosidic bonds. The general chemical formula of polysaccharides is $(C_6H_{10}O_5)_n$, where the number of repeating units (n) varies. In plants, polysaccharides can have either structure- or storage-related function, with starch and cellulose being the two most significant polysaccharides within this group. Both are biodegradable, abundant, renewable, environmentally friendly, and cost-effective materials commonly encountered within the paper and textile industries, as well as paper conservation.

Cellulose

Cellulose is a linear homopolymer. As such, cellulose consists of D-glucose units joined by β-1,4-glycosidic bonds [28]. While cellulose can be derived from various sources, such as bacteria, fungi, algae, or tunicates, it is usually extracted from plants or trees, which are more abundant and readily accessible. Cellulose is a constituent of the plant cell wall, to which it provides structural reinforcement. Within plants, cellulose molecular chains are

organized into microfibrils. Microfibrils form macrofibrils, constituting the cellulose fibres that comprise the plant cell wall [37].

Cellulose molecules, owing to their numerous hydroxyl groups, form hydrogen bonds with other cellulose molecules. This results in the formation of highly crystalline structures [38]. However, the cellulose structure is not entirely crystalline. It also contains amorphous regions. The proportion of these two regions varies depending on the cellulose source of origin. These two regions provide entirely different properties, as explained in the previous section (2.1.1. Polymer properties). The hydroxyl groups in cellulose are also responsible for its hygroscopic nature. Cellulose either absorbs or releases water, depending on the temperature and relative humidity levels. Typically, under room conditions, cellulose retains from 8% to 10% of water [39].

Cellulose is considered insoluble in water and most organic solvents and lacks odour and flavour. For this reason, cellulose is primarily used in the form of fibres and derivatives. The properties of cellulose and its derivatives can vary widely due to their structural differences [40]. Cellulose derivatives are typically classified into two main groups: cellulose ethers and cellulose esters. Both cellulose ethers and esters have good adhesive properties. However, cellulose esters have not been recommended for conservation treatments since recently [41]. On the other hand, cellulose ethers are often employed in the conservation of paper [42].

Cellulose ethers

Cellulose ethers are hydrophilic compounds that are mostly water-soluble. They easily transform into hydrogels after encountering water [43], which is a desirable property in many fields [44]. Cellulose ethers are commonly used as bio-adhesives but are also widely employed as coatings. Some of the most commonly used cellulose ethers include methylcellulose, ethyl cellulose, hydroxypropyl cellulose, hydroxyethyl cellulose, carboxymethyl cellulose, and sodium carboxymethyl cellulose.

Starch

Starch, a naturally occurring polymer of glucose, serves as an energy storage molecule in plants. In nature, starch exists in the form of semi-crystalline granules [45]. Considering that granules vary in shape, size, and chemical composition for each plant species [46], the properties of starch depend on its origin, similar to cellulose.

Starch consists of two macromolecules: amylose and amylopectin. While amylose is linear, amylopectin is highly branched. Both are polymers of α-D-glucose and "have different properties, both as dry films and in solution" [8]. Amylose is recognized for its strong films, as opposed to amylopectin [8]. In statistics, starches comprise 20–25% of amylose and 75–80% of amylopectin [47,48].

Starch's ability to form films and transparency make it an attractive option for protective coatings. However, starch also presents several disadvantages as a coating material. Its significant hydrophilicity, attributed to many hydroxyl groups, stands out as a major disadvantage. When in contact with water, starch tends to swell. Additionally, most starch-based films have low water-barrier properties [49]. Such behaviour is undesirable for many applications related to paper, from the packaging industry to paper conservation. Despite their poor water-barrier properties, starches can form films with good oxygen-barrier ability [49,50].

Starch dissolves in certain organic solvents and is soluble in water after reaching gelatinization (55–80 °C) [8], as heating swells and structurally degrades granules [51].

Some of the disadvantages of starches include high viscosity following the gelatinization process, weak solubility in cold water [52,53], and bioreceptivity[7] [54]. The bioreceptivity of historic starch adhesives poses a significant challenge in paper conservation as this material tends to attract various biological agents [55].

To expand their application and improve their existing properties, natural starches are typically modified. This can be achieved through physical, genetic, chemical, and enzymatic methods, or combinations of these methods [53,56].

[7] Bioreceptivity represents "the ability of a material to be colonized by living organisms" [316].

2.2. PAPER

2.2.1. The history of papermaking and coating paper

The term “paper” originates from the Greek word for papyrus, an earlier writing and drawing material used by Egyptians around 3000 B.C. Papyrus is referred to as the earliest version of paper. The material we recognize today as “paper” was invented around A.D. 105 by Ts’ai Lun in ancient China. The acceptance of paper as a replacement for other writing materials (e.g., parchment) came much later. Early papers also had certain flaws. Due to the translucency and thin structure of paper [2], the Chinese used sizing, coatings, and dyes to improve its performance. The Chinese also tried to prevent the biological attack on more valuable papers. According to Hunter, a toxic dye derived from the *Amoor cork tree* was used to deter insects [57]. Despite these advancements in paper quality, its dissemination beyond China remained slow until the Battle of Talas. During that period, the Chinese captives revealed the procedure of papermaking to Muslim Arabs. Facing a shortage of fresh fibres, Arabs employed linen as an alternative to mulberry, which was used by the Chinese [58]. The papers from this period were usually surface sized with wheat starch [59], while white chalk was sometimes added as the filler to the mixture [54].

Paper initially spread over the Middle East and Africa before expanding into Europe, commencing with Sicily and Spain. Spaniards were introduced to papermaking by the Moors from North Africa during their reign [57]. Paper from that period was sized with a thick layer of starch [59,60]. During the 13th century, papermaking emerged in Italy, with the first papermakers based in Fabriano. In Italy, papermaking flourished as Italians introduced various advancements such as sizing with gelatine, watermarking, mechanization of the pulping process, and the wire mesh mould [2,61]. Italian papermakers such as Fabriano, Fedrigoni, and Burgo Group are, up to this day, still relevant.

European papermaking blossomed in 1450 with the invention of the movable-type printing press. This innovation, pioneered by Johannes Gutenberg in Mainz, Germany, catalysed the mass production of books, leading to a significant increase in the demand for paper. Different printing requirements and distinct types of paper later contributed to the development of several printing methods. In Europe, pieces of clothing or rags that were deemed unusable for any other purpose, were repurposed for papermaking. For this reason, in the 17th century, the invention of the Hollander beater in the Netherlands facilitated more

efficient processing of rags into fibres [54], further increasing the demand for paper. Though paper quality declined, some improvements were made, resulting in more homogeneous and whiter sheets [2].

Throughout history, several attempts have been made to control microbial growth on paper. From the 16th to the mid-17th century, alum (aluminium sulphate) was added to the sizes [60]. Alum was sometimes substituted by zinc sulphate, yet both of these compounds promoted acidity in the presence of water [4], affecting the longevity of paper.

To further improve paper quality, George Cummings developed a paper coating using lead white pigment and other substances, obtaining an English patent for it in 1764 [57]. The first continuously operating paper machine was invented at the end of the 18th century by Frenchman Nicolas-Louis Robert, who aimed to reduce the number of workers needed in the manufacturing process [62]. Due to the French Revolution, the machine was further improved outside of France by Bryan Donkin and the Fourdrinier brothers [63]. As paper gained popularity and rags became scarce, alternative sources of cellulose (e.g., straw, grass) were introduced by that time.

In the 1840s, alongside advancements in mechanization and the development of chemical processes for converting wood into pulp [64], wood fibres began to be widely adopted. The use of these lignin-abundant materials drastically reduced paper quality. Further improvements in production machinery and increased operational speeds led to a greater output of materials, which deteriorated fast due to the presence of acidic substances. During the mid-20th century, the paper industry experienced a transformative phase characterized by growth, adaptation, and modernization, driven by automation. This revolutionized production processes, expanded the range of paper-based product offerings, and fuelled technological innovation.

To this day, paper has remained indispensable in our everyday lives. In the 21st century, amid a global shift towards sustainability, the paper industry is assuming a new role. With over 70% of all paper in Europe being recycled, paper surpasses all other materials in recycling rates [65]. Moreover, wood fibres can be recycled around 6–7 times before being repurposed for bioenergy [66].

2.2.2. Paper components

Paper is a heterogeneous material. Its geometrically complex surface can be viewed as a "multi-layered composite structure of a 2D fibrous network" [67], where fibre serves as the "fundamental unit of the paper structure" [68].

The main and most stable constituent of fibres is cellulose. Although cellulose used in papermaking is usually derived from plants or trees, other types of fibres from non-cellulosic sources (e.g., synthetic) are occasionally utilized. Aside from cellulose, fibres can also contain lignin and hemicellulose. Other than fibres, paper may contain pectin, fillers, resins, sizing, pigments, dyes, inks, or coatings, all of which influence the properties of the sheet. Therefore, paper is also considered a composite material.

Cellulose fibres

The properties of cellulose used in papermaking are influenced by several factors, including its origin, purity, fibre characteristics, degree of polymerization, and crystallinity [2]. Cellulose is "structured into fibres" [6], whose quality is of particular importance. Cellulose fibres also impart strength, colour, opacity, density, and porosity to the paper sheet. According to Szczepanowska, the quality of the fibres can be determined by several factors, including their ends, length, surface, shape, and lumen[8] [69]. Cellulose fibres exhibit distinctive properties and morphological features based on their source of origin. Plants such as jute, flax, and hemp contain over 50% of cellulose, while cotton contains up to 98% of cellulose [2,3]. On the other hand, wood contains around 40–45% of cellulose, 15–25% of hemicellulose, and 20–30% of lignin [6]. Over the course of history, the cellulose content in paper varied, and so did the quality of paper. Between the 15th and 17th centuries, paper was made exclusively from hemp and flax rags, while cotton was used from the mid-17th century to the mid-19th century [70]. These raw materials produced high quality paper compared to wood, which was used in the latter period (post-1840).

Hemicelluloses are polysaccharides that comprise around 20% of plant cell walls [6]. Hemicellulose is linked to cellulose with pectin, forming a "network of crosslinked fibres with structural role" [71]. Although the composition of cellulose and hemicellulose is similar [2], their properties differ. Hemicellulose possesses lower strength than cellulose.

[8] Lumen refers to space inside the fibre [69]

Lignin is an aromatic polymer that provides support and strength to wood by acting as a binding material that holds cellulose and hemicellulose together [72]. It is also the most unstable component of paper. Lignin easily undergoes oxidation under the influence of light, leading to severe degradation of paper (darkening, yellowing, and crumbling). Lignin's high acidity is the main reason for the low stability and fast deterioration of paper. Acidity stems from the presence of phenols in lignin's structure [2], which also impart antimicrobial properties to this compound [73]. The presence of lignin in paper can be determined using several methods, among which the phloroglucinol colour test [74,75] is commonly employed in paper conservation laboratory analysis.

Pectin is another polysaccharide present in the cell walls of plants. Its main component is pectic acid. Both pectin and pectic acid are soluble in water [2]. Pectin also possesses gel-forming ability [76] and when used in the form of an additive, it can increase the strength properties of paper [77].

Sizing involves the addition of an adhesive material to paper to achieve targeted characteristics. It was originally employed to reduce the hydrophilicity of cellulose fibres and facilitate writing on historic paper [4,59]. This also made the surface smoother due to reduced porosity and roughness [78]. In paper conservation, this process is referred to as resizing [59]. Paper could either be surface-sized or internally-sized. Early sizes such as gypsum, starch, rice flour, and lichen were applied as surface coatings to paper [60]. Gelatine, introduced in the 13th century, brought a different approach, as paper was immersed in the sizing solution [4]. Historic papers that were extensively sized are stronger and less water-absorbent than non-sized papers. In the 19th century, the practice of incorporating sizing (i.e., alum-rosin) into pulp emerged [70]. In more recent times, a range of materials, including alkyl ketene dimer (AKD), alkenyl succinic anhydride (ASA), and stearic anhydride, have been utilized for sizing [2,79]. Nowadays, sizing is still used in papermaking for enhancing the surface properties of paper, e.g., finishing, printability and print quality, smoothness, and surface bonding strength.

Fillers are water-insoluble substances. They typically range from 0.1 μm to 10 μm in size [80]. The selection of a filler, along with its quantity, depends on the requirements for the specific paper. In papermaking, fillers are used for increasing opacity, smoothness, and brightness, as well as buffering [2]. Excessive amounts of fillers can compromise paper

integrity and printing performance [80,81], as well as alter its structural, optical, and surface characteristics. The inclusion of fillers lowers the cost of paper and the amount of other materials within the formulation [8]. The common fillers in papermaking are calcium carbonate (ground calcium carbonate, precipitated calcium carbonate), kaolin clays, chalk, talc, aluminium trihydroxide, gypsum, and titanium dioxide (rutile) [80,81].

Pigments are water-insoluble components of inks derived from animals, plants, or minerals. Pigments possess higher lightfastness than dyes. Some of the most important traditional black, red and white pigments include carbon black/lamp black, bone black/ivory black (blacks), red ochre, madder lake/alizarin, red lead/minium, vermilion, cochineal (reds), lime white/chalk, lead white, zinc oxide, and titanium dioxide (whites) [82].

Dyes differ from pigments. Based on their origin, dyes can either be organic or inorganic. Throughout history, natural sources of dyes included leaves, lichens, insects, shells, roots, and bark. Dyes are utilized by papermakers either through direct or indirect application (colouring fibres). The main types of dyes used in papermaking include direct dyes, acid dyes, basic dyes, and sulphur dyes [83]. Most paper dyes are water-soluble and vulnerable to UV radiation, acids, and gaseous pollutants. Dyes need to possess compatibility with the substrate, wet fastness, and lightfastness [84] to be able to impart colour properly.

Inks are categorized into two main categories: printing inks and writing inks. The basic ingredients of inks include colouring substances (pigment or dye), solvents (water or oil), binders, and additives (thickeners, optical brighteners, antiseptics, surfactants, plasticizers, buffers, and waxes). Some inks, such as iron gall ink, also contain binding agents known as mordants [85]. Printing inks also contain varnish. Some of the most important early writing inks were carbon black, bistre, sepia, and iron gall ink [86]. Early printed works predominantly employed black and red printing inks. Black printing ink was typically made from linseed oil and carbon black from the soot residue of burning oil, bones, trees, or resins [86,87], while red was derived from a mineral pigment known as vermilion. Today, the properties of printing inks depend on the nature of the specific printing technique (classic or digital).

2.2.3. Papermaking process

The fundamentals of papermaking have not changed much over time, with several key steps still being integral to the process today. Initially, fibres are extracted from the raw material through steaming, mechanical beating, or cooking and subsequently suspended in water [69]. The quality of water is crucial for the quality of the resulting paper, as explained by Neumann [88]. Various fillers may be incorporated into the slurry mixture to meet specific application requirements. The slurry is then collected on a fine wire screen to allow water drainage and sheet formation. In the end, dried paper sheets can undergo additional surface treatments, such as coating, burnishing, or similar [54]. The appearance of a paper sheet is affected by the features of the screen used in the papermaking process [89]. Quality papers both from contemporary times (e.g., Fabriano Ingres) and historical periods showcase a range of distinctive features formed during their production, such as chain lines, laid lines, watermarks, and more.

Over the course of history, the composition and physical appearance of paper varied depending on the geographical location where paper was produced and the characteristics of the papermaking process. These factors are the reason behind the large variations in the properties of different papers. As a result, paper is broadly classified as: (i) Western or Eastern (Asian); (ii) handmade or machine-made.

Eastern papers, made from the bark of trees and other vegetation, feature strong and long fibres (e.g., paper made from *kozo* fibres). For this reason, they are minimally sized and have no fillers [69,90]. In contrast, Western papers, particularly those from the latter period, have shorter fibres, and contain several additives intended to improve their quality.

Handmade papers can be produced from a wide range of plant fibres, including hemp, flax, cotton, bamboo, banana, corn, rice straw, mulberry, and more. On the other hand, machine-made papers are mainly produced from wood fibres. For this reason, handmade and machine-made paper differ in both quality and appearance. Machine-made paper is characterized by short fibres, while handmade paper typically has longer fibres (>1 mm) [50]. Longer fibres convey strength to the paper sheet [50,91], as a result of additional contact points, greater fibre entanglement, and fibre flocculation during the papermaking process [67]. The tendency of long cellulose fibres to flocculate during papermaking [92] results in variations in paper thickness [67], which contributes to the heterogeneity of the sheet.

2.2.4. Paper-based cultural heritage

Cultural heritage is defined as anything human-created that holds significant value for specific communities [93]. As such, cultural heritage plays a "crucial role in the recognition, definition, and affirmation of our cultural identity" [94], encompassing both tangible and intangible assets with social, symbolic, historic, aesthetic, ethnological, anthropological, artistic, and scientific significance [95]. As this legacy of humanity is unique and irreplaceable, it needs to be protected, well-preserved, but also accessible.

The profound importance of protecting and preserving cultural heritage gained global recognition with the adoption of the *World Heritage Convention (Convention concerning the Protection of the World Cultural and Natural Heritage)* by the General Conference[9] of the United Nations Educational, Scientific and Cultural Organization (UNESCO) in Paris, France, on November 16, 1972. This "unique international instrument" [96] seeks to encourage all nations to protect and preserve their cultural and natural heritage. In the ensuing decades, a plethora of crucial documents emerged [97], all sharing a common goal: to preserve the significance of heritage for the well-being of both present and future generations. These international documents serve as the basis for many national documents on preservation, from which professional operational documents and procedures arise.

Today, cultural heritage is predominantly endangered by environmental influences and climate change. According to the Canadian Conservation Institute, heritage items face the ten primary threats, including "incorrect temperature, incorrect relative humidity, light, ultraviolet and infrared, fire, water, physical forces, theft and vandalism, pollutants, pests, and dissociation" [98]. While heritage items may vary in shape, size, or properties and may have different constituent materials, these ten agents of deterioration affect them in similar ways. Preventing the detrimental impact of these factors presents a particularly formidable challenge, as it necessitates the implementation of various preservation strategies.

Preservation is an initiative-taking effort aiming to slow down or prevent deterioration or damage to cultural heritage items. It is achieved through the "control of their environment and/or treatment of their structure," with the goal of "maintaining them as much as possible unchanged" [99].

Cultural heritage, as the "physical carrier of information and human thought" [1], encompasses a variety of printed and handcrafted works, including books, pamphlets,

[9] The General Conference is the highest governing body of UNESCO.

documents, artworks on paper, musical notes, letters, photographs, manuscripts, globes, and more. These works, predominantly found in the form of loose sheets or bound in books or pamphlets, are composed of materials such as leather, parchment, wood, metals, textiles, paper, waxes, inks, and adhesives. Among these materials, paper serves as the dominant medium used for writing, drawing, and printing. As a result, the preservation efforts for printed and handcrafted works for the most part revolve around paper-based materials.

On the other hand, preservation decisions are based on the type of institution that holds historic items and the needs of its users [100]. Ensuring the preservation and protection of historic paper is the responsibility of conservators, technicians, librarians, curators, registrars, collection managers, and other professionals working within galleries, libraries, archives, and museums (GLAM). Among these professionals, conservators are personally and ethically responsible for the performance of conservation-restoration treatments [21,23]. Therefore, to successfully prevent the degradation of historic paper, paper conservators need a comprehensive understanding of the paper's structure, composition, production processes, state of preservation, deterioration factors, degradation mechanisms, and available conservation methods.

2.3. PAPER DETERIORATION

Historic handmade paper, particularly from medieval times, is recognized as a resilient and durable material [4]. Despite its longevity, paper ages, as the natural ageing of paper is an inevitable process. Although it cannot be prevented, the process of ageing can be slowed down by employing certain preservation methods. Although passage of time plays a role in the natural ageing of paper, premature deterioration is predominantly triggered by a range of internal (endogenous) and external (exogenous) factors [4], which may directly and/or indirectly contribute to degradation. Degradation results in physicochemical damage to materials and sometimes leads to the loss of information, rendering historic paper items inaccessible and diminishing their value [101].

Internal factors of deterioration

Internal factors of deterioration are usually introduced during the papermaking process and are associated with the composition of paper, covering aspects such as fibre characteristics (type, strength, length), degree of polymerization and crystallinity of cellulose, and the presence of fillers, additives, acidic components, functional groups, and metal ion impurities [5,6]. In the realm of paper preservation, the longevity of paper is assessed through two key attributes: stability and durability. Stability refers to paper's "resistance to chemical changes," while durability denotes its "physical resistance to stress and strain" [102]. In the long term, chemical changes are more detrimental than physical changes. That is why it is important for paper to stay stable for as long as possible. For a paper to remain stable, its main component, cellulose, has to stay stable [2]. As pointed out at the beginning of the theoretical part, cellulose is a polymer and therefore undergoes similar degradation processes as other polymers.

The lifespan of paper is significantly influenced by its pH level. Both acidity and excessive alkalinity pose risks to paper. However, acidity is of particular concern as it readily migrates from material to material and its detrimental effects are more damaging. As cellulose ages, it generates formic, acetic, oxalic, and lactic acids [103]. These acids further accumulate within paper and accelerate its degradation. As frequently observed in paper works from the mid-19th century, highly acidic paper is fragile and prone to cracking and crumbling, which results in the loss of material. These visual indications of acidity are readily recognized, even by non-professionals. The pH value of paper is usually determined by the cold extraction

method [104] or by surface pH measurement [105]. In order to prevent further acid-catalysed degradation, it is necessary to deacidify paper. At pH values lower than 5.5 [3], deacidification cannot be avoided. Buffering should not be overdone, as pH values of 9 or higher can lead to alkaline degradation [3]. Therefore, paper should be buffered to a neutral or slightly alkaline pH value to ensure its longevity. The main causes of acidity in historic papers are particularly well-known to conservators. They include the presence of alum, verdigris pigment [106], impurities, degradation products, oxidation of lignin, atmospheric pollutants (sulphur dioxide, nitrogen oxides, ozone, hydrogen sulphide), and migration of acids from other materials (e.g., inks, cardboard) [107]. Acidity negatively affects not only paper but many other organic materials.

Although paper requires an optimal amount of moisture to retain its flexibility, excessive amounts of water in paper can catalyse hydrolysis, cause bleeding or corrosion of inks, and encourage microbial attack. Regardless of the mechanism responsible for water presence (capillary suction, wetting, or water condensation), water remains one of the main causes of paper deterioration.

External factors of deterioration

External factors of deterioration refer to environmental conditions during storage, exhibition, and handling of paper, such as temperature, humidity, light exposure, oxygen levels, atmospheric pollutants, and more. In a chemical sense, these factors catalyse or initiate a series of reactions whose detrimental impact on paper collections is well-documented [108–110]. In reality, most conservation interventions arise from the improper environmental conditions under which paper is kept. Experts indicate that this proportion is as high as 95% [69]. For this reason, historic papers need to be kept in a controlled environment.

Paper is best preserved in a dark and clean storage place, with temperatures ranging from 16 °C to 20 °C and relative humidity maintained between 45% and 55%, without fluctuations [111]. Light levels should be maintained at 50 lux, with UV levels reaching up to 75 μW/lm [112]. Exposure to pollutants, heat, high relative humidity, and direct light should be prevented. Paper can also deteriorate due to interactions with various adjacent materials and structures, including writing inks, adhesives, preservation enclosures, furniture, or other paper items. Overall, deterioration can be initiated by various chemical, physical, and biological causes, with their collective and combined interplay causing severe damage to paper. Nonetheless, regardless of the triggering mechanism, cellulose degradation commonly arises from photodegradation, biodeterioration, acid hydrolysis, and oxidation [7].

2.3.1. Light as a physical cause of deterioration

Light is a component of the electromagnetic (EM) spectrum, which encompasses a wide range of forms, including gamma rays, X-rays, UV radiation, visible light, IR radiation, microwaves, and radio waves. As a result of irradiation, light is absorbed, transmitted, or reflected by a material. However, only absorbed light has the potential to induce degradation. The reaction leading to organic material's degradation requires the absorption of sufficient energy by a molecule [113], as illustrated by **Equation 1** [108].

$$R + h\nu \rightarrow R^* \quad (1)$$

where R is the organic molecule (e.g., polymeric), $h\nu$ is the energy of the absorbed photon of frequency ν (or wavelength c/ν; where h is the Planck's constant and c is the velocity of light), and R^* is the electronically excited molecule.

Organic materials commonly exhibit a higher vulnerability to light than inorganic materials [113], and given the density of their structure, they experience mainly surface degradation [108]. In addition to the organic material's vulnerability, the key parameters associated with light-induced degradation include energy, frequency, wavelength, and exposure characteristics.

Energy and frequency are both related to waves. As the frequency of a wave increases, so does its energy. This relationship is crucial when considering the different degradation potentials that come from light exposure. The longer-wavelength, low-frequency waves (IR) carry less energy compared with the shorter-wavelength, high-frequency waves (UV). However, IR waves can still induce degradation through the "localized heating of objects" they interact with [108]. On the other hand, energetic UV waves cause severe physicochemical damage to polymeric materials. The extent of degradation also depends on the intensity of light and the exposure characteristics (e.g., duration).

Light-induced damage is cumulative and irreversible. While it primarily manifests through changes in paper's optical properties (gloss or colour shift; yellowing, bleaching, or darkening), other changes (chemical, mechanical, or surface) also occur. These mechanisms are well-documented by several sources [114–117].

Both natural and artificial light can induce degradation. Sunlight, which contains high-energy UV radiation, is extremely harmful. Other types of light sources, such as fluorescent or incandescent lamps, emit lower UV doses of energy, so they are considered less dangerous. The solar spectrum covers a broad range of wavelengths, starting at 280 nm up to around 2500 nm. During the daytime, light within the spectral range of 300–550 nm is the most detrimental to cellulose [115,116]. During light exposure, damage occurs due to many chemical reactions. These reactions are not only caused by light, but also by elevated temperatures [108,114], as all absorbed radiation is converted to heat.

In polymers, the light-induced degradation results from photolysis and photo-oxidation. The absorption of photons within the UV-C region (100-280 nm) "leading directly to chemical reactions that cause degradation" is photolysis [114,118]. On the other hand, photo-oxidation typically occurs through the absorption of photons in the near-UV (300–400 nm) or visible region (400–750 nm). These two mechanisms have been previously described by many researchers [2,115,116]. UV radiation can be absorbed by various paper components. Some of these components include fillers (e.g., TiO_2), impurities, unsaturated functional groups, or printing ink [119,120]. Photodegradation results in changes of colour (yellowing, browning, fading, and bleaching) and structure (embrittlement, loss of mechanical properties, gloss, or adhesive power of the coatings) of paper [121], but the exact changes depend on the particular paper and its unique history, i.e., internal and external factors.

2.3.2. Heat as a physical cause of deterioration

Heat can be transferred through a variety of mechanisms, including conduction, convection, and radiation. Typical heat sources include the local climate, sunlight, incandescent lamps[10], heating devices, open fires, and various other means. Irrespective of the mode of transfer, heat has the potential to adversely impact polymeric materials by inducing accelerated ageing.

Polymers, such as cellulose, exhibit different behaviours and rates of degradation at different temperatures [122]. Elevated temperatures pose significant risks as they cause changes on the molecular level. The most apparent outcome of thermal degradation is the physical deterioration of paper.

[10] Measures to ban incandescent bulbs are currently implemented throughout the world [317,318].

Temperature is inversely related to relative humidity. Paper, being hygroscopic, experiences dimensional changes in response to drastic changes in temperature and relative humidity levels in its environment. Although cellulose remains stable at lower temperatures [2], elevated temperatures will accelerate its rate of ageing. While it is widely acknowledged that the rate of chemical reaction doubles with each 10 °C rise, the degradation of cellulose proceeds at an even faster rate. According to Thomson, cellulose degradation accelerates around 2–2.5 times with each 5 °C increase [108,123].

Elevated temperatures and dry conditions accelerate the natural ageing of cellulose and dry out paper, causing structural damage due to brittleness, cracking, and tearing. Yellowing is also known to result from prolonged heat exposure, as observed in accelerated thermal ageing tests [102,115].

Thermolysis and thermo-oxidative degradation are the main heat-induced degradation processes that affect paper. Thermolysis involves heat-induced degradation in the absence of oxygen, while thermo-oxidative degradation involves the combined action of heat and oxygen [124].

2.3.3. Oxidation as a chemical cause of deterioration

As explained in the previous sections (2.3.1. and 2.3.2.), upon exposure to heat or light energy, cellulose degrades as a result of oxidation. While heat and light serve as initiators of oxidation, cellulose can undergo oxidation under various circumstances, facilitated by oxidizing agents (e.g., reactive oxygen species (ROS) of radical nature) [110], an electronically excited molecule, or microorganisms [120].

Cellulose undergoes oxidation due to its many hydroxyl groups as well as the presence of aldehydes in its structure [110]. Oxidation of cellulose promotes the further formation of carbonyls (aldehydes, ketones) and carboxyls, inducing changes in the molecular structure of cellulose [125]. The degradation of cellulose can occur with or without the opening of the pyranose ring. This mechanism is well-documented by several sources [126–128]. The oxidation process accelerates in the presence of copper (Cu) and iron (Fe) [2], while it slows down in the presence of titanium (Ti), aluminium (Al), or zinc (Zn). [119].

Organic materials within the paper (fibres, colouring agents, coatings, adhesives, lignin) are all vulnerable to oxidation, particularly under the influence of UV radiation and

high temperatures. Among these materials, polymers with oxygen in their structure are particularly vulnerable [8].

The main consequences of oxidative reactions are chain scissions and crosslinking [129]. In paper, oxidation results in colour changes, diminished gloss, embrittlement, and changes in the mechanical properties of the paper [22]. Some of these changes (e.g., yellowing) can occur even in the initial stages of oxidation [8]. The oxidation of cellulose can promote acidity. This mechanism takes place when primary alcohol groups are oxidized to aldehydes and subsequently to carboxylic acids [120].

2.3.4. Microorganisms as a biological cause of deterioration

The high bioreceptivity of paper makes it vulnerable to attack by various macroorganisms and microorganisms [130], with insects, fungi, and bacteria being the most common ones. While insect activity typically results in loss of material (i.e., perforations in paper, missing corners) and accumulation of dirt (i.e., dead insects, larvae waste, frass), microorganisms can cause severe physical and chemical damage due to the production of organic acids and enzymes. Fungi and bacteria degrade paper primarily through the secretion of cellulase enzymes. These enzymes can break down cellulose through the hydrolysis of the β-1,4-glycosidic bonds [131].

In the paper collection areas, microorganisms are found either as dormant spores or active propagules [132]. Their activity and growth depend on several factors, including pH value, microclimate conditions (temperature and moisture level), oxygen level, the presence of macronutrients [133], and dirt [134]. Most bacteria thrive within warm temperature ranges (around 40 °C) [135] and exhibit optimal growth at pH levels between 6 and 7.5 [133]. On the other hand, fungi prefer temperatures around 25–30 °C for their growth [136–138] and develop and thrive across a broad range of pH levels, depending on the specific species [135,139]. According to Szczepanowska, microbial growth on paper depends on water activity[11] and the paper's absorbency [69]. However, the presence of water on the paper surface is not enough, as water needs to be present in an unbound state on the paper surface to facilitate microbial action [69]. Water activity for bacteria ranges from 0.8 to 1.0, while for fungi, it typically falls between 0.61 and 0.8 [140]. Requiring less moisture than bacteria,

[11] "Water activity (a_w) refers to the amount of water available for microbial growth, expressed on a scale of 0 to 1.0, with pure water having a water activity of 1.0." [69].

fungi can develop and thrive more easily in paper collection storage areas. In addition, fungi are also widely known for their adaptation mechanisms [141], making them the primary microbial colonizers of paper.

Fungi

Fungi are neither animals nor plants, although they are considered to be more closely related to animals [142]. They are heterotrophic organisms that obtain nutrients from organic materials they colonize. In paper, fungi commonly target starch and cellulose, although they are capable of degrading other natural and synthetic polymers [132] typically found in paper collection storage areas.

Fungal infestation of paper can involve several detrimental actions, including the secretion of organic acids and enzymes, the production of pigments, oxidation, and more [130,132]. However, fungi are not only detrimental to paper. Their presence can also pose a serious threat to people working with or managing infested items. Certain species may induce respiration issues upon inhalation, trigger allergic reactions, or even be toxic to people [143].

Fungal spores in a dormant state are constantly present in our environment and commonly activate as soon as the conditions become favourable. In storage spaces for paper collections, a high relative humidity (> 70%) and a lack of air circulation can trigger their growth on a suitable substrate. The attachment of activated spores to the paper surface takes only a few hours [68]. While fungi may initially respond to favourable environmental changes, they also play an active role in adapting to their surroundings.

The growth of fungi on paper is influenced by the paper's physicochemical characteristics, including hygroscopicity, pH value, roughness, porosity, and other surface irregularities [144]. Surfaces with such characteristics provide protection against airflow, offering oxygen and space where fungi can grow undisturbed [68]. Although polysaccharide-based adhesives are considered to encourage fungal growth [42], Szczepanowska's research indicates that in the form of thin sizing, adhesive materials can inhibit fungal growth by preventing the entrance of water into the pores of paper [68].

The onset of a fungal infestation involves the development of colonies on the paper surface. The growth is commonly accompanied by a distinctive odour. As with other causes of deterioration described in previous sections (i.e., heat, light), the damage caused by fungi can also affect the surface (staining, colour changes) and/or the structure (weakening, cracking, disintegration) of paper.

The release of fungal pigments, which cause colour changes and staining of historic paper, is aesthetically unacceptable. It is also known to promote the further deterioration of paper. The excreted fungal pigments are either waste byproducts or a stress mechanism protecting fungal structure [145]. The phenomenon of foxing, usually observed in books from the latter historic periods (18^{th}–20^{th} century), is also attributed to fungal pigment activity [146]. Fungi are known to produce many types of pigments. Some of these pigments include carotenoids, flavins, melanins, phenazines, quinones, indigo, monascins, and violacein [147]. Among these pigments, the dark-coloured melanins are especially dangerous to paper-based collections as they enter the paper structure [132]. Melanin-containing fungi are recognized for their high resistance and adaptability. These properties allow them to survive extreme conditions, including UV radiation exposure, high temperatures, and high concentrations of salts [145,148].

Fungi degrade cellulose by producing hydrolytic enzymes called cellulases. Cellulases are "capable of depolymerizing cellulose into smaller molecules" [149]. The three major cellulase enzymes that contribute to cellulose breakdown include exoglucanases, endoglucanases, and β-glucosidase [150]. Aside from cellulases, certain species produce amylases (starch-decomposing enzymes) and proteases (gelatine- and leather-decomposing enzymes) [143]. The most common cellulolytic fungi found in paper collections include *Aspergillus*, *Penicillium, Chaetomium, Fusarium,* and *Trichoderma* species [130]. The ability to produce enzymes makes fungi crucial in various industries. However, nowadays, fungi are utilized for several other purposes [151].

The deactivation of fungi is particularly challenging due to their adaptability. The most effective approach to preventing fungal growth in paper collection storage areas involves implementing preventive strategies, such as controlling environmental conditions and performing housekeeping and cleaning. While mechanical removal of the dry spores from the shelves or book surfaces can reduce their numbers, chemical and physical methods are utilized in more serious cases of infestation. Chemical methods encompass the use of alcohols [152], essential oils [153], azole antifungals, phenol derivatives, photocatalysts, salts and esters of acids, and more, while physical methods involve dehydration, γ-radiation, freezing, high temperature, UV radiation, low oxygen environments [154–156], and plasma [157,158]. Alcohol solutions are the most widely used antifungal agents used by paper conservators. Fungi detection and disinfection treatment control can be performed using adenosine triphosphate (ATP) bioluminescence devices [159].

2.4. PAPER PRESERVATION

2.4.1. Paper conservation principles

According to the International Council of Museums Committee for Conservation (ICOM-CC), conservation involves “all measures and actions aimed at safeguarding tangible cultural heritage while ensuring its accessibility to present and future generations.” [160].

To control the influence of degradation factors and extend the life of a historic item, two main conservation methods are employed: (i) direct treatment of an item (curative treatments) and (ii) indirect treatment of an item (preventive measures). These two methods are entirely different but also interrelated.

Curative treatments (remedial conservation, restoration)

Prior to undertaking any curative treatment, a detailed assessment of the deterioration level of a paper item is performed. This assessment encompasses a visual and microscopical examination of the physical state of an item and laboratory analysis aimed at characterization (e.g., analysis of the fibres, lignin content, starch detection). When necessary, additional scientific methods are employed for non-destructive analyses of paper items [90].

Some of the examples of direct treatment performed on a paper item include surface cleaning, flattening, mending, repair, stain reduction, tape removal, strengthening, consolidation, sizing, resizing, deacidification, removal or deactivation of molds, protection, and more. The selection of the treatment method and materials for conservation depends on the specific conservation issue and the period of the item’s production.

While it is recognized that curative techniques successfully prolong the lifespan of paper, it is not feasible to perform treatment on all paper items. Therefore, curative treatments, while playing a significant role, are not sufficient for the comprehensive preservation of all items in the collection.

Preventive measures

To minimize the effects of deterioration factors on collections, it is necessary to enhance the quality of the environment surrounding paper items and implement a wide range of preventive measures. Some of the common preventive strategies include the improvement of the air quality through ventilation or filtration, conducting integrated pest management (IPM), housekeeping and cleaning, practicing emergency and disaster mitigation and

response, maintaining safe levels of microclimate conditions, and employing safe practices during storage, handling, transport, and exhibitions. Moreover, the principle of minimum intervention can only work when these proactive measures are implemented [161].

Paper conservation

The multidisciplinary cooperation of several professionals is essential for successfully addressing complex conservation issues [23]. Simultaneously, scientific advancements in the form of new conservation materials and formulations present a myriad of possibilities. To benefit from these possibilities, they must be rigorously assessed. Therefore, each novel conservation treatment should have all its phases (application, ageing, and removal) evaluated [8]. According to Horie, in the case of polymeric materials, the proposed conservation treatment should endure for up to 100 years [8].

The sole choice of conservation material used in conservation treatment affects the longevity of the treated item. A slightly modified application procedure or different amounts of materials added to the mixture can lead to undesired consequences, resulting in alterations to the appearance and structure of paper. Therefore, any new treatment should be evaluated by considering all aspects of application for the item, including aesthetic, technical, and ethical details [8]. This assumes undertaking preliminary research on model materials before treating historic paper items.

Japanese paper, also referred to as *washi*, stands as a prominent candidate among model materials for historic paper. Widely utilized in the repair and restoration of historic paper items, this paper is traditionally made from bast fibres sourced from *kozo, gampi,* and *mitsumata* plants native to Japan. But not all fibres in Japanese papers sold on the market belong to these three plants. Some fibres are derived from wood pulp [162] and are not of conservation grade. For this reason, only papers containing 100% of the aforementioned bast fibres (or their combination) should be used to treat fragile and valuable historic papers [163]. On the other hand, many Japanese papers that are not of conservation grade can serve as excellent model papers.

As mentioned previously, the rate at which degradation will proceed is determined by the paper's stability. The unstable, low-quality materials always degrade faster. The degree of degradation also determines the approach to paper's preservation. All materials used for conservation work are expected to be chemically stable and durable, with high purity and physicochemical properties compatible with those of the original materials, to avoid further degradation [164]. The proposed intervention should be purposeful, minimalistic, and

reversible [8], while also prioritizing the safety of the conservator-restorer, other people, and the environment [21]. Ultimately, the treated paper should retain its physical integrity, visual appearance, and tactile properties (grammage, thickness, roughness, smoothness, stiffness, or handle) to the fullest extent.

Over the decades, advanced conservation-restoration treatments have evolved, incorporating a range of solutions, such as inorganic nanoparticles, hybrid systems, microemulsions and gels, films, and protective coatings [12,165–167]. Each of these solutions is designed to address the specific challenge encountered in conservation-restoration work. In recent years, there has been a growing expectation for all new conservation treatments to align with the principles of green conservation as much as possible [168,169].

2.5. PROTECTIVE COATINGS

In essence, the coating procedure involves modification of the substrate by applying a thin layer of a new material, typically a polymer, in liquid form. Common industrial techniques for applying coatings include dip coating, brush coating, roll coating, bar coating, spray coating, drop coating, spin coating, or flow coating [170]. However, in certain instances, a monolayer coating does not provide adequate protection. In various fields, the application of multilayer coatings is a frequent practice to meet specific industry requirements [171]. Multilayer coatings are commonly utilized to impart several characteristics to the coating system, while the properties of each layer influence the properties of the coating itself [172].

Protection is typically the final step in conservation treatment, aiming at “slowing down the kinetics of surface deterioration and alterations” [173]. Protection often involves the application of coatings, serving as the first line of defence against environmental factors. Applying protective coatings is considered both a curative and preventive measure [174]. Coatings employed in paper conservation are expected to be compatible with paper, enhancing its targeted properties and prolonging its lifespan while also preserving its aesthetics and tactile characteristics. Ideally, they should remain invisible, appearing clear and transparent [175], without reflecting or scattering light extensively. Although achieving total reversibility is deemed impossible [176], coatings are expected to be reversible [8].

Coatings used in paper conservation should ideally provide a physical barrier to environmental factors (e.g., moisture, light, and oxygen), offering the appropriate protection

to paper items during exhibitions, storage, or research [2]. To achieve this, coatings sometimes carry protective substances incorporated into them in the form of fillers [8]. Other requirements for coatings in conservation include longevity, easy and fast preparation, and non-toxicity [175]. However, coatings also degrade and can be vulnerable to certain deterioration factors. Their vulnerability depends on the characteristics of both the coating structure (thickness, number of layers, morphology, adhesion) and the substrate, as well as the type of deterioration factor present [177].

2.5.1. Biopolymers as coating materials

Biopolymers are natural polymers that either originate from living organisms (natural biopolymers) or are chemically produced from natural sources (synthetic biopolymers). Natural biopolymers and their derivatives are commonly used in paper conservation due to their adhesive properties, film-forming ability, transparency, water solubility, abundance, low cost, biodegradability, low toxicity, ease of preparation and/or application, compatibility with paper, and more [178,179]. As such, biopolymers can serve multiple purposes, some of which include joining two materials [180], lining [181], consolidation [182,183], sizing/resizing [184], protection [12], or cleaning (hydrogels) [185,186].

When used for sizing or coating paper, biopolymers can increase the structural stability of paper, reduce surface roughness, or bind loose fibres [78] and pigments to a paper surface [187]. The selection of material for a particular surface treatment (coating, sizing, or consolidation) relies on its rheological and chemical characteristics, as well as potential deterioration mechanisms. Although they are beneficial for paper, biopolymers are also subject to physical, chemical, and enzymatic degradation [188,189]. Therefore, challenges with biopolymeric coatings could stem from undesired changes in the final properties of coated paper. Although there are a multitude of biopolymers used in paper conservation [178], among the most commonly used ones are starch and methylcellulose. These two materials are deemed compatible with paper and have excellent adhesion to cellulose fibres as a result of interfacial hydrogen bonding [29]. In the paper industry, starch is commonly employed to improve inter-fibre bonding and enhance paper strength [187,190]. The hydroxyl groups present in starch and cellulose molecules present in paper create hydrogen bonds, which facilitate their adhesion [191]. Wheat and rice starches are the most common starch types used in conservation work. Of these two types of starch, wheat starch exhibits greater

stability to natural ageing [8]. Starch has also been used as a sizing or adhesive since ancient times. The presence of starch in historical materials is usually detected with Lugol's solution, a diluted iodine-potassium iodide solution [192].

Starch products used in paper conservation are sold in powder form, which either requires cooking (starch for cooking) or can be prepared with cold water (precooked starch). In paper conservation, starch is usually applied to a certain substrate (e.g., paper, paperboard, leather) in the form of paste. The basic distinction between a paste and a liquid solution is based on their viscosity and method of application [29]. The viscosity of starch is easily modified with water, which determines its rheological properties and compatibility with the substrate. Compared with other adhesive materials commonly used in paper conservation (i.e., cellulose ethers), starch exhibits the highest stability to accelerated ageing [42]. However, starch is highly hydrophilic and swells in contact with water. The swelling of starch can induce planar distortions[12] in paper and cause additional damage. Other possible drawbacks include the brittleness and stiffness of starch films [187] and their high bioreceptivity when used as adhesives [42]. Starch is often combined with cellulose ethers to achieve better working properties [193,194]. Furthermore, water-soluble polymers can reduce the brittleness of starch films [39].

Methylcellulose ranks as the second most important adhesive in paper conservation [42]. As a cellulose ether, methylcellulose exhibits lower bioreceptivity compared with starch [42], but is not as strong [163]. In methylcellulose, hydroxyl groups of cellulose are replaced with $–OCH_3$ to give methoxy groups [195]. Methylcellulose is water-soluble and can be easily removed with water. As cellulose ethers are more mold-resistant than starch, they are the preferred choice for treating paper items that may be subjected to high moisture during storage [78]. Methylcellulose demonstrates high stability under accelerated ageing conditions, making it fit for long-term applications in paper conservation [189].

2.5.2. Titanium dioxide as a nanofiller

Nanoparticles

Substances that measure less than 100 nm in at least one dimension are referred to as nanomaterials. The most significant difference between micro- and nano-scale materials

[12] Planar distortion refers to the curling or cockling of paper.

involves their properties, which in nanomaterials are notably enhanced and distinctive, leading to a broader spectrum of potential applications. Nanomaterials can be categorized as zero-dimensional (nanoparticles, quantum dots), one-dimensional (nanotubes, nanowires, nanorods), two-dimensional (graphene), and three-dimensional (nanoprisms, nanoflowers) [196].

Nanoparticles are zero-dimensional nanostructures[13] [197], produced naturally, incidentally, or deliberately through engineering processes [198]. Their enhanced surface area to volume ratio, as well as the number and arrangement of surface atoms, govern their size and properties [198]. As a result, nanoparticles can exhibit unique chemical, physical, electronic, optical, mechanical, or biological characteristics that are utilized across multiple fields. However, prioritizing safety and understanding the implications of nanoparticles on human health and the environment are equally important and are regarded as paramount concerns.

The commercially available nanoparticles are usually sold in the form of dry powders. As nanopowders tend to agglomerate[14] more than powders of larger scales, effective control of nanoparticle dispersion during the preparation process is essential to fully leveraging their benefits [199]. This is particularly important for coatings. If optimal dispersion of TiO_2 NPs within the liquid medium is not achieved, the protective ability of the coating formulation may be decreased. Nanoparticles should also be compatible with the coating to avoid the destabilization of the formulation [200]. Such unstable dispersions are recognized by their low zeta-potential values and fast particle agglomeration [201]. Ethanol, propanol, or isopropanol are commonly utilized media for dispersing nanoparticles [202], due to their low toxicity [3]. Solid nanoparticles can be dispersed using sonication, stirring, or ultrasonication. However, ultrasonication stands out as a particularly effective method for dispersion [203], as it can successfully disaggregate gathered particles [204] resulting from the action of Van der Waals forces [200].

Over the past two decades, extensive research has focused on the use of nanomaterials in the conservation of cultural heritage materials, driven by their heightened chemical activity that can enhance treatment performance. Among these nanomaterials, oxides and hydroxides of alkaline earth metals have emerged as the predominant choices for preserving cultural heritage materials, owing to their ability to provide consolidation,

[13] Zero-dimensional (0D) nanomaterials have all dimensions confined to the nanoscale.
[14] Agglomeration refers to the formation of particle assemblages [319], facilitated by Van der Waals attraction forces between these particles [320].

deacidification, and antioxidation of the substrate [17,167,200,205–207]. On the other hand, metal oxides such as titanium dioxide (TiO_2), zinc oxide (ZnO), silver oxide (Ag_2O), and copper (II) oxide (CuO) in nanoform also exhibit high chemical reactivity as well as good antimicrobial properties [198]. A decrease in particle size also enhances catalytic activity, leading to an increased utilization of TiO_2 and ZnO in photocatalysis. These properties make them valuable for the development of nanocomposites.

In materials science, nanocomposites are described as combinations of two chemically distinct components, with at least one component being nanoscale. They typically feature a polymeric matrix serving as a binder and inorganic particles as the filler. This combination was first adopted in the 19th and 20th centuries in surface coatings [79]. Nanocomposites are recognized for their capacity to improve several properties of materials, including mechanical characteristics, thermal resistance, chemical stability, rheological properties, barrier properties, and resistance to UV radiation and microorganisms [18].

In conservation, nanocomposites are utilized as consolidants [208], protective coatings [167] or cleaning agents [209]. Nanocomposites in paper conservation are frequently composed of biopolymers as the binding matrix and inorganic nanoparticles of metal oxides as nanofillers [12,210].

Titanium dioxide

Titanium dioxide (TiO_2) occurs naturally as a metal oxide. As such, TiO_2 is present in three crystalline phases: anatase, rutile, and brookite. This compound gained popularity during 20th century industrial development [82,211] as a white pigment, imparting whiteness and opacity to a range of products (paper, inks, and food). Nowadays, it is widely recognized as a UV blocker and commonly incorporated into sunscreens, coatings, toothpastes, and other products due to its strong absorption of UV radiation and high refractive index [212].

TiO_2 is known for its photocatalytic activity. Among the three phases, anatase is the most commonly used for this purpose [213], due to its high photocatalytic effectiveness. While the potential of anatase TiO_2 is related to its photocatalytic activity, its limitation lies in its requirement for UV irradiation ($\lambda < 385$ nm) due to its band gap of 3.2 eV [212,213]. To overcome this issue and expand the TiO_2 wavelength spectrum of absorption into the visible region, TiO_2 was the subject of many modifications. These modifications mainly involved doping with metal and non-metal ions [214].

Nano-TiO_2 shows significant potential for several applications in the preservation of cultural heritage items due to its ability for self-cleaning [215,216], odour neutralization,

environmental purification, antimicrobial action, UV blocking, and more [18,197,217]. Despite the concerns regarding its potential harmful effects [218], nano-TiO_2 is considered low-toxic as its toxicity and environmental impact are still being evaluated [219].

Nano-TiO_2 demonstrates enhanced photocatalytic activity, excellent chemical and thermal stability [220], low electron conductivity [221], anti-corrosiveness [222,223] and transparency, with low reflectance in the visible range [197]. Furthermore, TiO_2 NPs are "bound to cellulosics through physical interactions" [18]. These collective characteristics suggest that incorporating TiO_2 NPs into a cellulosic coating is unlikely to affect the coated paper's chemical properties and aesthetics [197]. However, by absorbing UV radiation, TiO_2 can catalyse other detrimental chemical reactions.

Previous research has indicated that direct application of TiO_2 NPs leads to the oxidation of cellulose following accelerated ageing [19]. However, applying TiO_2 to paper indirectly (incorporated into cellulose ether) can provide protection against heat, UV radiation, and microorganisms [14,19]. Hence, in paper conservation, cellulose ether coatings are used as TiO_2 carriers that prevent its direct contact with inks and paper.

3. EXPERIMENTAL

The experimental part of this research consisted of three stages. Each stage was dependent on the previous one, resulting in the preparation of three sets of samples.

- In ***Phase I,*** materials used in the research were characterized. The influence of wet film thicknesses of the monolayer coatings (starch and methylcellulose) on paper's properties was investigated. This stage aimed to identify the optimal coating formulations intended for use in the subsequent stages.
- In ***Phase II***, the nano-TiO_2 modified bilayer coatings were formulated. All samples underwent accelerated UV ageing, and the influence of each coating formulation was analysed to determine the level of paper protection and the impact on the model paper's properties.
- In the final stage **(*Phase III*)**, the nano-TiO_2 modified bilayer coatings were assessed for their protection against heat and cellulolytic fungi, along with an assessment of reversibility. This stage aimed to assess the effectiveness and long-term impact of the treatment on the model paper's properties.

3.1. MATERIALS

3.1.1. Model paper

Takogami B was selected as the model substrate, despite the limited technical details provided by the manufacturer about this paper. According to available information, Takogami B is declared to be a 43 g/m^2 handmade paper, comprising 70% *kozo* fibres and 30% pulp, with good printability [224].

3.1.2. Printing ink

The printing of the model paper samples was performed using the NOVAVIT F918 Supreme BIO offset ink (purchased from Flint Group, Stuttgart, Germany), which is based on renewable raw materials (100% vegetable oil-based, formulated for alcohol-free printing) [225]. It is suited for printing corresponding to ISO 12647-2:2013, and both yellow and magenta process inks have a lightfastness of 5, according to ISO 12040:1997 [226].

3.1.3. Coatings

Starch and methylcellulose were selected as coating materials due to their compatibility with paper and their extensive use in paper conservation. Wheat starch (trade name Wheat Paste No. 301, item # TAD002001) was purchased from conservation, archival, and bookbinding supplier Talas, N.Y., U.S.A. The product was manufactured by Archer Daniels Midland Company (ADM) from Quebec, Canada, under the name PAYGEL 290 [227]. According to the manufacturer, the product has a loose bulk density of 0.32 g/cc ± 0.05 and 30% solubility in water. Precooked starch was chosen due to its faster preparation time. Methylcellulose (trade name Methyl Cellulose, item # TAD016003) was also purchased from Talas, N.Y., U.S.A. It was manufactured by Ashland, Columbus, OH, U.S.A. The product is declared stable, possesses a density of 0.25 g/cm^3, and is of technical grade [228].

3.1.4. Nanofiller

TiO_2 was employed as a nanofiller, providing protection against UV radiation, fungi, and heat. TiO_2 NPs, anatase, particle size of 18 nm, 99.9% purity, bulk density of 0.24 g/cm^3 [229] were purchased from U.S. Research Nanomaterials, Inc. (Houston, TX, U.S.A.). The anatase polymorph was selected over rutile due to its superior photocatalytic activity [230].

3.2. SAMPLE PREPARATION

Paper samples were cut into rectangular pieces in the direction of the chain lines. All samples were conditioned at 23 ± 1 °C and 50 ± 5% RH prior to the experimental part.

3.2.1. Preparation of the model paper

The protective efficiency of the coating largely depends on the surface preparation. Paper from the batch often contains structural defects, impurities, and contaminants. To establish optimal coating-substrate contact, the surface to be coated should be dry and clean. The cleanliness aims to improve the coating's adhesion to the surface as well as its covering and wetting ability [231]. The clean surface should not be touched prior to treatment.

- To ensure the cleanliness of the surface, the model paper samples were immersed in distilled water for 15 minutes. Afterwards, samples were left to air dry on a piece of blotting paper.

3.2.2. Application of the printing ink

The felt side of the handmade paper samples was determined as suggested in the literature [232] and printed with the red ink prepared by mixing magenta and yellow process inks. The red shade was utilized as the first printed works (almanacs or religious works) used this colour to demarcate sections or to decorate title pages [87,233]. The printing was performed using the Multipurpose Printability Testing System (MZ II, Prüfbau, Peissenberg, Germany), with a printing speed of 1 m/s, a printing pressure of 150 N/cm^2, and an ink distribution time of 30 s at 23 ± 1 °C and 50 ± 5% RH. The printing technique was utilized to achieve more uniform coverage of the surface. The obtained CIE colour components of the dry prints were as follows: L* = 51.16 ± 1.39; a* = 57.25 ± 1.38; b* = 27.36 ± 1.02.

3.2.3. Preparation of the coatings

Different coating consistencies and preparations are used in paper conservation, depending on the particular application, substrate type, and nature of the coating. In this research, both starch and methylcellulose were intended to be diluted, so they were prepared as liquid solutions.

Phase I: Evaluation of the monolayer coatings on the model paper's surface

- 7 g of precooked starch was added to the 100 mL of demineralized water, followed by magnetic stirring for 15 minutes at 1000 rpm.
- 1 g of methylcellulose was dissolved in 100 mL of demineralized water and allowed to settle for 24 hours.

Phase II: Evaluation of the bilayer coatings on the printed model paper's surface

- 7 g of precooked wheat starch was added to 100 mL of demineralized water saturated with calcium carbonate ($CaCO_3$). The mixture was magnetically stirred for 15 minutes at 1000 rpm. The resultant pH value of the solution was 7,10.
- 1 g of methylcellulose was dissolved in 100 mL of demineralized water and allowed to settle for 24 hours. TiO_2 NPs were added to the prepared methylcellulose solution at 0.2%, 0.5%, 1.0%, and 2.0% *w/w*. The mixture was ultrasonicated using the Hielscher UP100H ultrasonic homogenizer at 100% amplitude (1 cycle). Each sample was processed for 20, 25, 30, and 40 minutes, reflecting the principle that higher dry content necessitates more time (energy) for proper dispersion of NPs.

- To avoid heating the solution during ultrasonication, the container with each solution was kept immersed in a cooling water bath (Julabo GmbH, Seelbach, Germany) at a constant temperature of 10 °C.

Phase III: Evaluation of the bilayer coatings on the model paper's surface

- Starch and methylcellulose were prepared as described in the previous stage.
- TiO_2 NPs were added to the methylcellulose solution at 0.5%, 0.75%, and 1.0% *w/w*. The mixtures were sonicated for 25, 27, and 30 minutes using the apparatus outlined in a previous stage.

3.2.4. Coating process

To provide optimal protection for the paper sheet, coatings are expected to spread all over the paper surface and have uniform thickness [231]. The coated surface needs to be entirely covered for proper protection. If the thickness (or amount) of the coating varies, the application of identical formulations can produce different results and change the physicochemical properties of the paper sheet in a negative way.

- To control the wet film thickness and spread the coatings uniformly over the paper surface, a laboratory coating unit was utilized. K Control Coater, model 202 (RK PrintCoat Instruments Ltd., Litlington, U.K.) at a speed of 4 m/min, was employed for coating samples, while various wet film thicknesses were obtained using different coating bars.

Phase I

Starch and methylcellulose were applied to the paper's felt side using metal coating bars No. 2 (12 μm), No. 3 (24 μm), No. 5 (50 μm), and No. 8 (100 μm) in a single pass. The coated samples were allowed to air dry at room temperature for 24 hours before analysis.

Phase II* and *Phase III

To prevent direct contact between TiO_2 NPs, cellulose, and printing ink and to mitigate the risk of paper degradation, the coatings were applied in two layers. The bilayer application also aimed to prevent the coating from cracking. Starch was selected as the bottom layer to provide maximum adhesion between the coating and paper.

- The bottom layer was applied using coating bar No. 3 (24 µm). The top layer (methylcellulose incorporating TiO_2 NPs) was coated over the dried bottom layer using coating bar No. 2 (12 µm). Subsequently, all coated samples were allowed to air dry at room temperature.

3.2.5. Denomination of the samples

Table 1, **Table 2**, and

Table *3* show the denominations of the samples at different stages of the research.

Table 1 - Denomination of the samples in ***Phase 1***

Sample code		Description
RP		Uncoated model paper
WSP12	**MC12**	Model paper coated using the wet film deposit of 12µm
WSP24	**MC24**	Model paper coated using the wet film deposit of 24 µm
WSP50	**MC50**	Model paper coated using the wet film deposit of 50 µm
WSP100	**MC100**	Model paper coated using the wet film deposit of 100 µm

WSP – starch, MC – methylcellulose

Table 2 - Denomination of the samples in ***Phase 2***

Sample code	Description
U	Uncoated model paper
S	Model paper coated with starch
S+MC	Model paper coated with starch and methylcellulose
S+MC+0.2TiO₂	Model paper coated with S+MC incorporating 0.2% TiO_2 *w/w*
S+MC+0.5TiO₂	Model paper coated with S+MC incorporating 0.5% TiO_2 *w/w*
S+MC+1.0TiO₂	Model paper coated with S+MC incorporating 1.0% TiO_2 *w/w*
S+MC+2.0TiO₂	Model paper coated with S+MC incorporating 2.0% TiO_2 *w/w*

Table 3 - Denomination of the samples in ***Phase 3***

Sample code	Description
P	Uncoated model paper
S	Model paper coated with starch
S+MC	Model paper coated with starch and methylcellulose
T0.50	Model paper coated with S+MC incorporating 0.5% TiO_2 *w/w*
T0.75	Model paper coated with S+MC incorporating 0.75% TiO_2 *w/w*
T1.00	Model paper coated with S+MC incorporating 1.0% TiO_2 *w/w*

3.2.6. Accelerated ageing

Accelerated ageing studies are designed to simulate the natural ageing of materials under different conditions in a significantly shorter time. As such, they seek to understand and predict the degradation processes of materials, compare materials, or evaluate new conservation materials or treatments [122].

The common techniques employed to accelerate paper ageing involve exposing paper to different temperatures and relative humidities, heat treatment, and light irradiation. The impact of other deterioration factors, such as pollutants, may be observed in parallel [234,235].

Thermal ageing

While accelerated thermal ageing of paper items safely stored in a museum, library, or archive may never occur, assessing the effects of heat on model materials can provide valuable insights. The resulting changes are regarded as a measure of paper's permanence, durability [5,236], and stability. Nevertheless, information gathered for a specific elevated temperature may not be applicable to other elevated temperatures [122].

According to Feller, exposing paper to 3 days (72 hours) at 100 °C corresponds to 25 years of natural ageing [102].

UV ageing

The absorption of UV radiation initiates chemical reactions that can cause substantial damage to paper. This risk can be mitigated by incorporating UV-absorbing fillers into the paper coating. These fillers "dissipate" the absorbed radiation "through a radiationless process" [114] and can deactivate oxidizing agents [26]. One of these UV absorbers is TiO_2.

- Assessing the changes resulting from both accelerated thermal and UV ageing can offer insights into the protection provided by coatings.

- In ***Phase I***, the samples coated with monolayer coatings were heat aged at 100 °C for 50 hours in a Memmert UNB400 dry oven (Memmert GmbH, Schwabach, Germany), as previously described by Darwish [237]. The procedure simulated the natural ageing of paper, equivalent to 17–18 years, according to Feller [189].

- To evaluate the protective properties of the bilayer coatings in ***Phase II***, samples were subjected to accelerated UV ageing in the test chamber Solarbox 1500e (CO.FO.ME.GRA, Milano, Italy), equipped with a 1500 W Xenon lamp[15] and controlled temperature.
Irradiation in the chamber was set to 550 W/m^2. The samples were exposed for 35 h at 50 °C using the indoor filter S208/S408 (artificial daylight).

-In ***Phase III***, all samples (coated and uncoated) were heat aged at 100 °C for 9 days (216 hours) in a Memmert UNB400 dry oven (Memmert GmbH, Schwabach, Germany), according to Indictor [238]. The procedure simulated the natural ageing of paper, equivalent to 75 years, according to Feller [189].

3.3. EXPERIMENTAL DESIGN

3.3.1. Determination of the coatings' properties

pH value and viscosity

The pH value of the newly introduced materials is a crucial factor, as it affects paper's stability and durability in the long term. For this reason, it is important to keep this parameter within the optimal range.
Viscosity is a rheologic property that describes a liquid's fluidity. The appropriate viscosity is essential for achieving the consistent and controlled transfer of the coating onto the paper surface, thereby ensuring a successful application.

- The pH value of the coatings was measured with a WTW 340 pH meter (Xylem Analytics, Weilheim, Germany).

- The dynamic viscosity of the coatings in ***Phase I*** was measured at 22 °C using a RheolabQC rotational rheometer (Anton Paar GmbH, Graz, Austria) in a constant shear rate mode with a value of 50 s^{-1}.

[15] The Xenon arc lamp is commonly employed in accelerated ageing studies to test the lightfastness of materials. The lamp emits a high rate of UV radiation. This allows for the evaluation of unfiltered daylight effects [113].

3.3.2. Evaluation of the physical characteristics of the samples

Thickness and grammage

The grammage of paper is a physical variable that encompasses fibres, fillers, process materials (e.g., coatings, sizing), and water [239]. The thickness of paper largely depends on grammage. Considering that coatings are expected to be extremely thin [231], assessing thickness and grammage before and after coating application can offer valuable insights into the suitability of the coating for conservation purposes.

- Grammage and thickness of the investigated samples were determined during ***Phase I.*** The weight of the samples (38 × 80 mm) was measured with a digital analytical electronic balance (Mettler Toledo Xs205, Greifensee, Switzerland), while thickness was determined using a digital micrometer DGTB01 (Enrico Toniolo s.r.l., Milano, Italy), with a weight pressure of 49.03 kPa and a resolution of 0.01 mm. The sample thickness was recorded at random positions.

3.3.3. Evaluation of the surface morphology of the samples

Observation of microstructure is a common characterization method in materials science that can provide insights into the material's composition and physicochemical properties [240].

Optical microscopy and scanning electron microscopy (SEM)

At low magnifications, optical microscopy can provide insights into the paper's morphology [69], as well as coatings' and inks' covering abilities. SEM, on the other hand, provides a much broader range of magnifications than optical microscopy and a greater depth of field [240]. Structural details, such as morphology, texture, coatings, filler distribution, or impurities, are revealed through 3D images. Instead of light, SEM uses electrons to generate images [241]. Combining SEM with energy dispersive X-ray spectroscopy (EDS) provides high magnification imaging coupled with compositional (elemental) analysis of the surface.

- Optical microscopy was employed to analyse the samples' surfaces (texture, structures, fibre orientation, and film formation).

- To assess its surface morphology in the preliminary stage, the model paper was placed on a LED light board with a light intensity of 150─220 lm and illuminated from above with the Dino-Lite Premier Digital Microscope AM4113FVT (AnMo Electronics Corporation, New Tapei City, Taiwan). Micrographs were obtained at a magnification of 54×, using a UV illumination of 395 nm.

- In ***Phase I***, the coating films were captured with a polarizing light microscope (Olympus BX51) equipped with a DP72 digital camera (Olympus, Tokio, Japan). The micrographs were captured at a magnification of 100 × with a camera resolution of 4140 × 3096 pixels.

- In ***Phase I**** and ***Phase III****, SEM analyses were employed to assess the homogeneity of the coatings, the distribution of TiO_2 NPs in the nanocomposite film, the presence of aggregates, and the reversibility of the coatings. EDS analyses were employed to obtain data on the elemental compositions of the materials and to confirm the extent of TiO_2 removal from the coating by water immersion.

- The micrographs were obtained with a JEOL JSM-6460 Scanning Electron Microscope (JEOL Ltd., Tokio, Japan) with an INCA Energy EDS system (Oxford Instruments, High Wycombe, U.K.). For imaging, samples were mounted on aluminium stubs and gold-coated via the Baltec SCD 005 sputtering unit. The micrographs were recorded at various magnifications (100×, 300×, 500×, and 1000×).

3.3.4. Evaluation of the surface properties of the samples

The surface properties of paper not only determine its visual impression and tactile properties but also its interaction with water. All cellulose-based materials have a strong interaction with water due to their hydrophilicity and hygroscopicity [242].

Contact angle and water droplet absorption time

The contact angle (θ) describes paper's wettability with a liquid. When a liquid droplet is applied to the paper surface, it forms an angle at the point where the droplet meets the substrate. The surface is considered hydrophilic when the contact angle is below 90 °, hydrophobic when it is higher than 90 °, and superhydrophobic when the contact angle exceeds 150 ° [243]. In addition, water droplet absorption time refers to a timeframe during

which the paper structure fully absorbs a certain volume of water. Many parameters influence the wetting of the paper surface, including surface roughness, porosity, structural unevenness, chemical heterogeneity of the surface, surface-active substances, and the presence of impurities and contaminants [244].

- The contact angles of the samples in this research (***Phase I***, ***Phase II***) were assessed by goniometric observation, for which the Dataphysics' OCA30 device and its controlling software, SCA 20, were utilized. The measurements, using a sessile drop method, were run on 20 x 20 mm strips using redistilled water as the test liquid. The applied water droplets' volume was set to 2 μL, and the contact angle measurements were performed 0.2 s after the initial water-substrate contact using the Laplace-Young fitting.

- Water droplet absorption time (***Phase I***, ***Phase II***) was investigated through time-resolved contact angle measurements using the camera framerate (IDS Imaging Development Systems GmbH, Obersulm, Germany) of 25 fps and utilizing a water droplet of 2 μL. Due to the heterogeneity of the samples, the contact angle was measured 7 times.

Average surface roughness (R_a)

The structure of paper consists of numerous heterogeneities, with surface roughness being one of them. Surface roughness is commonly determined as average roughness or root-mean-square roughness [240]. The average roughness represents the height of the surface texture [245]. This characteristic can significantly impact wetting and adhesion [244], as well as fungal attachment and growth on paper [68]. The measurement of paper roughness plays a key role in assessing the impacts of degradation or evaluating the effects of curative treatments, such as surface cleaning, coating, sizing, or resizing.

- The average surface roughness was determined to assess the morphological features of the samples before and after accelerated UV ageing. The selected model paper (U) was intentionally rough, as rougher surfaces are preferred over smooth ones for coating due to better "interlocking" between the coating and the surface [231]. However, rougher surfaces also tend to attract more water [68], an issue that is anticipated to be addressed by the application of coatings.

- The measurements of average surface roughness (R_a) in ***Phase II*** were performed using a MarSurf PS 10 device (Mahr GmbH, Goettingen, Germany). Based on the previous experience of the investigating paper with a heterogeneous surface, the total length of the measurement (traversing length, Lt) was set to 15 mm, with a sampling length of 2.5 mm and a stylus speed of 1 mm/s.

3.3.5. Evaluation of the optical properties of the samples

The interaction of paper with light (absorption, transmission, or reflection) affects both its propensity to degradation and its optical properties. For this reason, optical properties not only describe the visual perception of paper but also indicate the resulting chemical changes.

Colour

The colour of the material results from the absorption of visible light wavelengths (380–750 nm). The chromophore, a colour-bearing group, absorbs electromagnetic waves upon excitation [83]. Clear and transparent materials do not contain chromophores [246], although certain degradation reactions are known to generate these groups [2]. In polymers, absorption of visible radiation is attributed to the presence of C=O and C=C groups, so when molecules with these double bonds absorb light, free radicals [119] or excited states can be formed and lead to other degradative reactions [113].

The colour of an object is determined by the interaction between the object (sample), a light source (illuminant), and an observer. The colour values are perceived subjectively, based on the individual's ability to perceive them, previous experience, and personal preferences.

Spectrophotometry is a non-destructive method encompassing the quantified measurement of the interaction between UV, visible, and IR radiation and a material, while CIE *L*a*b** colour space is the universally accepted method for expressing colour properties. In the CIE *L*a*b** colour system, colours are described by their X, Y, and Z tristimulus values, from which the *L**, *a**, and *b** colour components are calculated.

While *L** refers to lightness (100 white, 0 black), *a** and *b** denote the positions of colours on the red/green (+*a**, -*a**) and yellow/blue (+*b**, -*b**) axes.

The quantification of change in colour is assessed by calculating ΔE_{ab} (total colour difference) according to **Equation 2** [247].

$$\Delta E_{ab} = \sqrt{(\Delta L^*)^2 + (\Delta a^*)^2 + (\Delta b^*)^2} \quad \textbf{(2)}$$

Colour differences as perceived by a standard observer are categorized as follows [247]:

$0 < \Delta E_{ab} < 1$: the difference could not be seen,

$1 < \Delta E_{ab} < 2$: the difference is hardly noticeable,

$2 < \Delta E_{ab} < 3.5$: the difference may be noticed,

$3.5 < \Delta E_{ab} < 5$: the colour difference is clearly visible,

$5 < \Delta E_{ab}$: the colour difference points to two different colours.

Some of the factors influencing colorimetric measurements include standard illuminant[16], standard observer angle[17], measurement illumination conditions (M0, M1[18], M2, M3) and measuring geometry[19].

Spectrophotometers make ΔE_{ab} calculations automatically. They can also measure several other parameters, including yellowness, whiteness, opacity, colour strength, and more.

In more recent years, the determination of colour change in cultural heritage objects has been monitored with micro fading testers [248].

Yellowness

The yellowing of paper usually indicates ageing. It is commonly attributed to the oxidation of cellulose and the behaviour of acidic compounds formed during ageing [114,249].

The degradation of paper in the UV-Vis range is commonly caused by the formation of carbonyls of aldehydic groups and conjugated diketones [250]. These compounds are also identified as the main chromophores contributing to yellowing [250].

Chromophores are also generated from coatings: their decomposition byproducts [251] or oxidized impurities [164].

[16] The standard illuminant represents the light spectrum generated by known sources under which samples are viewed. Several standard CIE illuminants (A, B, C, D, E, and F) at different colour temperatures exist. The D illuminants (D50, D55, D60, and D65) were developed to compensate for the lack of UV in earlier illuminants [113]. Today, the most commonly used illuminant in colorimetry is D65, while D50 is commonly used in the printing industry.

[17] Observer angle is the colour-matching function for the CIE standard colorimetric observer, which is based on the average human response to colours across the spectrum [321].

[18] M1 conditions specify that the instrument illumination corresponds to D50, which is correlated to standardized viewing conditions (ISO 3664:2009) and has a more defined UV component (spectral region < 400 nm) [322].

[19] Measuring geometry is used to exclude gloss. Some of these geometries are: 0/45 (0:45), 45/0 (45:0), d/0 (d:0), d/8 (d:8), di/8 (di:8) and more. In the 0/45 geometry, the illuminant is positioned "at 0° with respect to the normal of the object's surface, while the sensor is set at a 45° angle from the normal." [246].

Opacity

Opacity refers to the property of paper to be impermeable to light. It is determined through reflectance measurements [252]. The opacity of paper depends on the characteristics of cellulose fibres and may be enhanced with fillers. Changes in opacity can occur due to fibre "debonding" and the loss of coating material [253] resulting from degradation.

Gloss

Gloss refers to paper's ability to reflect light. Gloss is categorized as low (< 10 GU), semi (10–70 GU), or high (> 70 GU) [254]. The most appropriate measurement angle among the standard options (20°, 60°, and 85°) is determined by initially inspecting the surface at a 60° angle [254]. The loss of gloss is commonly caused by surface irregularities (e.g., microcracks, roughness).

Fluorescence intensity

Light can also induce the luminescence of materials, a phenomenon well-known to conservators. Most often, materials are observed under UV illumination, where many substances exhibit distinctive visual characteristics, which are then leveraged for material characterization, detecting earlier repairs, or assessment of conservation treatment. Fluorescence is a type of luminescence that arises due to the activity of fluorophores. When a molecule absorbs shorter-wavelength photons (i.e., UV region-photons), which excites a fluorophore, it results in the re-emission of longer-wavelength photons, in which the absorbed energy is released as fluorescence [122,255,256]. The common excitation wavelengths for fluorescence are 365 nm, 395 nm, and 400 nm [256]. The wavelengths of the absorbed or emitted light are measured as fluorescence intensity [257,258].

- Throughout this research, colorimetric measurements were performed on both unaged and aged papers, using at least three independent samples and several positions within the same sample. CIE *L*a*b** values were assessed with the Techkon SpectroDens spectrophotometer (Techkon, Königstein, Germany), using the following settings: standard illuminant D50, a standard observer angle of 2°, M1 measurement conditions, and the sample backed by a standard white tile. The total colour differences were calculated using the ΔE_{ab} formula.

- In ***Phase I***, yellowness and opacity were determined using the Techkon SpectroDens spectrophotometer (Techkon, Königstein, Germany) with a measuring geometry of 0/45

(0:45) and the following settings: standard illuminant D50, a standard observer angle of 10°, and M1 measurement conditions. Yellowness was measured on a white backing, while opacity was measured using SpectroDens' opacity function, which includes spectrophotometric measurements of the sample on a black-and-white backing. Before the tests, the measuring unit was calibrated to absolute white.

- Gloss levels were determined in ***Phase I*** and ***Phase III*** using an Elcometer 407L Glossmeter; 20 & 60 Degree (Elcometer, Manchester, U.K.) with a measurement angle of 60°.

- As compounds can move to a fluorescent state during oxidation [221], the fluorescence intensity of the samples before and after ageing was determined to assess the eventual changes. Fluorescence intensity in ***Phase II*** was measured using the Ocean Optics USB4000+ spectrometer (Ocean Optics, Orlando, FL, U.S.A.) in conjunction with a 30 mm-wide integrating sphere under a measuring geometry of (8:di) with diffuse geometry and specular component included. The LSM Series LED light source at 365 nm was used as the fluorescence excitation wavelength. The excitation light source was maintained at a constant current of 0.140 A. The fluorescence intensity was measured within the spectral range between 330 and 630 nm.

3.3.6. Evaluation of the mechanical properties of the samples

Mechanical damage to paper occurs through regular use (handling), carelessness, or deliberate action. Additionally, structural damage may arise due to frequent and drastic fluctuations in microclimate conditions. The mechanical properties of the paper sheet are known to depend on both the cellulose chain length and inter-molecular and inter-fibre bonding [28,122]. As a result of degradation, cellulose experiences depolymerization and chain scission [2]. These changes alter the characteristics of cellulose fibres, therefore affecting paper's mechanical properties.

Several tests can be performed to determine the extent of these changes. The three tests used for describing the mechanical properties of paper under the influence of a force include tensile strength, compression strength, and shear strength. Furthermore, flexural strength, hardness, and impact resistance tests provide information on additional forces [259].

Tensile strength

Tensile strength describes the ability of a material to withstand pulling. In paper, tensile strength is known to depend on fibre characteristics (strength, length) and the type of bonding [67,260]. As coating application influences these parameters, tensile tests were employed for comparing different samples in this research.

Short-span compression test (SCT)

Compression tests are considered to be the exact opposite of tensile tests [29]. The short-span compression test (SCT) is the commonly used method for evaluating corrugated board components. The compression load is applied to a small area of the material. The obtained results reflect the paper's intrinsic strength, thereby indicating its fibre strength [261].

Bursting strength

Commonly known as the Mullen test, bursting strength represents the maximum hydraulic pressure a paper can withstand [262]. It is known to depend on the tensile strength and elongation at break [236].

Taber stiffness

Stiffness refers to the lack of flexibility in paper. It is influenced by paper characteristics, including thickness, grammage, raw materials present, fibres, fillers, and moisture content [239]. As coating applications are expected to provide flexible films, preserving this property is crucial to preserving paper's tactile properties. In conservation, the physicochemical properties of the coating material should match those of the treated item. Similarity is crucial in preventing further damage to an item [231].

- In this research, coatings aimed to improve the strength of the model paper. To assess the extent of these changes, in ***Phase III***, an evaluation of the paper's four mechanical properties was conducted before and after accelerated ageing. At least six independent samples were used to test each mechanical property.

- In this research, the tensile force was measured using a FRANK device, type 800 (FRANK, Birkenau, Germany), equipped with a vertical force measurement system and a maximum load capacity of 5 kp.

- To assess the compressive strength of the paper samples, the Lorentzen & Wettre Compressive Strength Tester STFI device, code 282 (ABB AB / Lorentzen & Wettre, Kista, Sweden) with a measurement range of up to 20 kN/m was utilized.

- The bursting strength of the paper samples was assessed using the Lorentzen & Wettre Bursting Strength Tester SE 181 (ABB AB / Lorentzen & Wettre, Kista, Sweden), with a measurement range of 70–1400 kPa, and in compliance with the ISO 2759 standard.

- Taber stiffness (TS) of the paper samples prior and post-thermal ageing was assessed using a Lorentzen and Wettre bending tester, code 160 (ABB AB / Lorentzen & Wettre, Kista, Sweden) with the following settings: touch speed of 5°/s, touch force of 2 mN, bending length of 25 mm, and bending angle of 7.5°.

3.3.7. Evaluation of the chemical properties of the samples

IR spectroscopy

Spectroscopy relies on the interaction of light with matter. Spectroscopic techniques are usually categorized as vibrational, electronic, scattering, or magnetic resonance techniques [26]. IR spectroscopy is a vibrational technique in which "an organic molecule absorbs and converts IR radiation in the range of 10,000–100 cm^{-1} into energy of molecular vibration" [263]. Identification of chemical groups can be obtained using the vibrational frequencies of chemical bonds. IR spectra are easily recognized by distinctive and sharp absorption bands. Each band relates to a specific covalent bond in a molecule [259]. Band intensities are expressed either as transmittance (T) or absorbance (A), while band positions are displayed as wavenumbers (frequencies). They are reciprocally related to wavelengths. Spectra from 4000 cm^{-1} to around 1500 cm^{-1}, are known as the ID region, while those from 1500 to 600 cm^{-1} are called the fingerprint region (functional group region) [259,263]. Spectra can be obtained for a variety of samples, including solids, liquids, and gases in all their forms. IR spectroscopy is frequently employed in material characterization, encompassing tasks such as determining chemical species, identifying structural heterogeneity, analysing thin films, coatings, and more [240].

FT-IR-ATR spectroscopy is a commonly utilized method in the analysis of polymeric materials. The directness of the contact with the sample determines the quality of the captured spectra [68]. The penetration depth of an ATR element is between 0.5 and 2 μm [264].

- Throughout this research, FT-IR spectra were obtained to characterize the applied coatings and investigate the state of degradation of cellulose resulting from accelerated ageing.

- Spectra were determined with a Shimadzu FT-IR IRAffinity-21 spectrometer (Shimadzu Corporation, Kyoto, Japan) with the Specac Silver Gate Evolution as a single reflection ATR sampling accessory, featuring a ZnSe flat crystal plate (refraction index of 2.4). The IR spectra were recorded in the spectral range of 4000 to 600 cm^{-1}, with a resolution of 4 cm^{-1} and were averaged over at least 6 scans.

3.3.8. Evaluation of the antifungal properties of the coatings

Exposure of TiO_2 to UV radiation has been shown to deactivate microorganisms by inducing oxidative stress on their cell membranes through the resulting ROS (superoxide anion radicals, hydroxyl radicals, and hydrogen peroxide) [10,265]. TiO_2 concentration, UV range, and dose (the irradiation time and intensity combined) play a crucial role in this process [266].

- The antifungal properties of the coated paper were assessed by subjecting samples to two strains of filamentous fungi: *Aspergillus niger* and *Trichoderma citrinoviride.* Both species are cellulolytic enzyme producers [150,267] known to attack cellulose and starches. Moreover, *Aspergillus niger* is commonly employed in paper conservation studies [12,14,42,268] and is abundant in indoor environments worldwide [143].

Fungal strains

The antifungal properties of the coated paper were assessed by inoculating it with three isolates: two *Aspergillus niger* and one *Trichoderma citrinoviride. A. niger* used for indirect inoculation is isolate No. ATCC strain 16888, purchased as a reference strain by the Croatian Veterinary Institute. Two of the utilized fungi (*Aspergillus niger* and *Trichoderma citrinoviride)* used for direct inoculation are airborne isolates obtained from the culture collection of the Faculty of Biology, University of Belgrade, Serbia (*A. niger* isolate No. BEOFB345m, Gene Bank accession numbers MH630013, MH605080; *T. citrinoviride* isolate No. BEOFB1220m, Gene Bank accession number MH671315).

Indirect inoculation

The paper samples underwent TiO_2 photoactivation for 30 minutes under a Philips TUV15W G15T8 UV-C lamp (Philips, Eindhoven, Netherlands) with UV radiation (254 nm) at 15.5 W. After illumination, two sets of sterilized paper samples (diameter of 25 mm, coated side facing up) were placed on malt extract agar (MEA) inoculated with 10 μL of *Aspergillus niger* spores in a concentration of approximately 10^7 mL^{-1} in the middle of the Petri dish. Inoculum was obtained by inoculation of ATCC strain 16888 on MEA and incubation in the dark at 25 ± 1 °C for 5 days, after which the spores were washed with Buffer Peptone Water (Merck, Darmstadt, Germany) with Tween 80 (Sigma Aldrich, St. Louis, U.S.A.). By decimal dilution, the concentration was adjusted to approximately 10^7 mL^{-1}. Each set of samples was kept in different conditions for 5 days: (i) in total darkness, at 30 ± 1 °C and 60% RH, (ii) under an D50 noon sky daylight light source, X-rite Macbeth Judge II lighting (X-rite, Grand Rapids, USA), with a light level of 114-foot candles, at ambient conditions. The growth was monitored daily over a 5-day period.

Direct inoculation

This part of the research aimed to further investigate the previous findings by altering the parameters (UV dose and exposure time, inoculated substrate, environmental conditions, and/or fungi type). Isolates (*A. niger* BEOFB345m and *T. citrinoviride* BEOFB1220m) were inoculated on malt extract agar (MEA) and incubated for 7 days at 25 °C in a thermostat (Memmert). After the incubation period, the conidial suspensions were prepared by washing conidia from the surface of the slants with sterile saline solution (NaCl 0.85%, HemofarmhospitaLogica, Belgrade, Serbia) containing 0.1% Tween 20 (Sinex Laboratory, Belgrade, Serbia). Conidia were counted on a 1 mm^2 surface using a haemocytometer (Bürker) and the suspension concentration was adjusted to approximately 10^7 mL^{-1}.

The samples underwent TiO_2 photoactivation for 24 hours under a Philips TUV30W G30T8 UV-C lamp (Philips, Eindhoven, Netherlands) with UV radiation (275 nm) at 12.3 W. The lamp was kept at 100 cm from the samples. After illumination, samples were conditioned for 48 hours at 100% RH at 25 °C in a glass chamber. Paper samples (diameter of 50 × 50 mm, coated side facing up) were inoculated with 10 μL of conidia (concentration of 10^6 mL^{-1}) and incubated for 7 days at the same conditions (complete darkness). The humidity levels were kept at equilibrium using a saturated KNO_3 and KH_2PO_4 solution. The growth was monitored daily over a 10-day period. All paper samples were photographed using a Nikon SMZ745T stereomicroscope to assess the growth intensity of the tested fungi.

In tests involving *T. citrinoviride,* filter paper was used as the control paper instead of paper coated with starch (S) for better comprehension of the obtained results.

3.3.9. Evaluation of the reversibility of the coatings

The assessment of reversibility is an important aspect, as it considers the removal of materials that could contribute to the degradation of the historic substrate. It depends on the properties of both the substrate and the introduced materials, as well as their combination.
Today, there is a consensus that pursuing reversibility in conservation treatments is an acknowledged goal, which may not always be entirely achievable [173,176,269].
Nevertheless, the removal of surface layers is a delicate conservation intervention that requires careful execution to avoid harming the underlying substrate.
In paper conservation, most adhesive residues or coatings are removed from the paper through immersion in water or through exposure to moisture provided by an ultrasonic atomizer. Starches can also be removed with enzymes, such as α-amylase, which break down the amylose chains [56,270,271]. In more recent years, the localized removal of starch paste has been performed with hydrogels [272]. The ease of removal depends on the starch quality and production method [194].

- In this research, the proposed nanocomposite coating consisted of two layers. Due to the complexity and heterogeneity of the system (model paper, coating layers), reversibility was assessed using the traditional method (***Phase III****). Samples were immersed in a distilled water bath for 1, 2, 24, and 48 hours and "probed with a glass rod" as described by Indictor [238]. The immersion time was intentionally extended to promote starch removal. The wet samples were left to air dry, and their surface was subsequently analysed by a JEOL JSM-6460 Scanning Electron Microscope (JEOL Ltd., Tokio, Japan) with an INCA Energy EDS system (Oxford Instruments, High Wycombe, U.K.). For imaging, samples were mounted on aluminium stubs and gold-coated via the Baltec SCD 005 sputtering unit.

4. RESULTS AND DISCUSSION

The findings featured in ***Phase I, Phase II***, and ***Phase III*** have been previously published by the author [210,273,274], and are hereby included with the consent of the co-authors. Furthermore, the results from ***Phase I**** and ***Phase III*,*** though unpublished, have been included in this work with the agreement of the co-authors.

4.1. CHARACTERIZATION OF THE MODEL PAPER

The analysis of the model paper's characteristics served as a fundamental step in assessing upcoming applications.

4.1.1. Macrostructure

Model paper (Takogami B) exhibits a slight yellowish tint, a characteristic commonly observed in historic handmade paper prior to the end of the 18th century, before the bleaching technique became widely used [70]. The surface of model paper appears rough, as depicted in **Figure 1**, left, where it is captured under raking light using a Nikon D300 camera. Additionally, when captured in transmitted light, the chain lines spaced 35 mm apart are visible (**Figure 1**, right). The yellowish tint, printability, rough surface, and handmade quality were all factors contributing to the selection of this paper for research purposes.

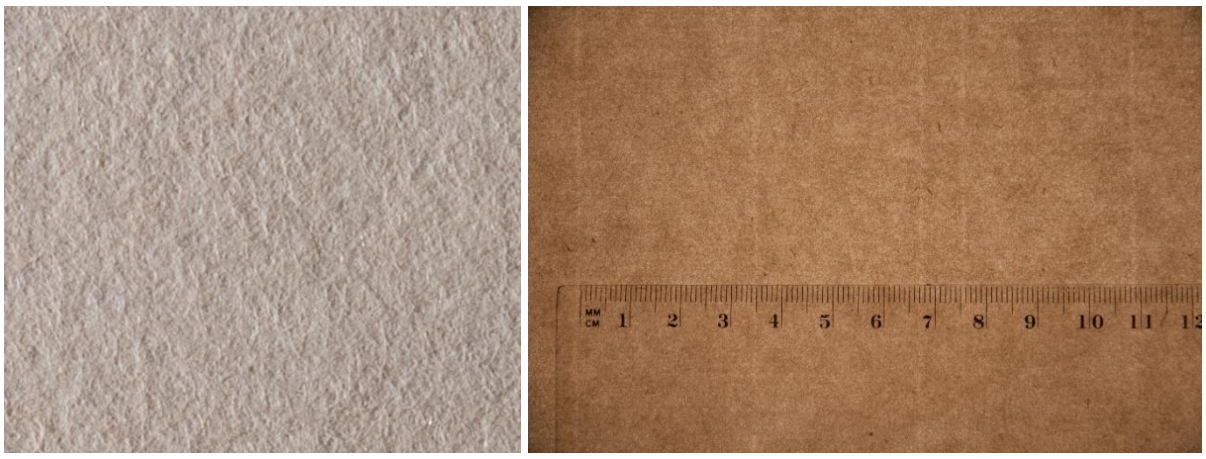

Figure 1 - Model paper's surface under raking light (left) and its chain lines captured in transmitted light (right).

4.1.2. Microstructure

Phase I: Evaluation of the monolayer coatings on the model paper's surface

In **Figure 2**, the fibre network of the model paper is shown under UV illumination of 395 nm, captured by a Dino-Lite Premier Digital Microscope.

By observing the measuring scale shown in the micrograph below (**Figure *2***), it can be concluded that individual fibres are long [50]. The fibres are also randomly arranged, without preference for orientation, with large pores between them.

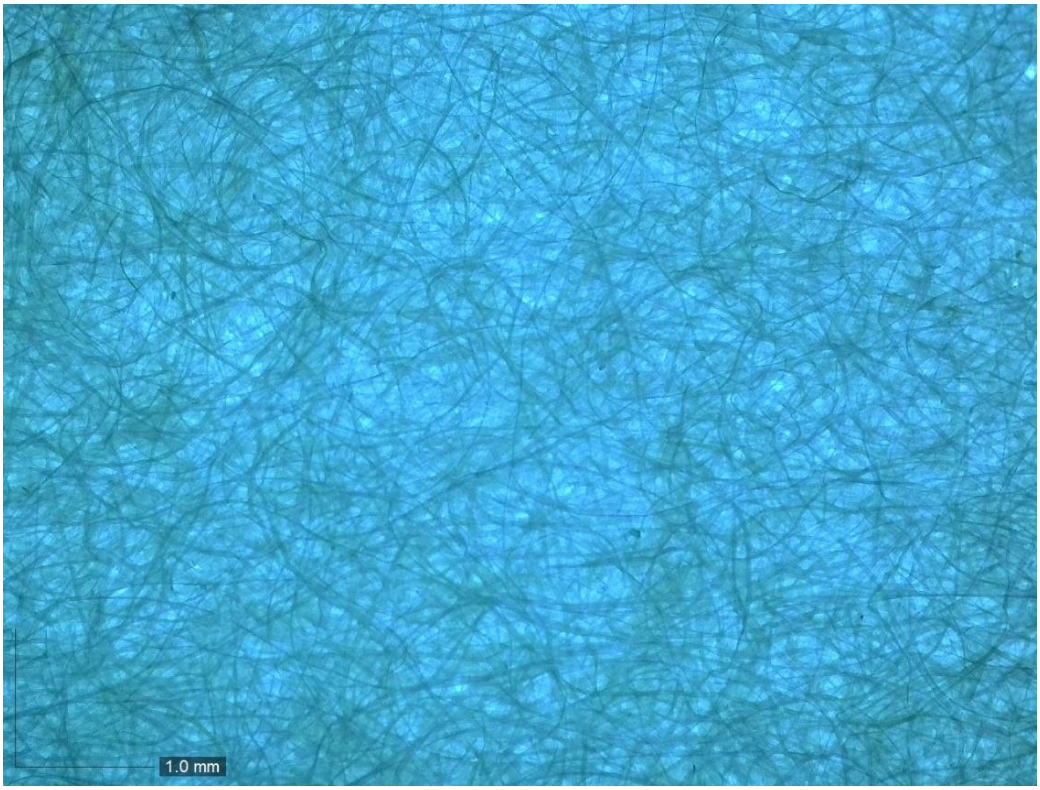

Figure 2 - Micrograph of the model paper at 54× magnification.

The SEM micrograph (**Figure 3**) more closely reveals the fibrous surface of the model paper, while the EDS spectrum (**Figure 4**) uncovers its elemental composition. The findings suggest that model paper is composed of carbon (C) and oxygen (O), with small amounts of silicon (Si), magnesium (Mg), calcium (Ca), aluminium (Al), and chlorine (Cl). These compounds are often found during the elemental analysis of paper from different periods [275]. The presence of Si, Mg, and Cl is also indicative of the pulp [276]. The presence of Cl and Si can increase the fungal resistance of paper [277].

Figure 3 - SEM micrograph showing the surface morphology of the model paper at 300× magnification.

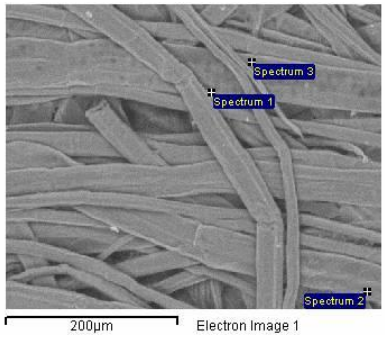

Spectrum	In stats.	C	O	Mg	Al	Si	Cl	Ca	Total
Spectrum 1	Yes	56.64	37.58		1.12			4.66	100.00
Spectrum 2	Yes	87.61	9.89	0.18	0.24	0.16	0.96	0.95	100.00
Spectrum 3	Yes	63.17	28.15	3.14	0.16	4.45	0.08	0.84	100.00
Max.		87.61	37.58	3.14	1.12	4.45	0.96	4.66	
Min.		56.64	9.89	0.00	0.16	0.00	0.00	0.84	

Figure 4 - SEM micrograph (left) and EDS surface elemental composition analysis of specific positions of the model paper in statistics (right).

4.2. pH VALUE AND VISCOSITY OF THE COATINGS

Phase I: Evaluation of the monolayer coatings on the model paper's surface

The coatings used in paper conservation should maintain a neutral or slightly alkaline pH value to prevent the degradation of cellulose due to acidity or excessive alkalinity, as highlighted in the previous section (2.3. Paper deterioration).

During preparation, the starch coating exhibited a slightly acidic pH value (**Table 4**), which was left unadjusted for observation purposes. However, this value was adjusted to neutral in the later phases. The pH value of the methylcellulose coating remained neutral in all measurements.

The role of viscosity is pivotal in conservation treatments, where different applications call for either high or low viscosity levels. Low-viscosity materials can more successfully enter the pores of paper, which makes them the preferred choice for coating applications [231].

The viscosity of the coating increases with the concentration of solids. Similarly, a higher molecular weight of the polymer or a higher viscosity of the solvent can increase viscosity [8]. On the other hand, viscosity decreases with a rise in temperature and *vice versa*.

The results of dynamic viscosity in this research are presented in **Table 4**.

At 23 ± 1 °C and 50 ± 5% RH, the dynamic viscosity of starch was three times higher than the viscosity of methylcellulose, resulting from the higher concentration of solids within the formulation.

Table 4 - pH value and viscosity of the coatings.

Coating	pH Value (1)	Dynamic viscosity (mPa-s)
Methylcellulose	7.07	107.4
Starch	6.11	363.1

4.3. THICKNESS AND GRAMMAGE OF THE SAMPLES

Phase I: Evaluation of the monolayer coatings on the model paper's surface

Application of the coatings has resulted in an increase in the thickness and grammage of the model paper (**Figure 5, Figure 6**).

Although methylcellulose film could not be seen in the micrographs (**Figure 7**) and was presumed to be absorbed by the paper's surface, the increase in thickness of the paper may indicate that film remained invisible due to its high transparency [278].

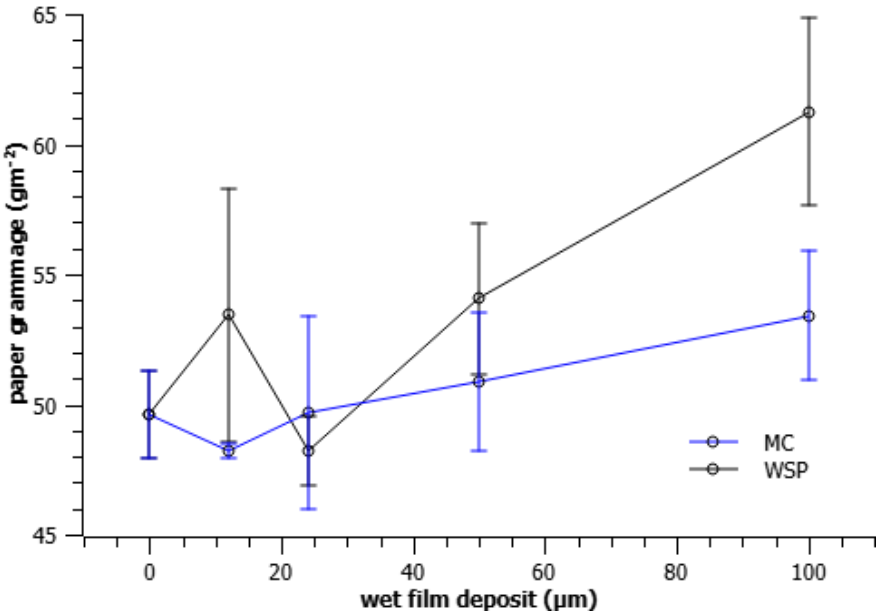

Figure 5 – Grammage (gm^{-2}) of the model paper samples coated with starch (WSP) and methylcellulose (MC) [273].

The highest increase in both thickness and grammage is observed in starch-coated samples (WSPs), which results from the higher concentration of solids. Large SD values showing variations in the thicknesses of the coated model paper samples could be explained by the heterogeneous structure of the model paper and the work of surface tension, which prevents wet films from retaining the same thickness after they are spread over the rough paper surface [231].

In addition to paper heterogeneity, the fluctuations in thickness can also be attributed to the Campbell effect [279], where cellulose fibres "shrink during drying as the capillary pressure closes the pores" within the fibres [50].

Although the application of each coating influences the physical characteristics of the model paper, the application of a 100-µm-thick starch coating (WSP100) results in an excessive increase in thickness and grammage of the aforementioned paper.

Considering that the application of coatings should not drastically change the original physical characteristics of paper, the results from ***Phase I*** were used to define the experimental setup for ***Phase II***.

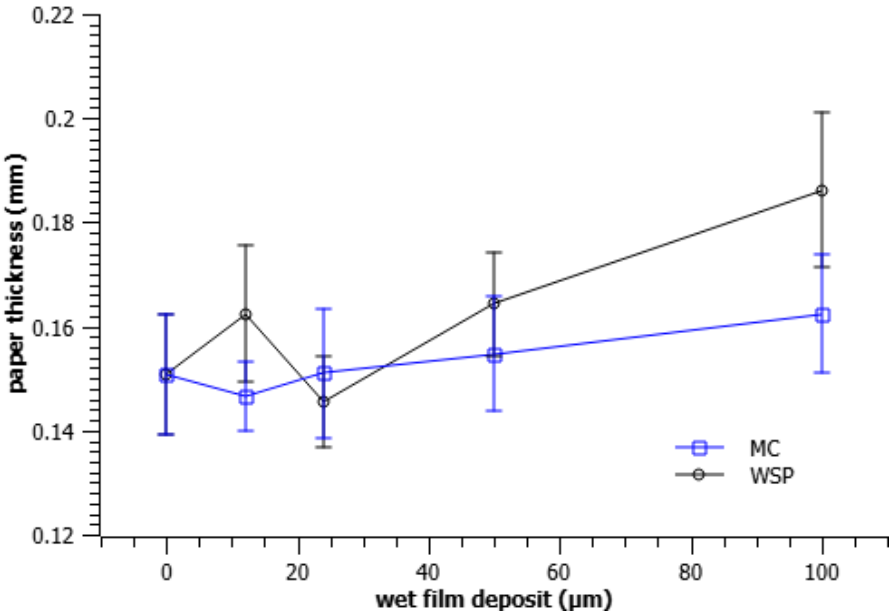

Figure 6 – Thickness (mm) of the model paper samples coated with starch (WSP) and methylcellulose (MC) [273].

4.4. FILM FORMATION PROPERTIES OF THE COATINGS

Phase I: Evaluation of the monolayer coatings on the model paper's surface

In this stage, the model paper samples were coated using different wet film thicknesses.

Figure 9 As the formation of film on the fibres surface modifies the entire paper surface, a visual assessment of the coating films served as the initial step in determining their future application. **Figure 7** shows micrographs of the uncoated model paper (RP) and model papers coated with starch (WSP) and methylcellulose (MC) using varying wet film thicknesses. Not all coated samples are shown in the micrographs below, as some appear to be too similar.

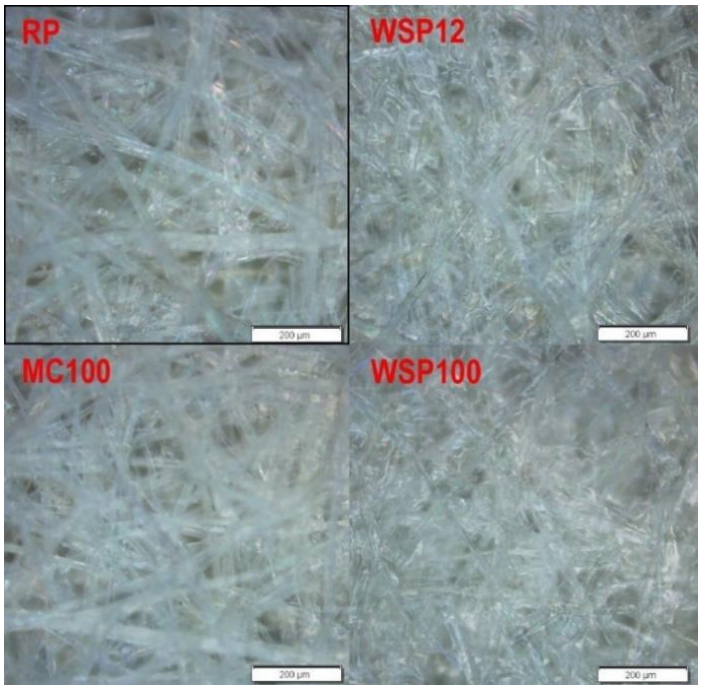

Figure 7 - Micrographs of the uncoated model paper (RP) and model paper coated with starch (WSP12, WSP100) and methylcellulose (MC100) at 100× magnification [273].

When observing the uncoated model paper (RP) and paper coated with a 100 μm thick methylcellulose coating (MC100), the fibres are clearly visible. Micrographs suggest that the dilute methylcellulose coating penetrates the paper's surface rather than forming a film, irrespective of the wet film thickness applied. However, it is important to note that the methylcellulose coating appears transparent, rendering it invisible in the micrographs. Micrographs also suggest that the starch film effectively fills most of the pores between the fibres, covering the paper's surface. Moreover, even when paper is coated with starch using a

wet film thickness of 12 μm (WSP12), the surface appears well covered and closed. This occurrence can be attributed to the strong film-forming ability of starches [51,280].

Phase I*: Evaluation of the monolayer coatings on the model paper's surface

SEM imaging conducted during this phase revealed coating imperfections that remained hidden under optical microscopy. **Figure 8** displays the surface of the model paper coated with buffered starch (S) using a wet film thickness of 24 μm. This particular coat served as the bottom layer of the proposed bilayer coating throughout this research. The starch layer is not entirely uniform, which is consistent with findings from the previous studies [281].

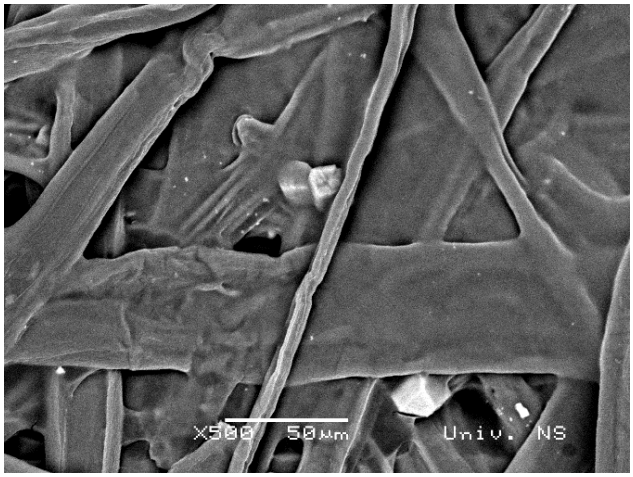

Figure 8 - SEM micrograph of the model paper coated with starch (S) at 500× magnification.

Phase II: Evaluation of the bilayer coatings on the printed model paper's surface

In the second stage, the model paper samples were first printed and then coated.

Figure 9 shows a micrograph of the uncoated model paper's surface. Consistent with previous observations, fibre direction is not visible, and the surface exhibits non-uniformity. Additionally, on the printed surface, a paper fibre network is evident, indicating non-uniform ink film formation. Based on the micrographs, none of the coatings seem to affect the visual appearance of the samples (**Figure 10, Figure 11)**. While certain changes in the visual appearance of the samples might be expected with coating applications, the starch and methylcellulose coatings cause minimal changes due to their transparency [278,282].

Visual assessment of the samples following accelerated UV ageing did not reveal changes indicative of degradation, even under higher magnifications. Therefore, the resulting micrographs are not presented here.

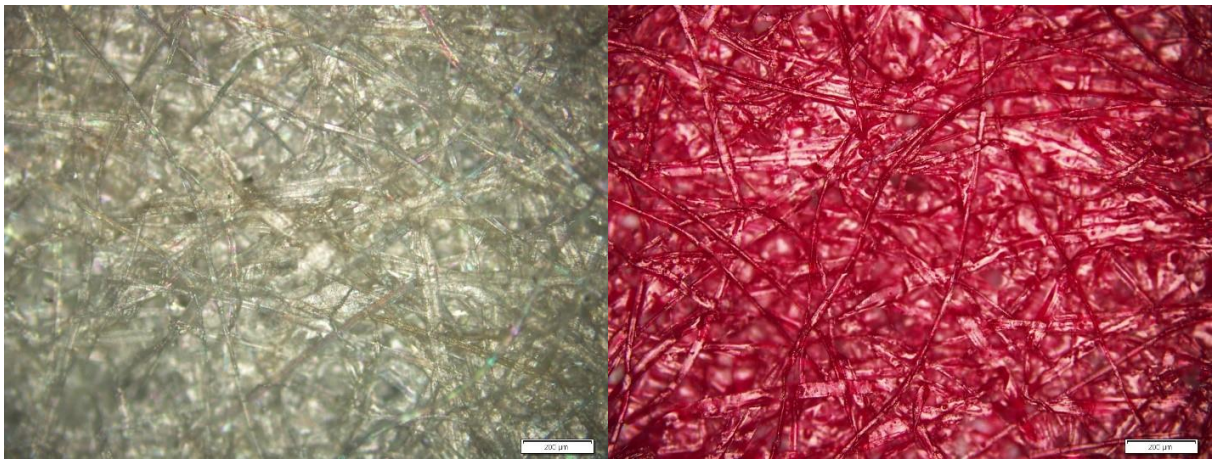

Figure 9 - Micrographs of the model paper's surface (left) and the printed model paper's surface (right) at 100× magnification [210].

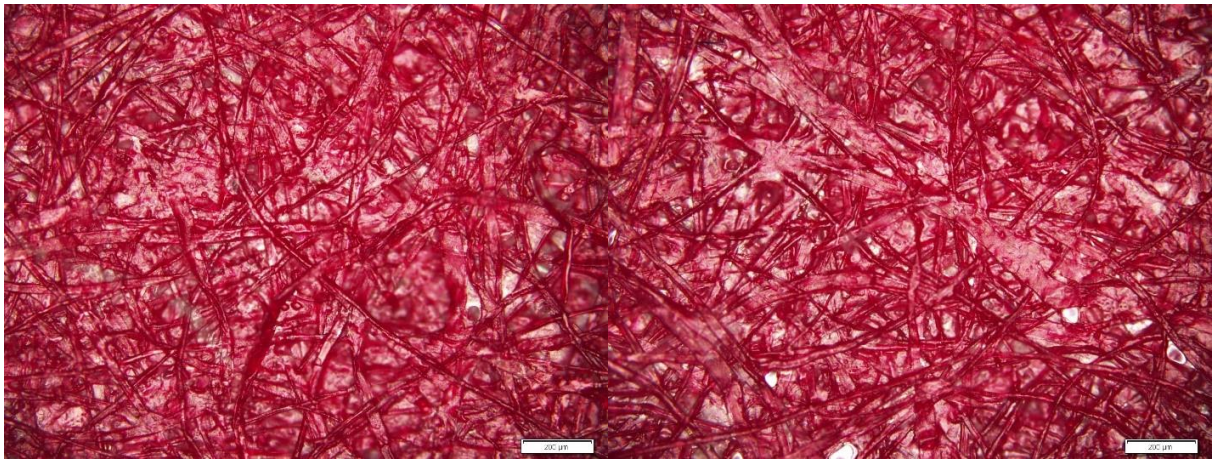

Figure 10 - Micrographs of the printed model paper's surface coated with starch (left) and the printed model paper's surface coated with starch and methylcellulose (right) [210].

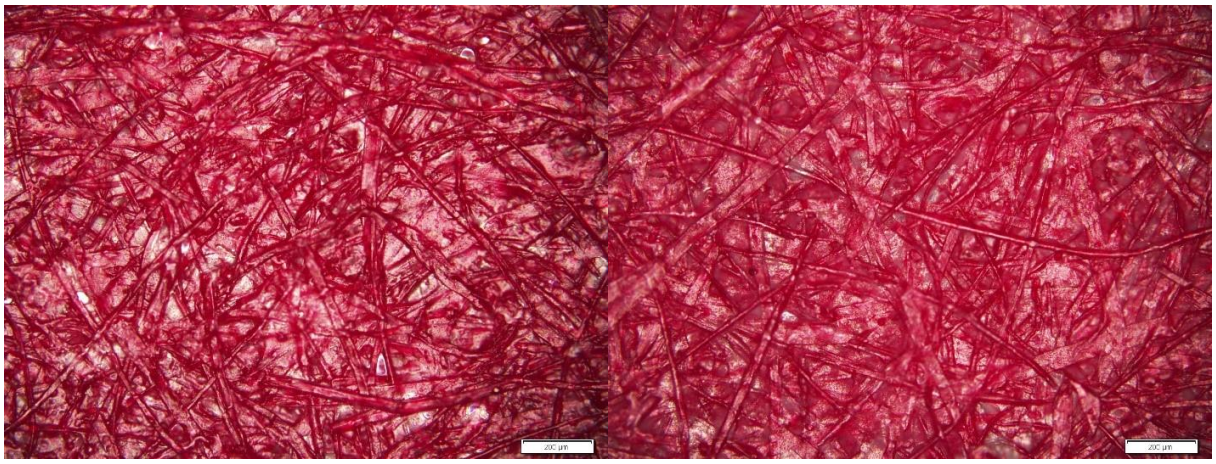

Figure 11 - Micrographs of the printed model paper's surface coated with the bilayer coating incorporating 0.2% TiO_2 *w/w* (left) and the printed model paper's surface coated with the bilayer coating incorporating 2% TiO_2 *w/w* (right) [210].

4.5. DISTRIBUTION OF TIO_2 NPS IN THE NANOCOMPOSITE FILM

Throughout this research, the model paper samples displayed non-linear behaviour. Such behaviour may result from both the substrate's heterogeneity and the non-uniform dispersion of (nano)particles in a colloidal solution.

The research, having previously established the heterogeneity of the model paper, will now assess the distribution of nanoparticles in the nanocomposite film.

Phase III*: Evaluation of the bilayer coatings on the model paper's surface

SEM-EDS analyses conducted during this stage aimed to assess the morphology and elemental composition of the nanocomposite films. For this purpose, samples coated with bilayer coatings incorporating 0.75% and 1% TiO_2 *w/w* were selected for examination.

Figure *12* and **Figure 13** display the SEM micrograph and elemental composition of the model paper's surface coated with the bilayer coating incorporating 0.75% TiO_2 *w/w* (T0.75). While elemental analysis confirms the presence of titanium (Ti), SEM micrographs reveal the relatively uniform distribution of TiO_2 NP aggregates in the nanocomposite film.

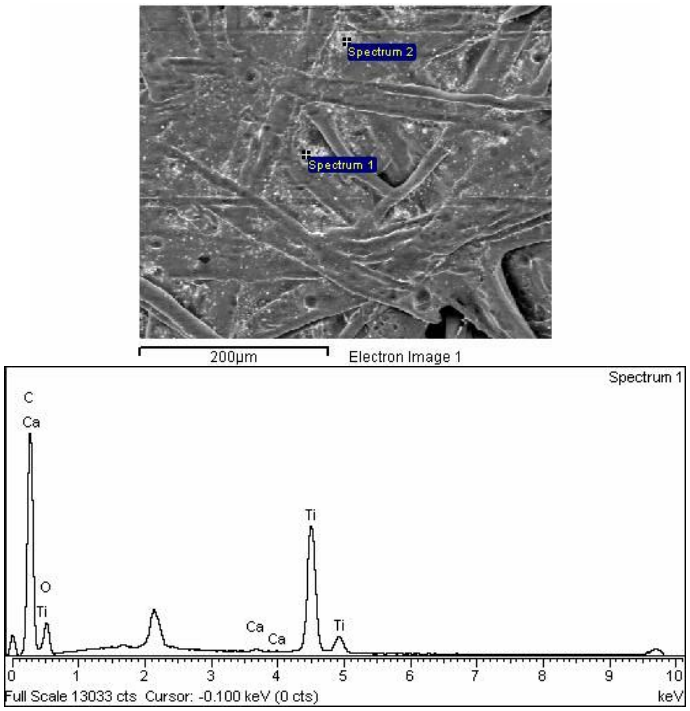

Figure 12 - SEM micrograph (above) and EDS surface elemental composition analysis of specific positions of T0.75 (below).

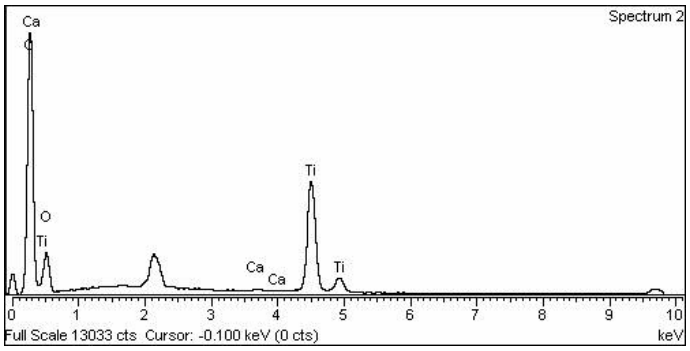

Figure 13 - EDS surface elemental composition analysis of specific positions of T0.75

The uniform dispersion of NPs in the polymer matrix is essential for ensuring the overall functionality of the protective coating [199]. Furthermore, adequate dispersion "increases the surface contact between the matrix and NPs" [283], promoting their physical interactions [283,284].

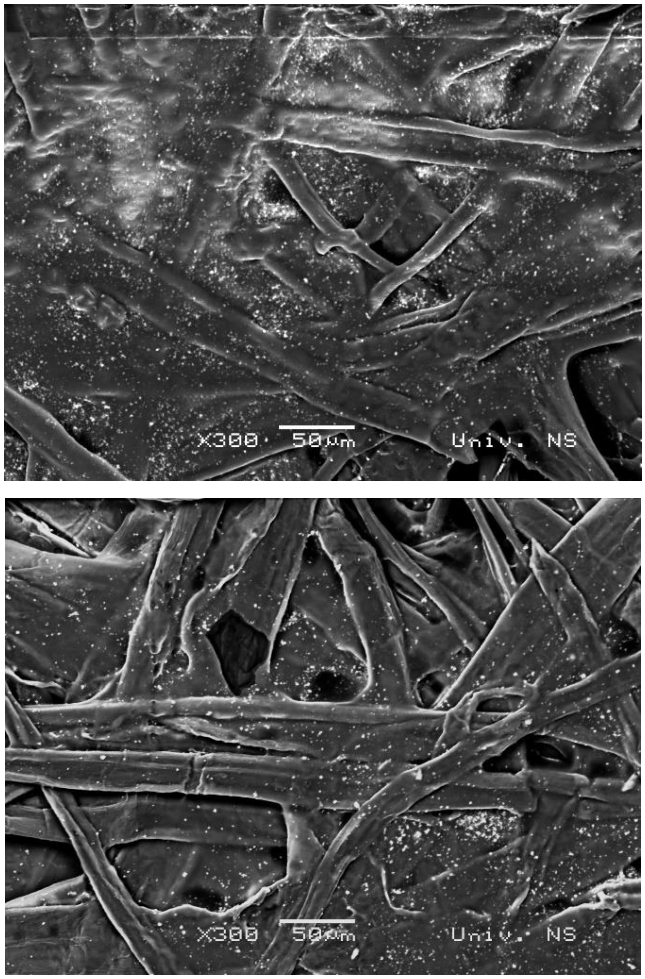

Figure 14 - SEM micrograph showing the distribution of TiO_2 NPs in the nanocomposite films on T0.75 (above) and T0.50 (below) at 300× magnification.

SEM micrographs shown in **Figure 14** and **Figure 15** reveal that the sizes and arrangements of aggregates are consistent for all three TiO_2 weight concentrations (0.5%, 0.75%, and 1%) used in ***Phase III****, therefore indicating uniform dispersion.

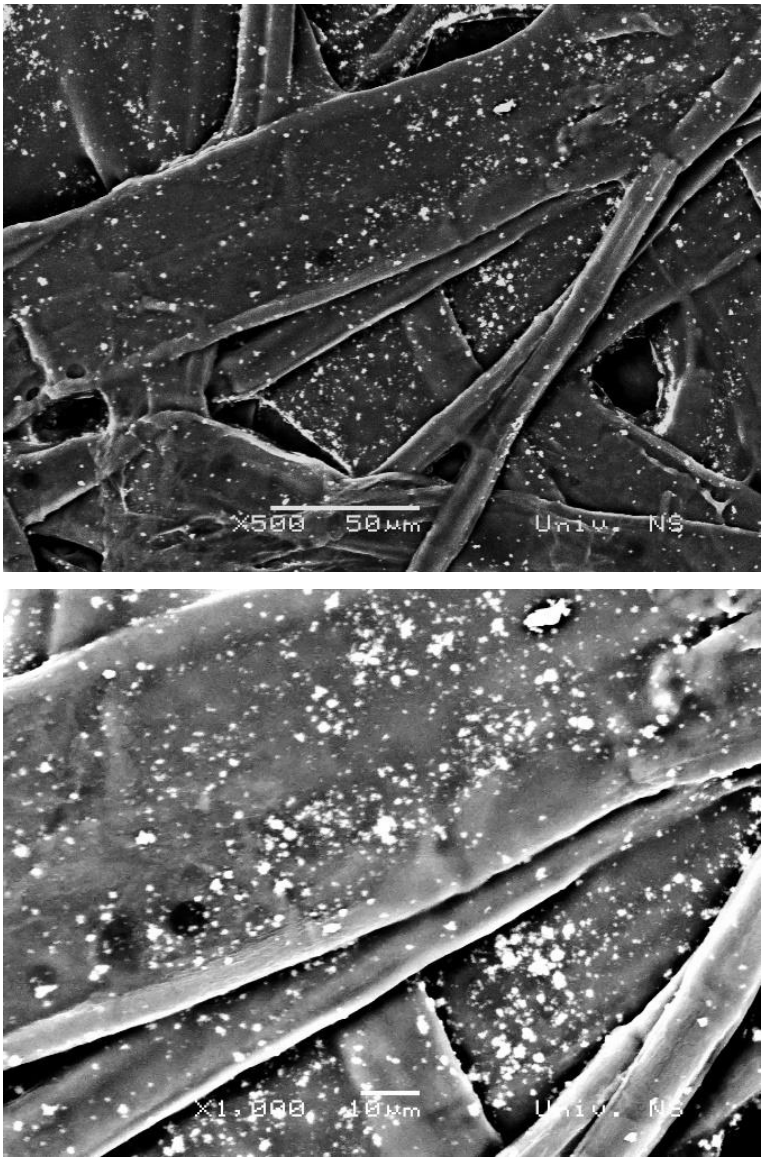

Figure 15 - SEM micrographs showing the distribution of TiO_2 NPs in the nanocomposite film on T1.00 at 500× (above) and 1000× (below) magnification.

4.6. SURFACE PROPERTIES OF THE SAMPLES

4.6.1. Contact angle and water droplet absorption time

Applying a polymeric coating is known to modify the surface properties of the paper sheet. In cases of increased wettability, fibre swelling and paper weakening may occur, which are considered undesirable outcomes that could contribute to the further deterioration of paper. Therefore, measurements of contact angle and water droplet absorption time were performed to evaluate how the application of coatings affected water-paper interaction.

Phase I: Evaluation of the monolayer coatings on the model paper's surface

As illustrated in **Figure 16**, prior to accelerated thermal ageing, the application of a methylcellulose coating increases the water contact angle of the model paper (RP). On the other hand, starch has lowered the water contact angle of the RP, making the surface more hydrophilic. Accelerated thermal ageing of the RP (**Figure 17**) results in an increase in the water contact angle ($\theta > 120°$), indicating the hydrophobic nature of the tested surface. Furthermore, ageing increases the contact angle of all coated samples, although the changes in samples coated with methylcellulose (MCs) are minimal.

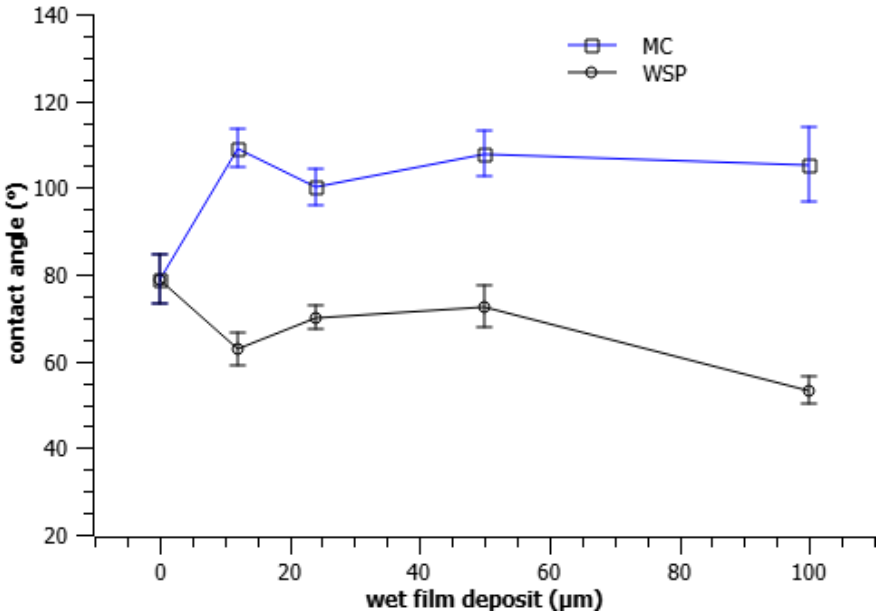

Figure 16 - Water contact angles (°) of the unaged samples [273].

In contrast with the unaged samples, the heat aged starch-coated samples (WSP) exhibit different wettability, depending on the amount of wet film applied. Namely, an increase in the wet film deposit results in a decrease in the contact angle on WSP-coated samples.

The changes in the wet film deposit of unaged samples do not seem to significantly influence the interaction between the coated model paper's surface and water. This can be explained by the formation of oxidation products, as confirmed by the FT-IR analysis (**Figure 33**).

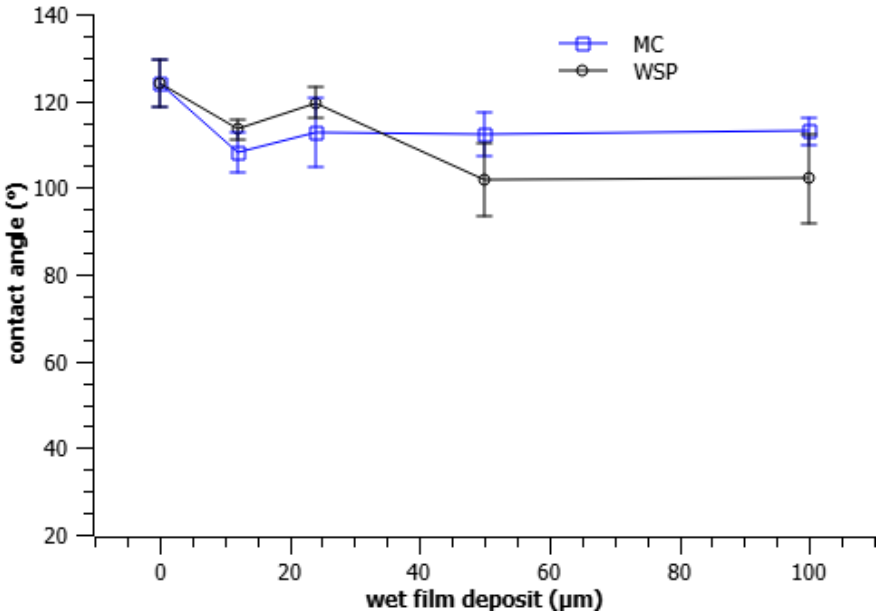

Figure 17 - Water contact angles (°) of the heat aged samples [273].

In addition to the determination of the water contact angle, the water droplet absorption was also assessed.

The results of the water droplet absorption measurements are presented in **Table 5.**

Table 5 - Water droplet absorption times (s) of samples.

Wet Film Deposit (µm)	Unaged		Heat aged	
	MC	WSP	MC	WSP
0	2.88 ± 0.39		76.54 ± 19.07	
12	3.71 ± 0.23	1.91 ± 0.27	25.47 ± 1.66	214.33 ± 16.43
24	3.50 ± 0.14	3.25 ± 0.29	25.53 ± 4.06	359.59 ± 25.96
50	3.97 ± 0.45	3.93 ± 0.45	15.34 ± 2.94	>720
100	4.94 ± 0.45	4.33 ± 0.45	17.39 ± 4.24	>720

The highest resistance to water droplet penetration was observed in the heat aged samples coated with starch (WSPs). Samples that contained the largest amounts of starch (50 μm and 100 μm) failed to complete the test in 12 minutes.

Importantly, it should be noted that accelerated thermal ageing may have contributed to the surface sealing, potentially impacting surface topology and, consequently, penetration.

The surface sealing could be attributed to the oxidation of cellulose, which is known to affect the hygroscopic properties of paper by inducing brittleness and reduced responsiveness to wetting [285].

Phase II: Evaluation of the bilayer coatings on the printed model paper's surface

Considering that the application of TiO_2 is recognized for significantly reducing contact angles and water droplet absorption times of materials [286], both properties were assessed before and after the introduction of TiO_2, as well as before and after undergoing accelerated UV ageing. The results of the contact angle measurements **(Figure 18, Figure 19**) show that each of the coatings has decreased the contact angle of the printed and non-printed model paper's surfaces.

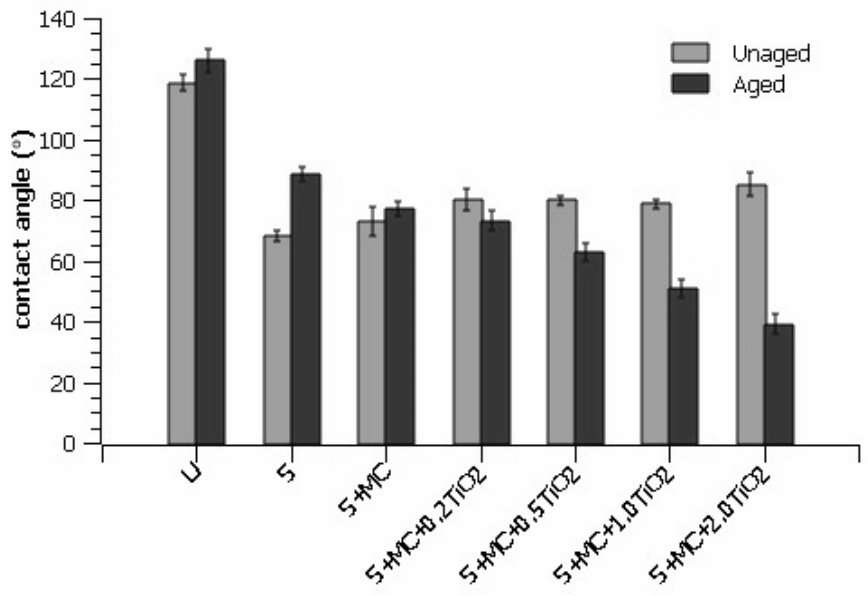

Figure 18 - Water contact angles (°) of the printed samples [210].

By increasing the TiO_2 NP weight concentration, the contact angle on the paper's surface slightly increases prior to accelerated UV ageing. This result can be explained by the decrease in roughness (**Figure 23**, right).

Although the coatings were not visible in the presented micrographs (**Figure 10**, **Figure 11**), the contact angles of both the printed model paper's surface and the non-printed model paper's surface were similar, indicating that the coatings have enabled proper coverage of the surface. The contact angles of paper coated with TiO_2 nanocomposites have further decreased after accelerated UV ageing. On the other hand, the contact angles of samples coated with starch and methylcellulose (S+MC) have increased.

The decrease in contact angles becomes more pronounced as the TiO_2 NP weight concentration increases, as highlighted by previous research involving anatase TiO_2 [287]. The increase in hydrophilicity of uncoated model paper samples can be attributed to the increase in hydroxyl groups [288].

By comparing the results of contact angle measurements for paper coated with starch from both phases (***Phase I*** and ***Phase II***), it appears that accelerated thermal ageing (**Figure 16**, **Figure 17**) has affected the contact angles of the paper more than accelerated UV ageing (**Figure 19**).

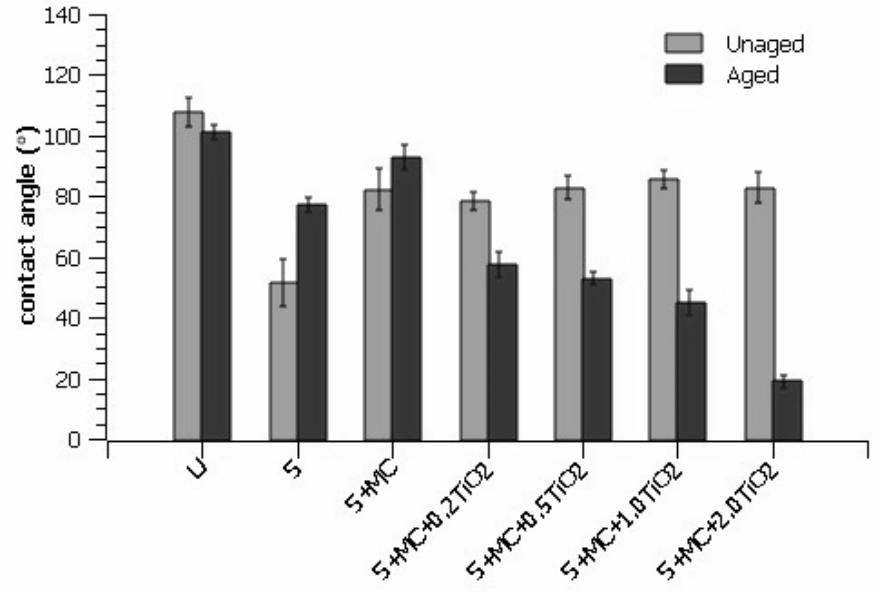

Figure 19 - Water contact angles (°) of the non-printed samples [210].

As shown in **Figure 20** and **Figure 21,** accelerated UV ageing has increased the water droplet absorption time of samples coated with starch (S) and starch and methylcellulose (S+MC). The reduction in the water droplet absorption time of the coated samples incorporating TiO_2 NPs can be explained by the photocatalytic activity of TiO_2 [289], where resulting radicals cause the degradation of the coatings by creating microcracks within their surface.

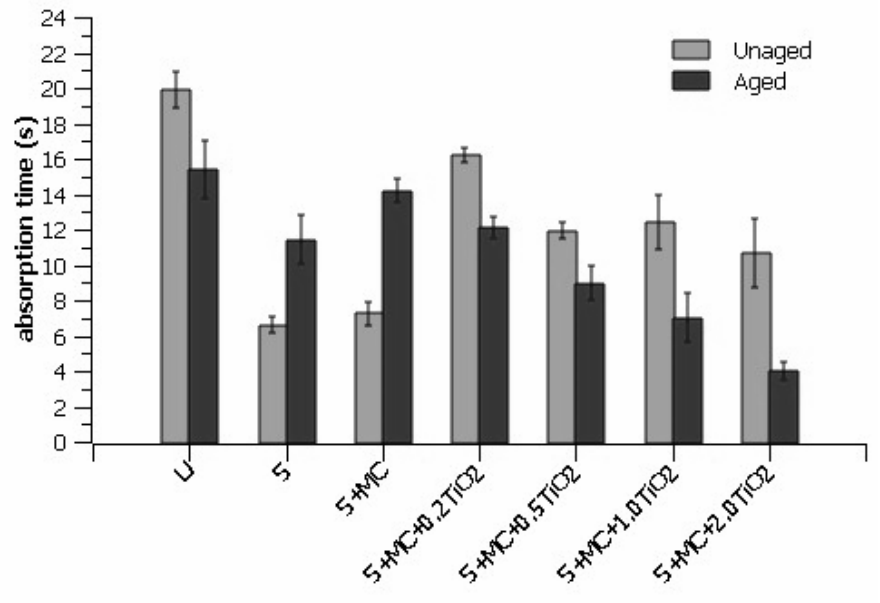

Figure 20 - Water droplet absorption times (s) of the printed samples [210].

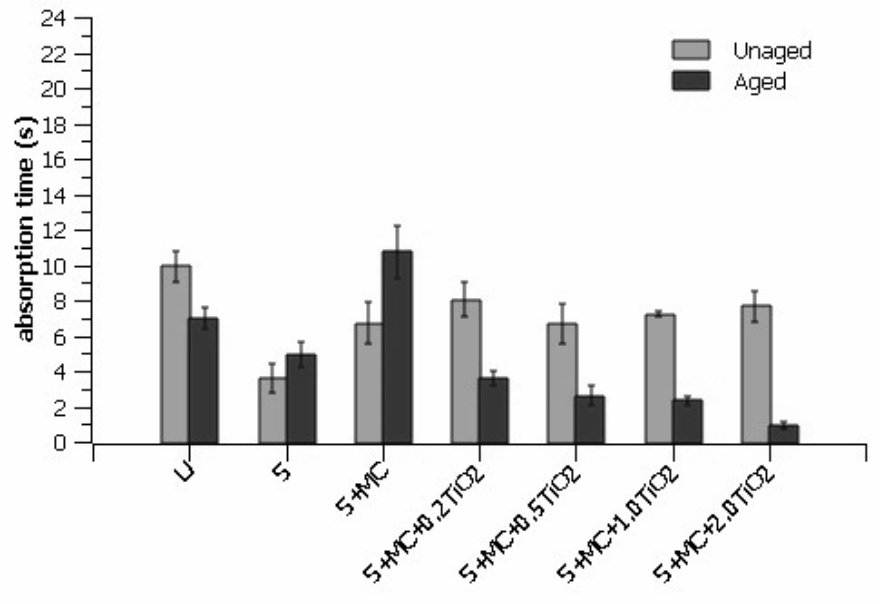

Figure 21 - Water droplet absorption times (s) of the non-printed samples [210].

4.6.2. Average surface roughness

Phase II: Evaluation of the bilayer coatings on the printed model paper's surface

The surface roughness measurements, as shown in **Figure 22** and **Figure 23**, exhibit high SD values, probably due to the non-uniformity of the analysed surfaces. The other surface characterization methods were presumably not affected by this issue due to the different

measuring resolution (the diamond tip of the perthometer measures 5 μm in diameter, while water droplets in the contact angle tests and the device's openings in optical characterization are given in milimeters). The surface roughness of the model paper has been reduced through the application of coatings, especially those incorporating TiO_2 NPs. Accelerated UV ageing has increased the average surface roughness of all coated samples. This finding could be attributed to the formation of microcracks on the coating's surface and corresponds with the findings obtained from contact angle and water droplet absorption time measurements on the model paper (**Figure 19**, **Figure 21**).

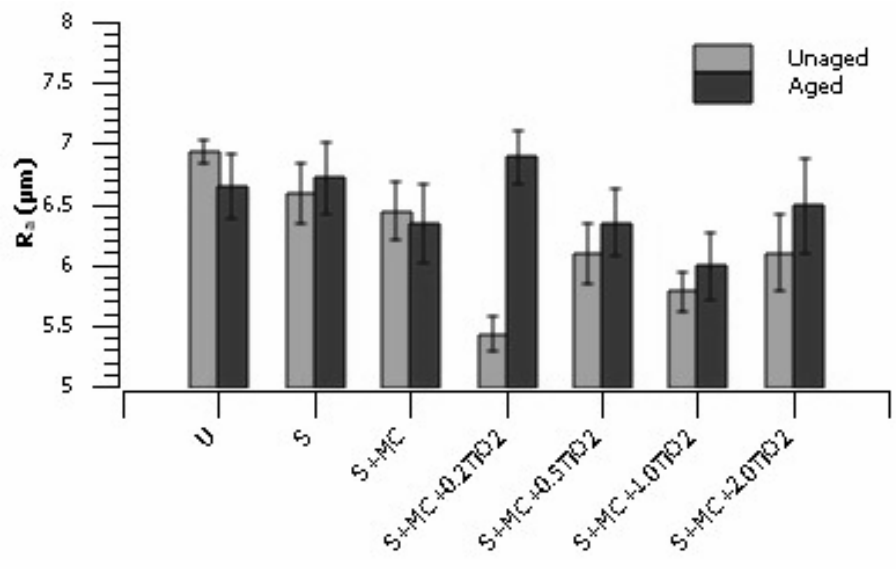

Figure 22 – Average roughness (μm) of the printed model paper's surface [210]

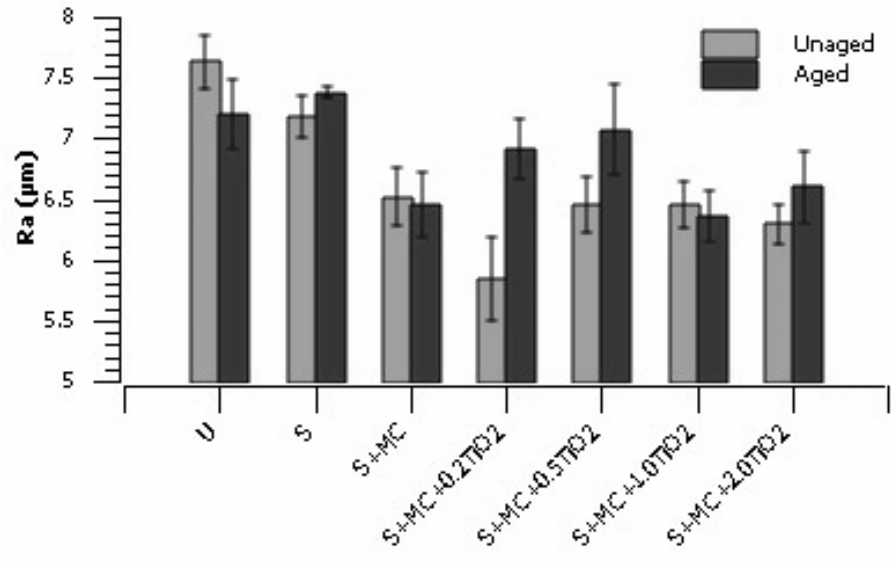

Figure 23 - Average roughness (μm) of the paper's surface [210].

4.7. OPTICAL PROPERTIES OF THE SAMPLES

Undesired changes in the optical properties of paper may result from ageing or conservation-restoration treatments. Most commonly, changes in optical properties reflect changes that occur at the molecular level. Within this context, the applied coatings are expected to provide transparent and colourless films that would not change significantly after accelerated ageing.

4.7.1. Total colour difference

Phase I: Evaluation of the monolayer coatings on the model paper's surface

The results presented in **Table 6** show that the investigated monolayer coatings (starch, methylcellulose) do not significantly affect the colour of the model paper (RP), which is consistent with previous studies [42,189]. The influence of the different wet film thicknesses on the colour of the model paper's surface is nearly insignificant. To determine how accelerated thermal ageing had affected the samples, the colour difference between the unaged and the aged samples was calculated.

The results shown in **Table 7** indicate that most coatings have effectively slowed down colour changes resulting from thermal ageing. In all aged samples, the observed colour changes were barely noticeable by the human eye ($\Delta E_{ab} < 3$) [247].

Table 6 - Total colour differences between the uncoated and the coated model paper.

Wet Film Deposit (µm)	MC	WSP
0	-	-
12	0.78	0.94
24	0.67	0.37
50	0.86	0.48
100	1.10	0.89

Table 7 - Total colour differences between the unaged and the heat aged samples.

Wet Film Deposit (µm)	MC	WSP
0	2.20	2.20
12	1.46	0.52
24	2.07	2.70
50	1.21	1.61
100	1.00	1.47

Phase II: Evaluation of the bilayer coatings on the printed model paper's surface

The colour measurements were conducted before and after each phase presented in the experimental section (paper preparation, printing, coating, and accelerated UV ageing).

In contrast with the micrographs presented earlier (**Figure 10, Figure 11**), these results (**Figure 24**) indicate that the coatings have indeed altered the colour of the prints. Notably, the starch coatings (S) and coatings incorporating 0.2% TiO_2 *w/w* (S+MC+0.2TiO_2) have produced the least noticeable changes. Additionally, an increase in the weight concentration of TiO_2 NPs in the methylcellulose coating led to a higher total colour difference. This behaviour stems from the fact that TiO_2 is also used as a white pigment [211].

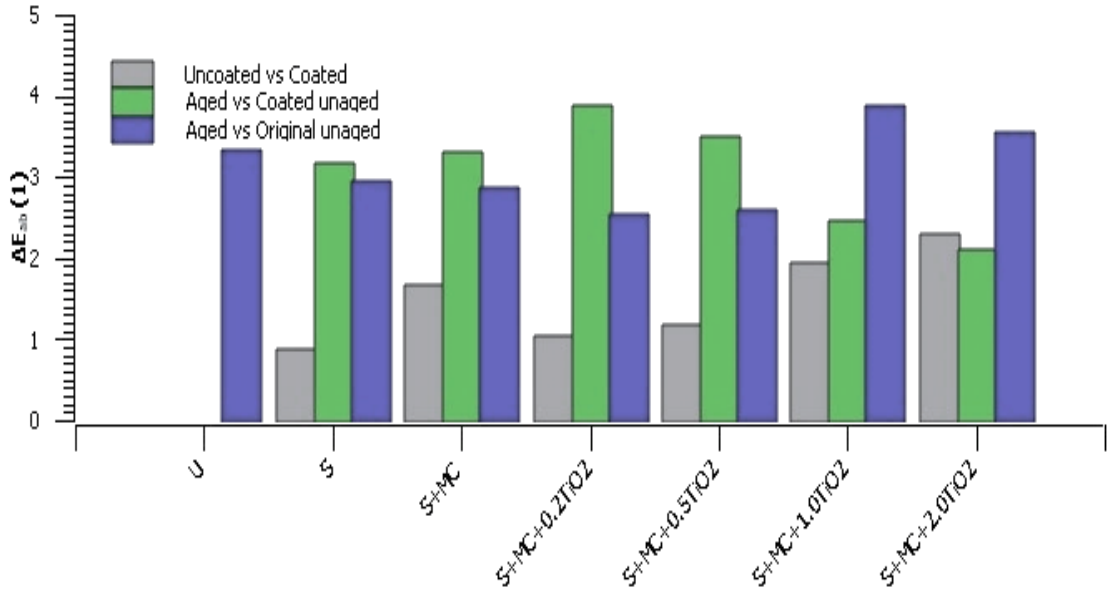

Figure 24 - Total colour differences between the unaged and the UV aged samples [210].

The influence of accelerated UV ageing was determined by observing colour changes between the model paper (U) and coated samples. From those samples, it can be observed that an increase in the TiO_2 NP weight concentration results in a decreased total colour difference in the aged samples, which could be attributed to the TiO_2's absorption of UV energy [290].
However, by comparing the results obtained from the uncoated model paper and the UV aged samples (both uncoated and coated), it becomes clear that the printed model paper's surface was least affected by coatings incorporating 0.2% (0.2TiO_2) and 0.5% (0.5TiO_2) TiO_2 NPs. These results are consistent with previous studies in which coatings with similarly low TiO_2 concentrations were able to slow down the colour change of the treated paper [19].

Phase III*: Evaluation of the bilayer coatings on the model paper's surface

Colorimetric measurements (**Figure 25**) reveal that accelerated thermal ageing affected the colour of all samples, with the samples coated with starch (S), starch and methylcellulose (S+MC), and the bilayer coating incorporating 0.5% TiO_2 *w/w* (T0.50) exhibiting comparatively lesser changes. The original colour of the paper was preserved the most (ΔE_{ab} < 3) by starch coating alone, which is consistent with previous studies on starch behaviour during ageing [42]. An increase in TiO_2 concentration resulted in a higher total colour difference after accelerated thermal ageing. Similar to the author's previous research [210], the colour properties were most effectively preserved in a sample with a lower TiO_2 concentration (T0.50).

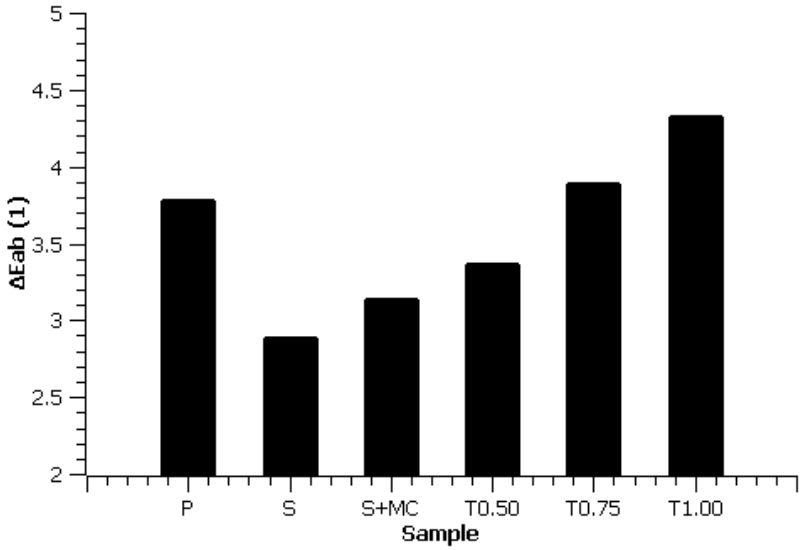

Figure 25 - Total colour difference between the unaged samples and the heat aged samples.

As a result of accelerated thermal ageing, the *b** colour component exhibits an increase in the yellow colouration, while the *L** and *a** values have not changed significantly (**Table 8**).

Table 8 - CIE colour components of the samples before and after accelerated thermal ageing.

	Unaged			Aged		
Sample	***L****	***a****	***b****	***L****	***a****	***b****
P	89.60±0.46	1.66±0.15	12.05±0.53	88.48±0.15	2.31±0.13	15.60±0.32
S	89.11±0.45	1.77±0.21	12.87±0.62	88.40±0.72	2.08±0.20	15.65±0.53
S+MC	88.97±0.43	1.69±0.18	12.91±0.60	88.48±0.48	2.09±0.24	15.98±0.55
T0.50	88.86±0.59	1.85±0.23	13.07±0.45	88.19±0.48	2.29±0.24	16.33±0.46
T0.75	89.35±0.31	1.65±0.17	12.98±0.55	88.61±0.47	2.24±0.31	16.75±0.61
T1.00	89.59±0.36	1.54±0.17	12.67±0.51	88.77±0.39	2.17±0.23	16.86±0.49

4.7.2. Yellowness

Yellowness of paper is an undesirable effect that can result from heat exposure [102,115].

Phase I: Evaluation of the monolayer coatings on the model paper's surface

As demonstrated in **Table 9**, the yellowness of the coated paper is nearly unaffected by accelerated thermal ageing. Nonetheless, ageing has led to an increase in the yellowness of all samples, a change attributed to oxidation products, as detected through FT-IR analysis (**Figure 34 – Figure 38**).

Table 9 - Yellowness of the samples before and after accelerated thermal ageing

Wet Film Deposit (µm)	Unaged		Heat aged	
	MC	WSP	MC	WSP
0	25.78 ± 0.56		28.12 ± 0.51	
12	26.10 ± 0.47	26.48 ± 0.97	28.38 ± 0.54	27.00 ± 1.63
24	26.42 ± 0.62	25.04 ± 0.74	28.94 ± 0.64	28.28 ± 0.39
50	26.39 ± 0.53	25.76 ± 0.81	27.95 ± 0.79	28.05 ± 0.61
100	26.96 ± 0.59	26.28 ± 0.35	27.89 ± 0.64	28.72 ± 0.63

4.7.3. Opacity

The opacity of paper is associated with the amount of air it contains, specifically the arrangement of numerous small air pores with a large total surface area [291]. Higher levels of opacity result from an increased quantity of light scattered from the surfaces of numerous small pores [292].

Phase I: Evaluation of the monolayer coatings on the model paper's surface

The results obtained from measuring the opacity of samples (**Table 10**) indicate that the coatings do not drastically influence the opacity of the model paper (denominated as „0“ in the table). On the other hand, accelerated thermal ageing leads to higher porosity and opacity in paper. This results from a larger number of small pores resulting from the drying out of paper due to the elevated temperature in the accelerated thermal ageing process, as fewer hydrogen bonds are formed between the cellulose fibres [293].

The alterations in the FT-IR spectra within the 1307–1340 cm^{-1} range confirm the rearrangement in hydrogen bonding (**Figure 34 – Figure 38).**

Due to the heterogeneity of both the model paper and coated samples, the opacity changes that may have resulted from accelerated thermal ageing were not detected. This is corroborated by the high SD values of all measurement sets.

Table 10 - Opacity (%) of the samples before and after accelerated thermal ageing.

Wet film deposit (µm)	Unaged		Heat Aged	
	MC	WSP	MC	WSP
0	81.06 ± 1.69		84.62 ± 1.87	
12	79.49 ± 1.16	79.73 ± 3.16	81.58 ± 1.46	80.84 ± 2.52
24	80.26 ± 1.98	76.61 ± 1.92	83.18 ± 1.27	81.98 ± 2.91
50	81.45 ± 2.38	78.44 ± 2.43	79.22 ± 2.33	80.82 ± 3.30
100	81.72 ± 1.89	80.63 ± 2.85	79.43 ± 2.16	81.05 ± 3.40

4.7.4. Gloss

An excessively shiny surface is an undesirable outcome of the curative treatment, occurring due to an over-application of the coating. The reduction of gloss, on the other hand, may indicate degradation.

Phase I: Evaluation of the monolayer coatings on the model paper's surface

The results of the gloss measurements are shown in **Table 11**. The initial gloss value of the model paper (denominated as „0" in the table) is low and nearly unaffected by the dilute methylcellulose coating. The increase in the wet film deposit raises the gloss value of all samples coated with starch (WSPs). This can also be observed in the micrographs of the coating films presented earlier (**Figure 7**).

Table 11 - Gloss value (GU) of the samples before and after accelerated thermal ageing.

Wet Film Deposit (µm)	Unaged		Heat aged	
	MC	WSP	MC	WSP
0	4.21 ± 0.08		4.18 ± 0.09	
12	4.23 ± 0.09	4.56 ± 0.09	4.23 ± 0.08	4.60 ± 0.11
24	4.18 ± 0.07	4.57 ± 0.11	4.23 ± 0.05	4.58 ± 0.07
50	4.19 ± 0.09	4.81 ± 0.09	4.18 ± 0.10	4.75 ± 0.05
100	4.20 ± 0.07	5.17 ± 0.11	4.17 ± 0.05	5.15 ± 0.11

The gloss value is increased by nearly a whole 1 GU in WSP100 (model paper coated with starch using a wet film coating thickness of 100 μm). The accelerated thermal ageing of the samples has not affected the gloss of the samples significantly.

Phase III*: Evaluation of the bilayer coatings on the model paper's surface

The results shown in **Figure 26** indicate that the gloss value decreases with the addition of TiO_2 NPs. The decrease seems more pronounced with an increased TiO_2 NP concentration.

On the other hand, accelerated thermal ageing did not affect the gloss value of the samples significantly. The gloss value of samples has slightly decreased, probably due to oxidation [114], as detected through FT-IR measurements (**Figure *41*** – **Figure *46***).

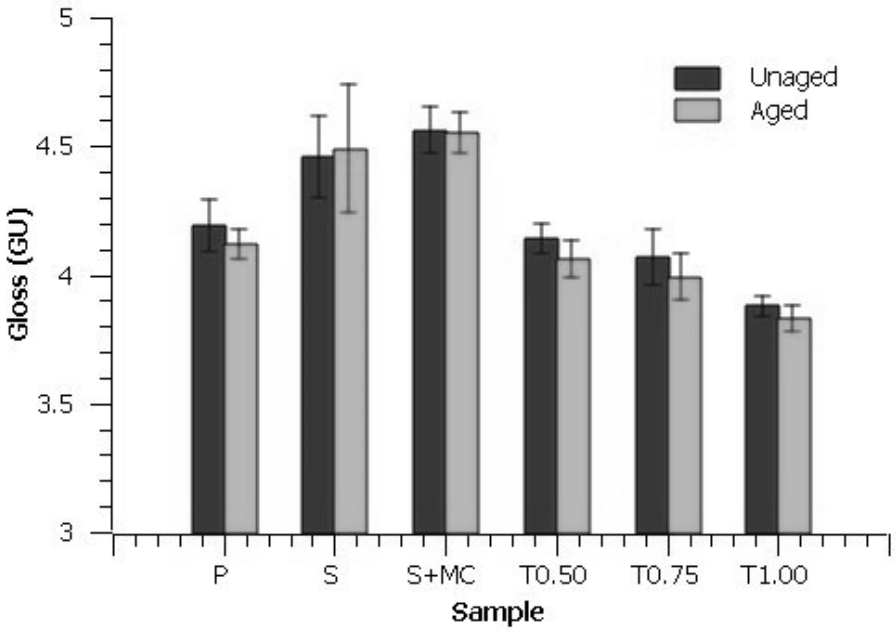

Figure 26 - Gloss value (GU) of the samples before and after accelerated thermal ageing.

The decrease in gloss observed in the heat aged samples incorporating TiO_2 NPs could be attributed to the formation of agglomerates [294], as observed through SEM imaging (**Figure 14**, **Figure 15**).

4.7.5. Fluorescence intensity

Phase II: Evaluation of the bilayer coatings on the printed model paper's surface

The fluorescence intensity measurements have confirmed the absence of a response in the visible part of the spectrum. This result indicates that components within the paper structure do not exhibit fluorescent behaviour.

Figure 27 and **Figure 28** show the intensities of the reflected light at a wavelength of 365 nm. Uncoated model paper displayed the highest degree of dispersion, aligning with expectations due to the heterogeneity of the model paper's surface. UV exposure led to surface-layer degradation, resulting in increased light scattering on the fibres.

The starch coating has increased light absorption in the UV range. After subjecting model paper coated with starch (S) to accelerated UV ageing, a significant increase in reflected light was observed, suggesting that degradation of the coating has occurred. On the other hand, the addition of a methylcellulose layer (S+MC) reduces paper reflectance in the UV spectral range. A similar increase in reflectance was observed in the aged model paper (U).

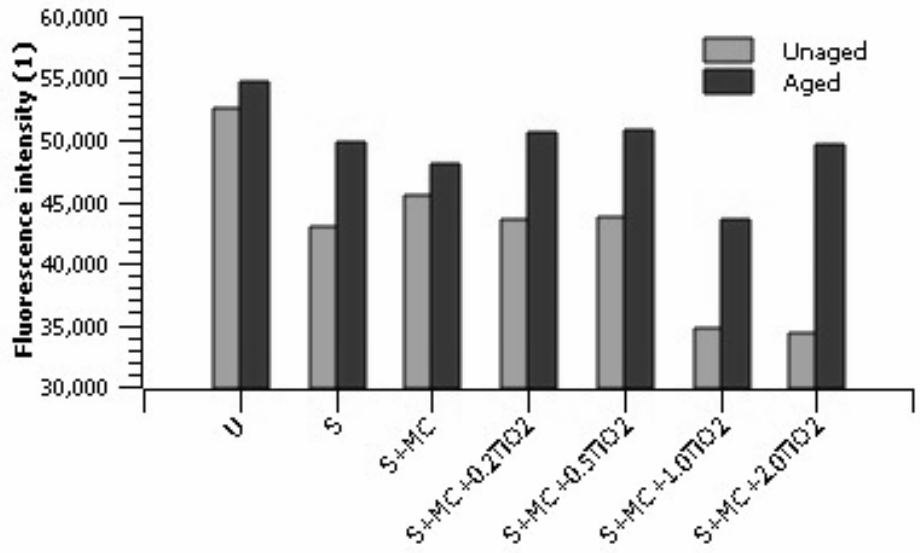

Figure 27 - Fluorescence intensity of the model paper's surface [210].

It is also important to note that the size of TiO_2 NPs in the nanocomposite film affects the absorption of UV radiation. On the other hand, the addition of TiO_2 also affects the degree of UV reflection [295].

Previous research has shown that TiO_2 NPs strongly absorb UV radiation in the 330–370 nm range [296], and increasing the TiO_2 weight concentration enhances UV absorption, thereby reducing reflectance from the sample.

Interestingly, there was no significant difference in the reflectance between samples that incorporate 0.2% and 0.5% TiO_2 (S+MC+0.2TiO_2, S+MC+0.5TiO_2). However, an increase in the TiO_2 weight concentration (1% TiO_2) significantly reduces reflectance. The further increase in the TiO_2 weight concentration reduces reflectance levels to an infinitesimal amount.

After exposure to UV radiation, the bilayer coating incorporating 1% TiO_2 *w/w* (S+MC+1.0TiO_2) proved to be the most promising, indicating the satisfactory filling of the spaces between the fibres, whose structure was not significantly compromised despite the surface layer coating cracking. By introducing an ink layer, absorption is increased. With the application of starch or starch (S) and methylcellulose (S+MC), reflectance at 365 nm increases. With the addition of TiO_2, reflectance is expected to decrease due to the absorption characteristics of TiO_2 NPs in the UV spectral region. An increase from 0.5% to 2% TiO_2 *w/w* results in a slight jump in reflection. This could have resulted from the fact that ink, starch, methylcellulose, and TiO_2 NPs have significantly filled the spaces between the fibres, resulting in the coating's heterogeneity and enhancing the light scattering.

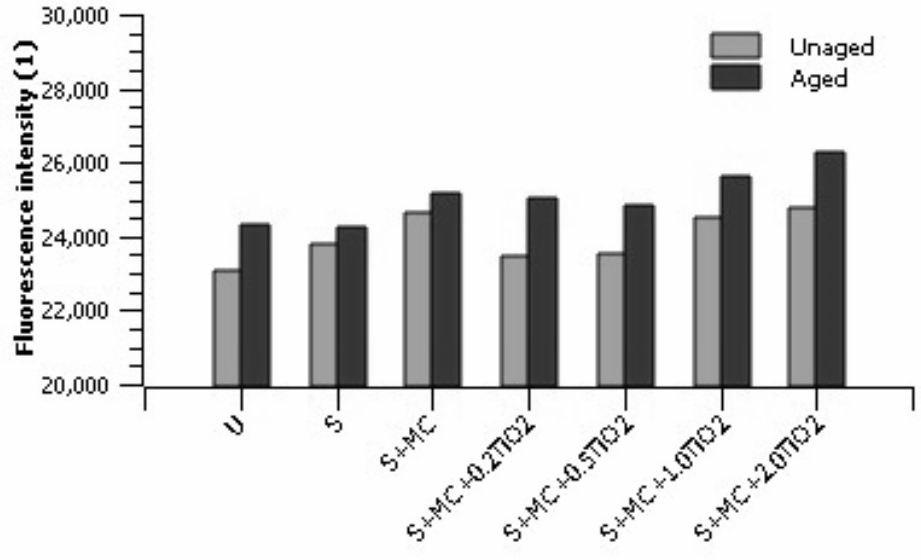

Figure 28 - Fluorescence intensity of the printed model paper's surface [210].

4.8. MECHANICAL PROPERTIES OF THE SAMPLES

Phase III: Evaluation of the bilayer coatings on the model paper's surface

Due to the heterogeneous structure of handmade paper, mechanical properties have provided only overall insights into the coating effects before and after accelerated thermal ageing.

4.8.1. Tensile force

Figure 29 displays the results of the tensile force measurements. All coatings have increased the tensile force of the model paper, likely as a result of hydrogen bonding between the coatings and cellulose fibres. The highest values of tensile force were provided by bilayer coatings incorporating 0.5% and 0.75% TiO_2 *w/w* (T0.50 and T0.75). Lower values of tensile strength were obtained from the samples with the highest TiO_2 weight concentration (1% TiO_2), which can be attributed to the agglomeration of NPs or their poor distribution within the nanocomposite film, as suggested by previous studies [297].

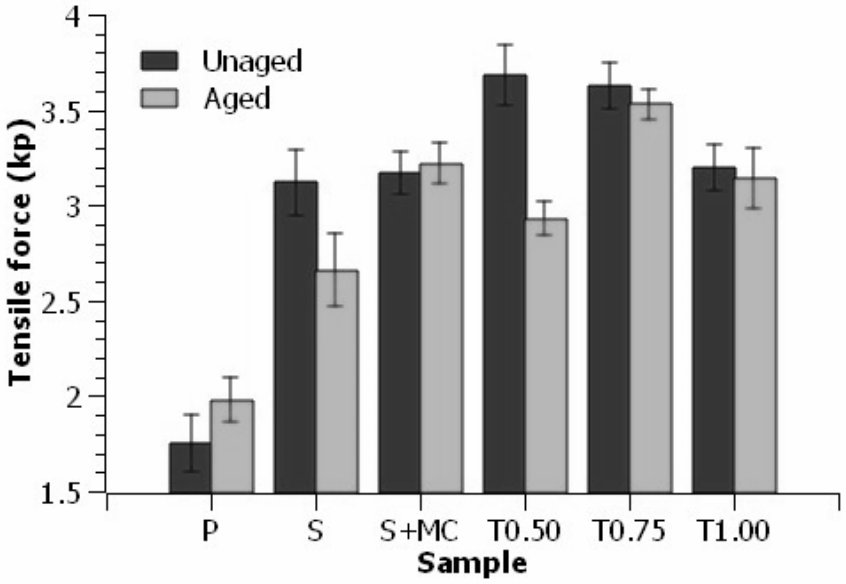

Figure 29 - Tensile force (kp) of the samples before and after accelerated thermal ageing [274].

Degradation due to heat exposure typically results in a loss of strength in paper [298], although tensile strength may not initially be affected as much as the other properties (i.e., folding endurance) [102].

Following accelerated thermal ageing, the tensile force decreases in most samples. However, both the uncoated model paper (P) and paper coated with starch and methylcellulose (S+MC) seem to exhibit a slight increase. The unusual result could be attributed to the large SD values resulting from the heterogeneity of the model paper. The most significant decrease in tensile force after accelerated thermal ageing is observed in model paper coated with starch (S) and model paper coated with the bilayer coating incorporating 0.5% TiO_2 *w/w* (T0.50). For other samples, the change in tensile force is less pronounced.

4.8.2. Bursting strength

Contrary to the tensile force measurements (**Figure 29**), the bursting strength decreases with the application of the coatings (**Figure 30**). The decrease follows an almost linear pattern, becoming more pronounced with the addition of a methylcellulose layer and with an increasing weight concentration of nano-TiO_2 within methylcellulose.

Following accelerated thermal ageing, the bursting strength decreases in all samples. The decrease in bursting strength may be associated with crosslinking resulting from elevated temperatures [5].

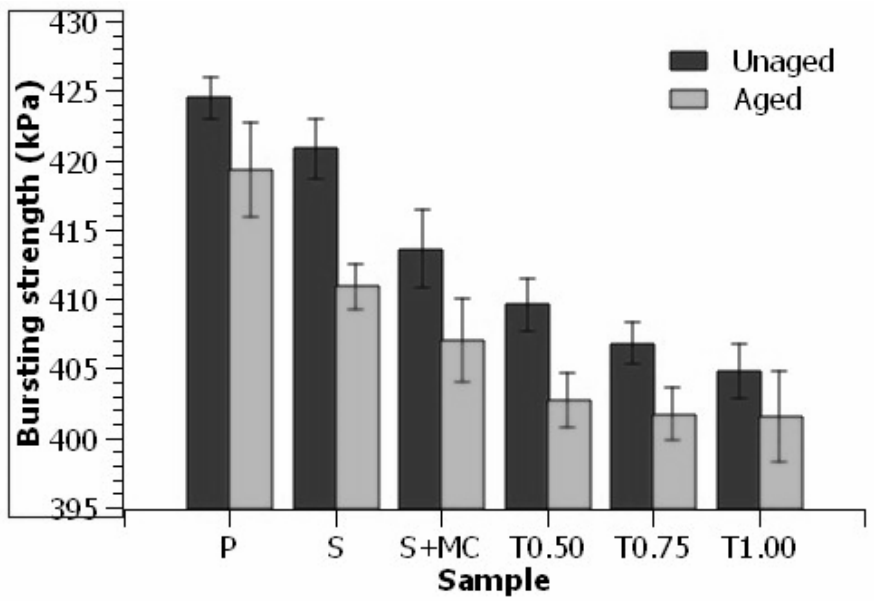

Figure 30 - Bursting strength (kPa) of the samples before and after accelerated thermal ageing [274].

4.8.3. Taber stiffness

The application of a polymer coating is known to increase the stiffness of the paper sheet [50]. The excessive coating application can also make paper less flexible or prone to cracking, which can lead to the loss of material.

The results presented in **Figure 31** confirm that the stiffness of the coated samples is higher than that of the uncoated ones (P). The increase in stiffness for most samples is moderate. Accelerated thermal ageing results in a decrease in stiffness, but this decrease is not as significant due to high SD values. The high SD values can be attributed to the sensitivity of the testing unit and the heterogeneous structure of handmade paper.

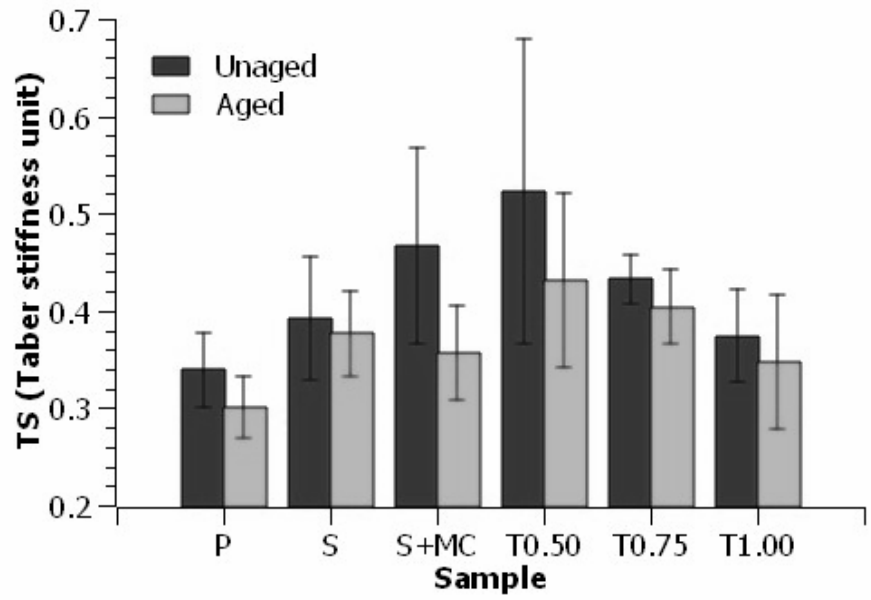

Figure 31 - Taber stiffness (TSU) of the samples before and after accelerated thermal ageing [274].

4.8.4. Short-span compression (SCT)

The loss of paper's stability as a result of degradation can manifest itself not only through strength reduction or increased stiffness but also through increased brittleness [22]. However, while brittle materials easily break under one type of force (i.e., tensile force), they can withstand other types of forces (i.e., compression) [231].

The results presented in **Figure 32** show an increase in short-span compression as a result of coatings' application. Notably, there are minimal differences observed among the unaged coated samples. The introduction of nano-TiO_2 into the methylcellulose results in a reduction of short-span compression, whereas an increase in the nano-TiO_2 weight ratio leads to its enhancement. Previous studies have addressed the difficulties in accurately capturing the mechanical response in compression strength measurements, attributing the complexities to the physical characteristics of paper [299].

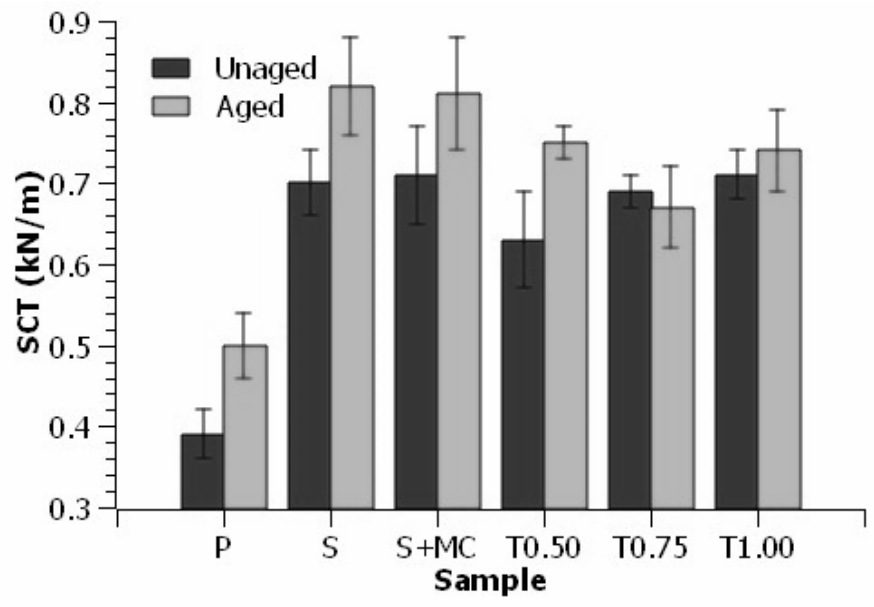

Figure 32- Short-span compression (kN/m) of the samples before and after accelerated thermal ageing [274].

4.9. CHEMICAL PROPERTIES OF THE SAMPLES

The following spectroscopic analyses are mainly concentrated on the most significant cellulose bands in order to characterize the samples and investigate the state of degradation of cellulose following accelerated ageing (thermal and UV). The degradation of paper is commonly monitored by observing regions between 1800–1400 cm^{-1}. Within this range, "carbonyl vibrations occur at different degrees of freedom" [2].

* As the figures from ***Phase I*** were previously published by the author [273], the FT-IR spectra also show another material (i.e., cellulose nanocrystals, CNCs) used in preliminary research. These results should be disregarded.

Phase I: Evaluation of the monolayer coatings on the model paper's surface

Figure 33 shows the FT-IR spectra of the uncoated and coated model paper.

The FT-IR spectra of the model paper are similar to those of other Japanese papers [300,301].

Bands at 1030 cm^{-1}, 1050 cm^{-1}, and 1170–1150 cm^{-1} are characteristic for cellulose [302]. There are also other strong bands of cellulose: 1159 cm^{-1} (anti-symmetric bridge stretching of C–O–C groups), 1105 cm^{-1} and 1024 cm^{-1} (C–O stretching in cellulose and hemicellulose molecules). The most pronounced band in the spectrum, observed at 1024 cm^{-1}, is accompanied by two characteristic peaks at 1051 cm^{-1} and 981 cm^{-1} [301].

The vibrational band at 893 cm^{-1}, assigned to C–O–C stretching at β-(1,4)-glycosidic linkages [303], is known as the "amorphous" absorption band, while the vibrational band around 1429 cm^{-1}, assigned to a symmetric CH_2 bending vibration, is known as the "crystallinity" band [301,304]. These characteristic vibrational bands are observed in both the uncoated model paper and in the model paper coated with methylcellulose (MCs), while samples coated with starch (WSPs) exhibit slightly different vibrational bands, although the vibrational bands of cellulose (paper) can also be detected, especially in the fingerprint region.

A vibrational band observed around 1639 ± 1 cm^{-1} is assigned to the bending vibration of water molecules (i.e., adsorbed water) [2,303]. However, considering the large noise coming from the model paper's (RP) spectra, it is assumed that some oxidation of the surface has

occurred. An increase in the wet film deposit makes the vibrational bands more pronounced, while the amount of adsorbed water increases, as observed from the broadening and the increase of the vibrational band located around 1640 cm^{-1} in samples coated with methylcellulose and starch.

In the FT-IR spectra of the starch-coated paper (WSP), the vibrational band at 1639 cm^{-1} can be attributed to the presence of bound water, while the band at 3420 cm^{-1} is caused by the stretching vibration of free O–H [284], due to the presence of hydroxyl groups [303]. The stretching of vibrational bands in the C–O and C–O–H groups results in the formation of a 1540 cm^{-1} band. The band at 1470 cm^{-1} can be assigned to the stretching vibration of C–O [305], while the band at 895 cm^{-1} is that of β-glycosidic linkage between glucose units [303].

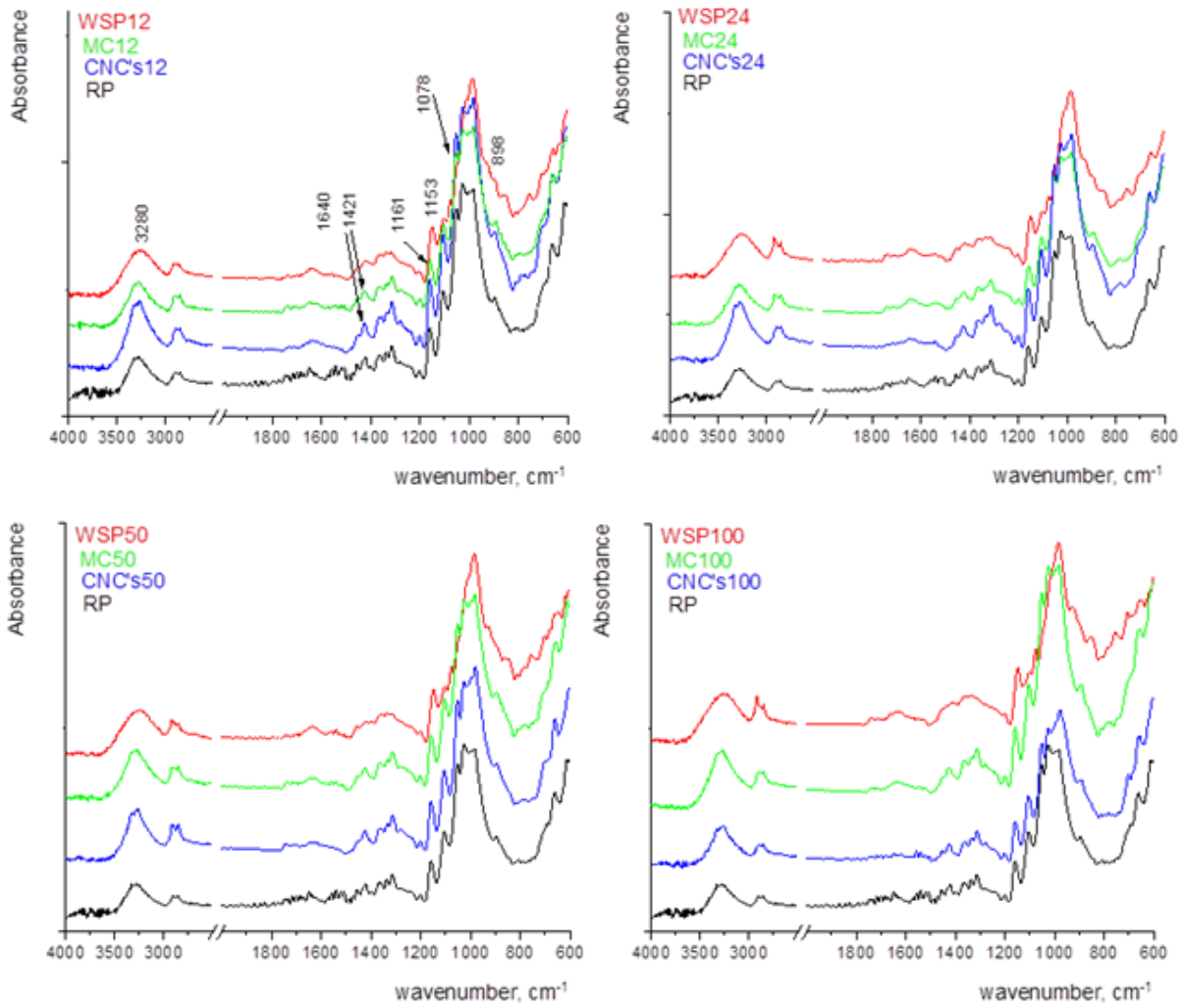

Figure 33 - FT-IR spectra of the model paper (RP) and the model paper coated with methylcellulose and starch (MCs, WSPs) [273].

In the samples coated with methylcellulose (MCs), the change in bands at 1370 cm^{-1}, 1340 cm^{-1}, and 1317 cm^{-1} within the spectrum indicates the rearrangement of the hydrogen-bonded network [301].

There are no significant changes in the spectra of the unaged and aged samples. The most notable changes can be observed in the range of 1500–1600 cm^{-1}. The loss of adsorbed water is also evident, indicating that accelerated thermal ageing has affected the paper's residual water content (i.e., desorption of water molecules) [306].

The broadening of the band at 893 cm^{-1} reflects the more disordered structure of the model paper (RP), resulting from accelerated thermal ageing (**Figure 34**).

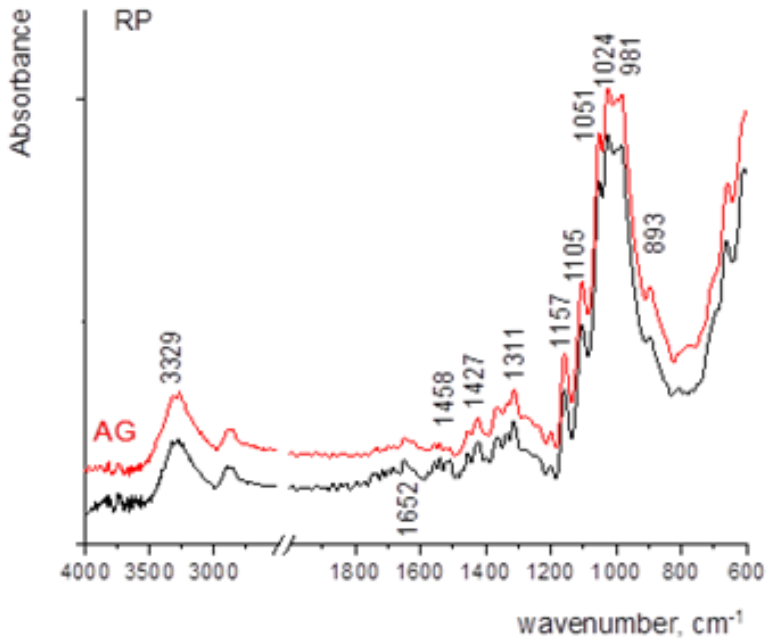

Figure 34 - FT-IR spectra of the model paper (RP) before and after accelerated thermal ageing [273].

In the model paper sample coated with a 12 μm thick methylcellulose coating (MC12) (**Figure 35**, left), the heat-induced changes may be attributed to the penetration of the coating into the model paper's structure, the oxidative mechanisms of the cellulosics (paper and methylcellulose), and the overlapping of their vibrational bands.

In the heat aged MC24 sample (paper coated with a 24 µm thick methylcellulose coating), the most notable change is the decrease of the vibrational band at 1639 cm^{-1}, signalling the loss of adsorbed water (**Figure 35**, right).

In MC50 (paper coated with a 50 µm thick methylcellulose coating), the peak of crystalline cellulose and adsorbed water decreases (**Figure 36**, left). The most significant changes occur in the spectrum of MC100 (paper coated with a 100 µm thick methylcellulose coating), where the peak of crystalline cellulose and adsorbed water decreases (**Figure 36**, right).

Supplementary bands can be attributed to the formation of oxidation products [124], as indicated by the appearance of new vibrational bands in the range of 1800-1500 cm^{-1}.

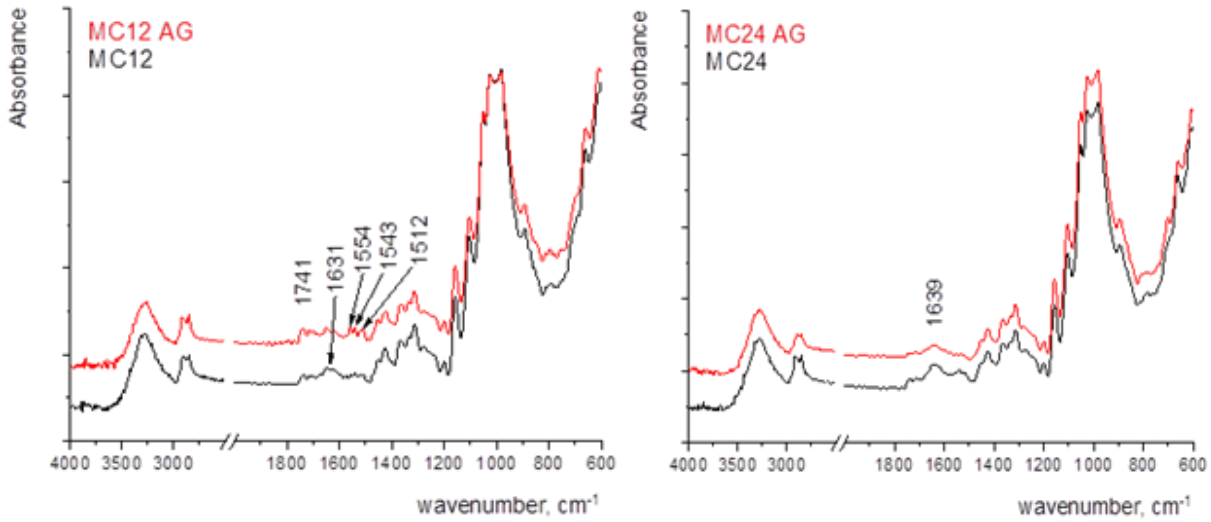

Figure 35 - FT-IR spectra of the MC12 (left) and the MC24 (right) before and after accelerated thermal ageing [273].

The formation of vibrational bands in the range of 1741–1707 cm^{-1} can be explained by the hydrolysis of the hemiacetal bonds [126], which may generate aldehydes upon opening the terminal rings. These bands represent the final oxidation stage of carbon (C) atoms in glucopyranose rings [306].

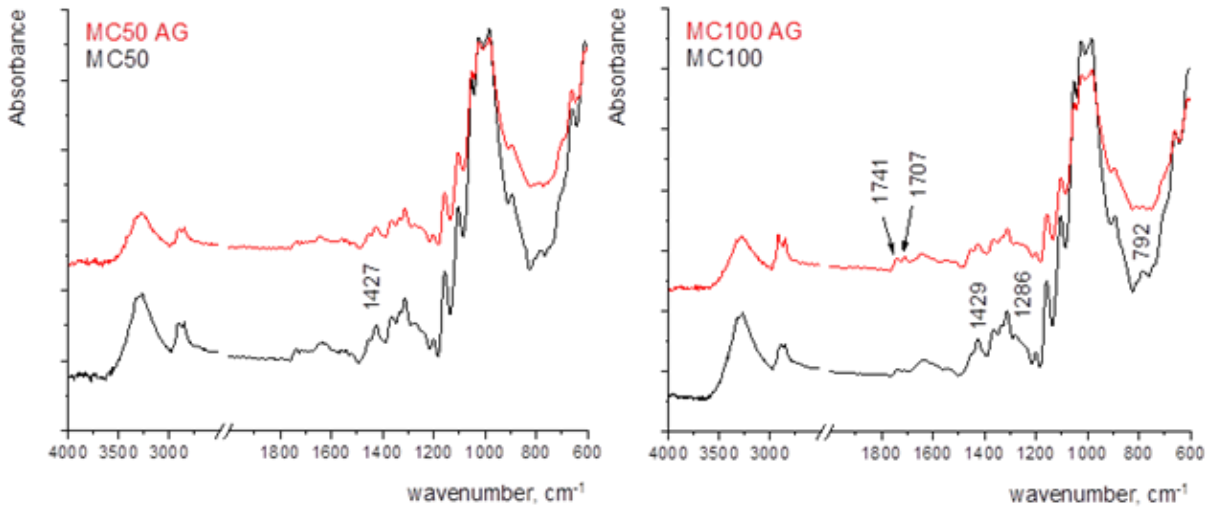

Figure 36 - FT-IR spectra of the MC50 (left) and the MC100 (right) before and after accelerated thermal ageing [273].

In samples coated with starch (WSPs), the alterations in the oxidation state of the samples with progressing degradation are observed in the FT-IR spectra within the 1500–1850 cm^{-1} range, where carbonyl groups appear in various chemical environments.

However, an issue may arise from the presence of water molecules at 1640 cm^{-1} masking the products of cellulose oxidation (**Figure 37, Figure 38).**

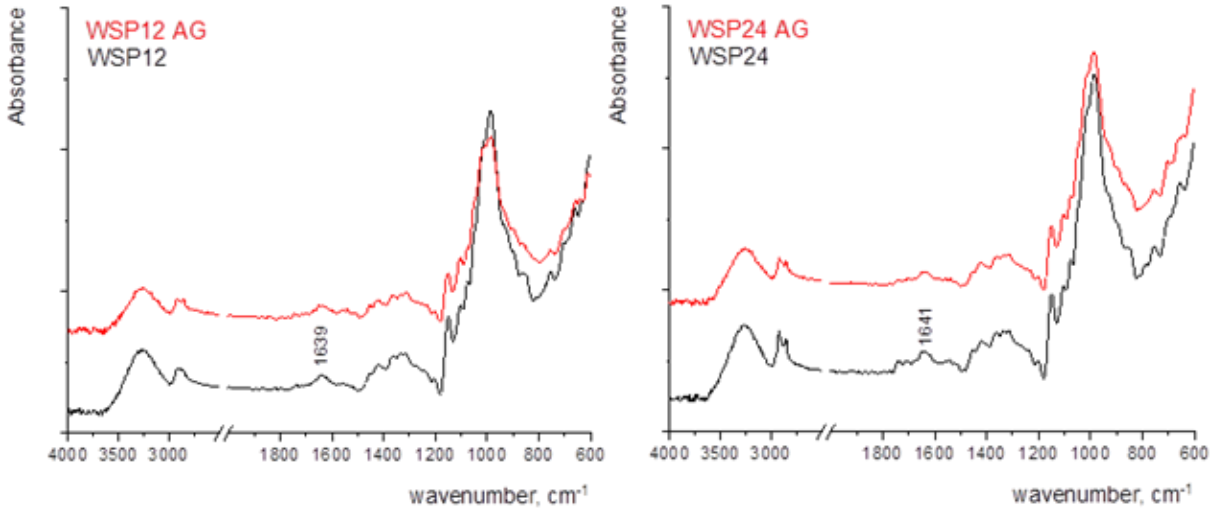

Figure 37 - FT-IR spectra of the WSP12 (left) and the WSP24 (right) before and after accelerated thermal ageing [273].

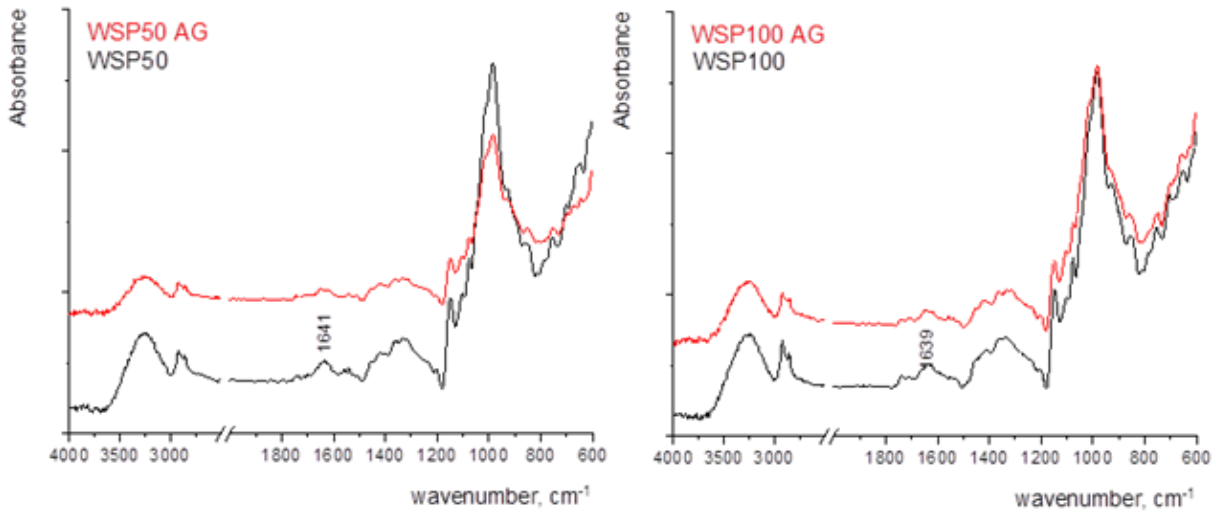

Figure 38 - FT-IR spectra of the WSP50 (left) and WSP100 (right) before and after accelerated thermal ageing [273].

Phase II: Evaluation of the bilayer coatings on the printed model paper's surface

In **Figure 39**, the FT-IR spectra of the uncoated printed paper (P) show distinct vibrational bands of cellulose, such as the C–O stretching (1105 cm^{-1} and 1024 cm^{-1}) and the anti-symmetric bridge stretching of C–O–C groups (1159 cm^{-1}). The most pronounced band at 1024 cm^{-1} is accompanied by peaks at 1051 $^{-1}$ and 981 cm^{-1} [301]. These bands are present in the printed model paper (P) and in the samples coated with starch (S) and starch and methylcellulose (S+MC), which are denominated P/S and P/S/MC in the spectra. However, paper coated with starch (P/S in the spectra) displays slightly different vibrational bands.

The bending vibration of adsorbed water is located around 1639 ± 1 cm^{-1} [303].

In the model paper coated with starch (P/S in the spectra), vibrational bands are observed at 3420 cm^{-1} due to the presence of –OH groups, while stretching of the C–O in the C–O–H groups results in a band at 1540 cm^{-1}. The β-glycosidic linkage vibration band is observed at 895 cm^{-1} [303].

The application of methylcellulose alters the bands at 1370 cm^{-1}, 1340 cm^{-1} and 1317 cm^{-1}, suggesting that a rearrangement of the hydrogen bonded network has occurred [301]. For both unaged and aged prints, the FT-IR spectrum remains relatively stable.

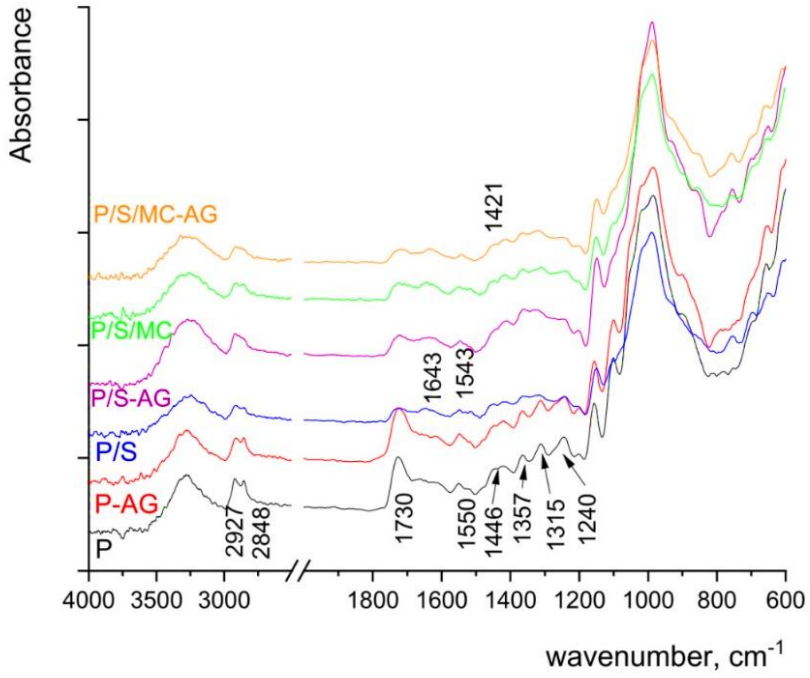

Figure 39 - FT-IR spectra of the unaged and the aged samples [210].

P - model paper, *P/S* - paper coated with starch, and P/S/MC - paper coated with starch and methylcellulose, AG - aged

The FT-IR spectra of the prints also show vibrational bands of printing ink binder, containing dispersed ink pigments. As pigments are covered in ink binder, they cannot be detected by FT-IR spectroscopy. Therefore, the FT-IR spectra changes resulting from accelerated UV ageing occur due to printing ink binder degradation, not pigment degradation.

The vibrational bands in model paper (P) ranging from 2925 to 2850 cm^{-1} can be attributed to aliphatic chains (–CH, $–CH_2$ and $–CH_3$ stretching bonding vibration) present in oils, such as fatty acids [307]. Vegetable oils also exhibit bands at 3014 cm^{-1}, 1463 cm^{-1}, 1166 cm^{-1}, 1101 cm^{-1} and 709 cm^{-1}.

The presence of the ester group in triglycerides is signalled by the carbonyl stretching band ranging from 1737 to 1722 cm^{-1}, usually accompanied by the bands at 1232 cm^{-1} and 1155 cm^{-1} [308]. When exposed to UV radiation, the ester carbonyl functional group spreads in width and moves towards lower wavenumbers. This behaviour indicates the formation of secondary oxidation products (i.e., carboxylic acids) [2].

In printed paper, the formation of oxidative products creates new vibrational bands at 1649 cm^{-1} and 1512 cm^{-1}, while the carbonyl vibrational band at 1722 cm^{-1} widens.

In the FT-IR spectra of the sample coated with starch (S), the vibrational band at 1630 cm^{-1} indicates the presence of bound water, while the band at 3420 cm^{-1} signals the presence of hydroxyl groups [303].

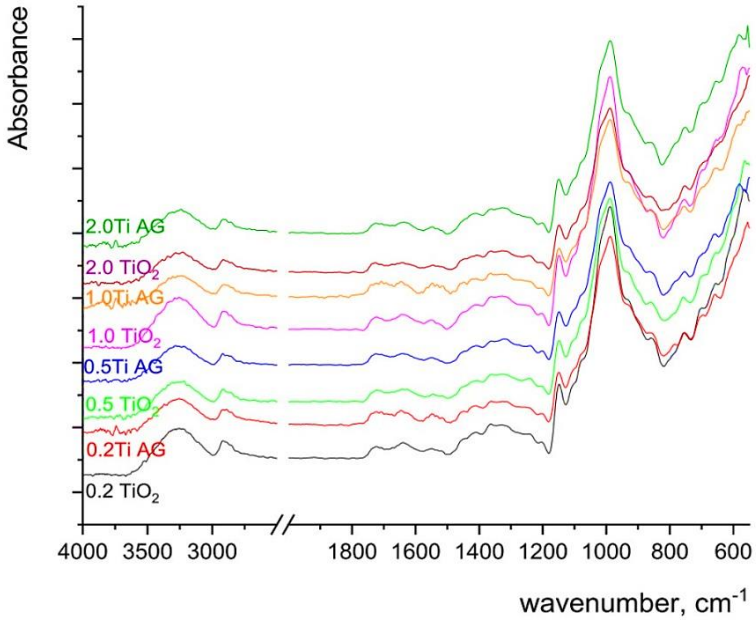

Figure 40 - FT-IR spectra of the unaged and the UV aged samples incorporating different TiO_2 *w/w* [210].

The band at 1540 cm^{-1} was formed due to the stretching of vibrational bands associated with the C–O bonds in the C–O–H groups. A stretching vibration of C–O is represented by the band at 1470 cm^{-1} [305].

Applying starch and methylcellulose coatings significantly changes the FT-IR spectra. This change can be observed in the carbonyl spectral range around 1730 cm^{-1}. Degradation occurs due to the presence of light-absorbing chemical species and chromophores (i.e., carbonyl groups), which absorb UV radiation and are most prone to photo-oxidation [119]. However, if the carbonyl groups in polymers are covered, as shown in the FT-IR spectra (**Figure 40),** the protective ability of coatings is present [309].

The masking of carbonyl groups in FT-IR spectra, indicating the protective ability of the applied coatings, could also be confirmed by the total colour difference results (**Figure 24**).

The signal of TiO_2 can sometimes be observed in the 800-600 cm^{-1} region [19,302], although it usually "escapes the FT-IR analysis" [79].

The addition of TiO_2 NPs to the coating did not alter the FT-IR spectra. This suggests "only a physical interaction between the nanofiller and the biopolymer matrix had occurred" [284]. The masking of the carbonyl band from the printing ink binder is still present (**Figure 40**).

Phase III*: Evaluation of the bilayer coatings on the model paper's surface

Figure 41 shows the FT-IR spectra of the model paper, where the strong bands of cellulose appear. The band at 1159 cm^{-1} corresponds to antisymmetric stretching of C–O–C groups and C–O stretching at 1105 cm^{-1} and 1024 cm^{-1}.

The band at 1024 cm^{-1} is accompanied by two characteristic peaks at 1051 and 981 cm^{-1} [301,310]. The vibrational band assigned to C–O–C stretching at β-(1-4)-glycosidic linkages at 893 cm^{-1} is known as an "amorphous" absorption band, while the vibrational band around 1425 cm^{-1}, assigned to a symmetric CH_2 bending vibration, is known as the "crystallinity" band [304].

The sharpening of the vibrational band after accelerated thermal aging at 894 cm^{-1} indicates an increase in less-ordered regions of the cellulose structure. In addition, the changes in the band at 1640 cm^{-1}, assigned to adsorbed water, are also noticed.

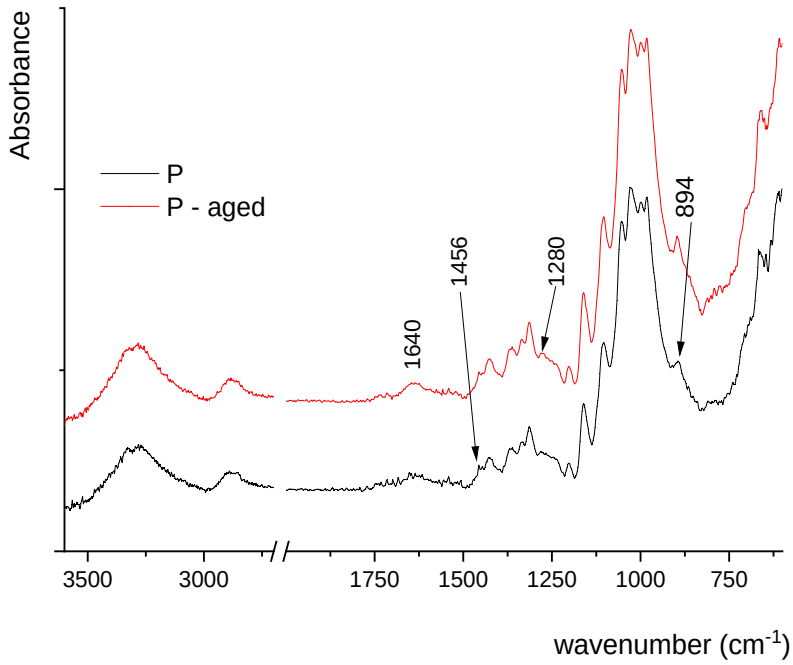

Figure 41 - FT-IR spectra of the unaged and the heat aged model paper (P).

From **Figure 42**, it can be noticed that model paper coated with starch (S) shows somewhat different vibrational bands compared with uncoated model paper, especially in the fingerprint region. In the FT-IR spectra of paper coated with starch, the presence of bound water can be indicated by the vibrational band at 1635 cm^{-1}, while the band at 3300 cm^{-1} signals the presence of hydroxyl groups (O–H).

When exposed to accelerated thermal ageing, the most pronounced changes occur in the fingerprint region between 1300 cm^{-1} and 1400 cm^{-1} due to the rearrangement of hydrogen bonds [301]. The sharpening of bands at 1201 cm^{-1}, 1313 cm^{-1} and 1421 cm^{-1} occurs during accelerated thermal ageing.

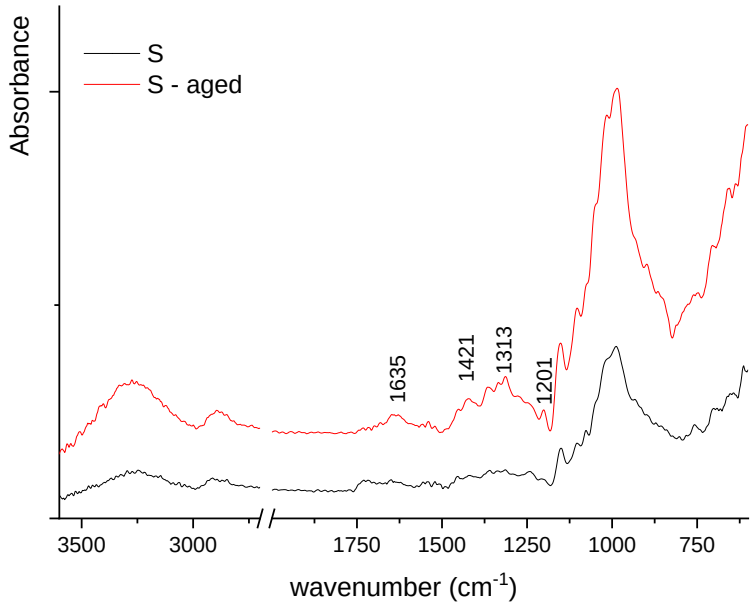

Figure 42 - FT-IR spectra of the unaged and the heat aged model paper coated with starch (S).

In the obtained FT-IR spectra of the paper coated with starch and methylcellulose (S + MC) (**Figure 43**), a large noise appears, probably due to its hydrophilic nature, as observed in ***Phase II*** (**Figure 19**, **Figure 21**).

The model paper coated with starch and methylcellulose (S+MC) also shows slightly different vibrational bands, especially in the fingerprint region.

In addition, after accelerated thermal ageing, the highest contribution is clearly seen in the changes of the vibrational band at the characteristic β-glycosidic linkage at 895 cm^{-1}, indicating an increase in amorphous structure [304].

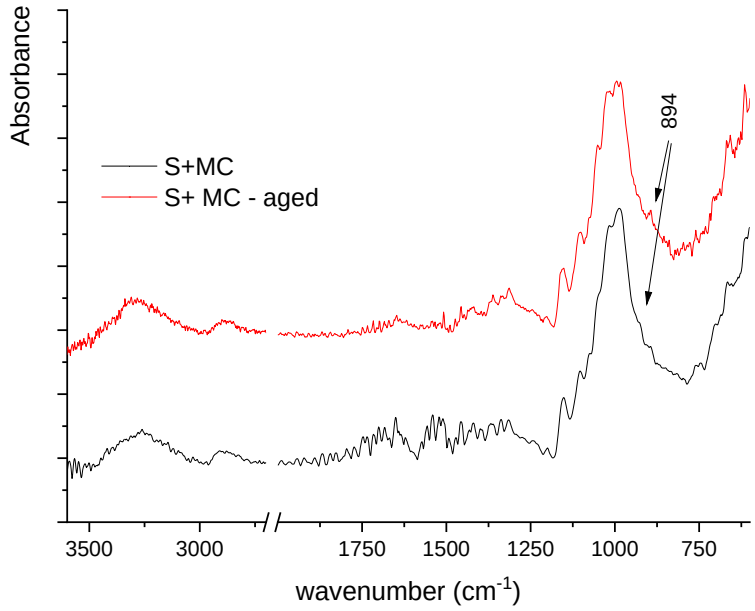

Figure 43 - FT-IR spectra of the unaged and the heat aged model paper coated with starch and methylcellulose (S+MC).

From **Figure 44,** it can be seen that, with the accelerated thermal ageing process, a slight increase in band at 898 cm^{-1} occurs, pointing to an increase in less ordered structures as a result of oxidation. In addition, even larger noise in the FT-IR spectra occurs as a result of ageing.

Figure 45 shows that, again, a larger noise in the FT-IR spectra occurs after ageing of the sample due to oxidation. This may result in the masking of some oxidation products formed during ageing.

Greater changes in FT-IR spectra are recorded for the aged T0.75 (model paper coated with the bilayer coating incorporating 0.75% TiO_2 *w/w*) in comparison with the T0.50 (model paper coated with the bilayer coating incorporating 0.5% TiO_2 *w/w*), considering the higher proportion of NPs in the coating and their interactions with IR radiation during the FT-IR analysis.

As NPs can act as reflectors, absorbers, or scatterers of IR radiation, this can increase the background noise or change the intensity of spectral peaks [296].

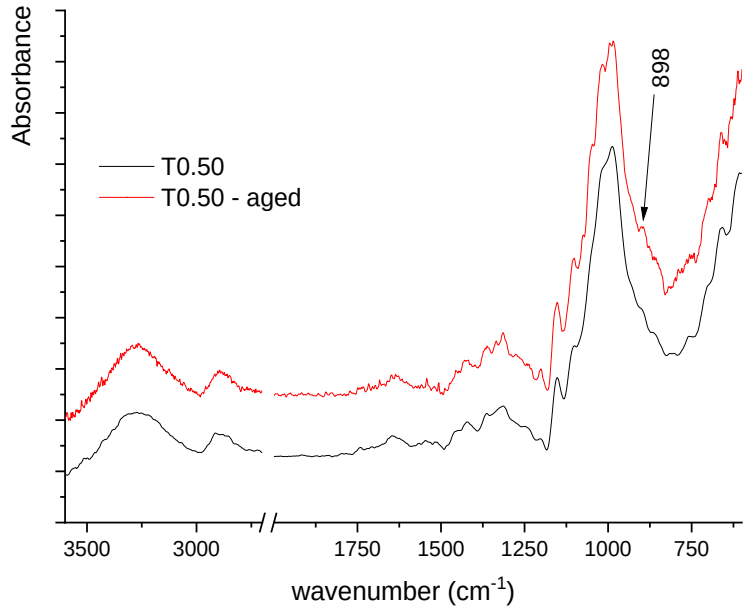

Figure 44 - FT-IR spectra of the unaged and the heat aged model paper coated with the bilayer coating incorporating 0.5% TiO_2 *w/w* (T0.50)

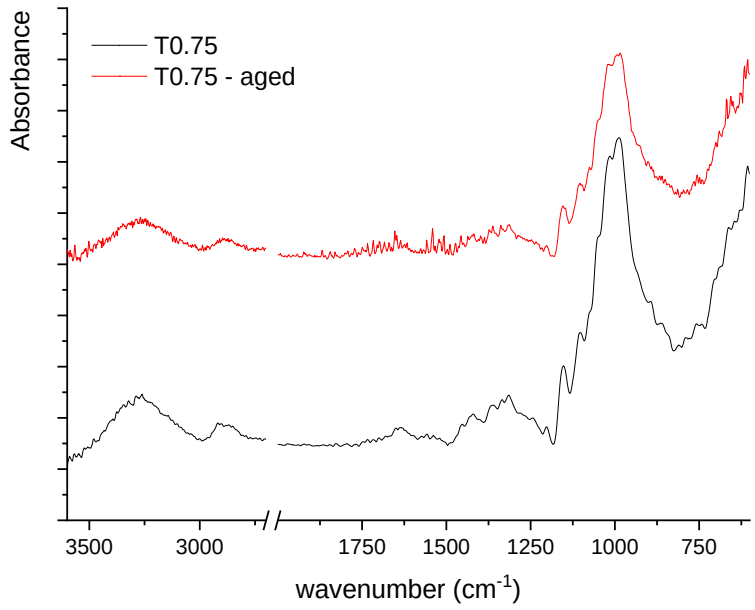

Figure 45 - FT-IR spectra of the unaged and the heat aged model paper coated with the bilayer coating incorporating 0.75% TiO_2 *w/w* (T0.75)

Similar behaviour is detected for the T1.00 (model paper coated with the bilayer coating incorporating 1% TiO_2 *w/w*) (**Figure 46**). In addition, the similarities between the FT-IR spectra of the unaged and aged samples point to higher stability to oxidation.

The addition of TiO_2 NPs to the methylcellulose coating increases the stability of the model paper subjected to accelerated thermal ageing compared with other coated samples. This is visible through the increase of the amorphous vibrational band and the rearrangement of hydrogen bonds.

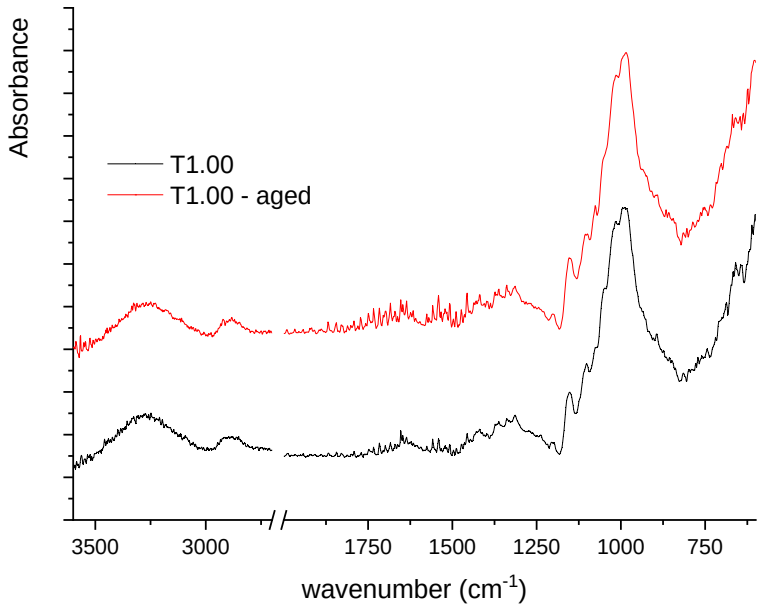

Figure 46 - FT-IR spectra of the unaged and the heat aged model paper coated with the bilayer coating incorporating 1% TiO_2 *w/w* (T1.00)

4.10. ANTIFUNGAL PROPERTIES OF THE COATINGS

4.10.1. Indirect inoculation

Phase III*: Evaluation of the bilayer coatings on the model paper's surface

The colonies that were inoculated on agar spread to paper on the fourth day of inoculation.

The results of the tests shown in **Figure 47** and **Figure 48** suggest that the bilayer coatings incorporating TiO_2 NPs (T0.50, T0.75 and T1.00) do not demonstrate inhibiting activity against *Aspergillus niger*. Moreover, the bilayer coatings appear to trigger fungal growth on the model paper compared with other samples (P - model paper, S - model paper coated with starch, S+MC - model paper coated with starch and methylcellulose).

To further investigate the lack of inhibition of TiO_2 NPs in the tested conditions, another series of experiments were performed with samples kept under an D50 daylight light source for 5 days (**Figure 49**). Again, the highest fungal growth was observed in the coated model paper samples incorporating TiO_2 NPs.

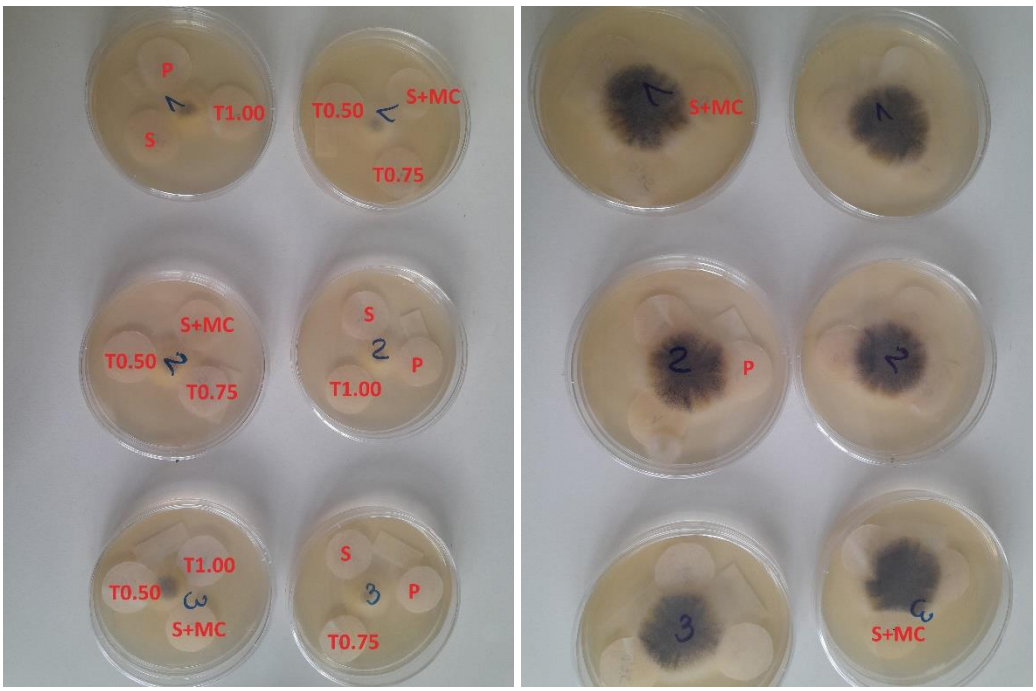

Figure 47 - Samples placed on inoculated agar after 48 hours (left) and 72 hours (right).

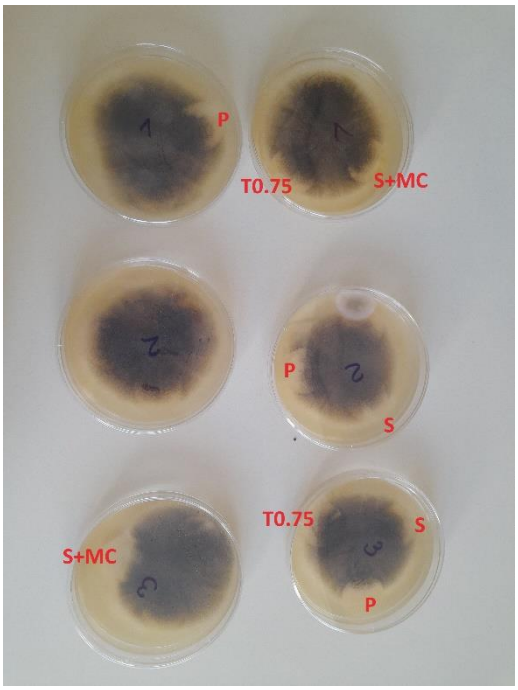

Figure 48 - Samples placed on inoculated agar after 96 hours.

In both experiments involving agar, the fungal growth appears to proceed at the slowest rate on S+MC samples (denominated as „0“ in **Figure 49**). The reduction in fungal growth can be attributed to the lower levels of roughness of the S+MC surface compared with other samples' surfaces (**Figure 23**).

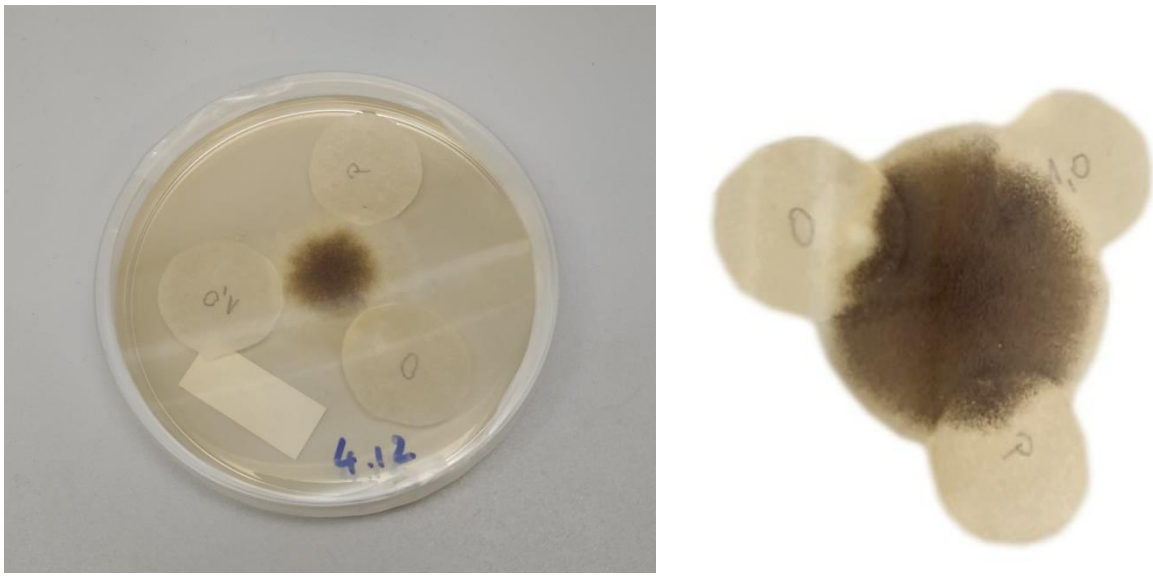

Figure 49 - Samples placed on inoculated agar under a daylight source after 72 hours (left) and 96 hours (right).

4.10.2. Direct inoculation

Phase III*: Evaluation of the bilayer coatings on the model paper's surface

The growth and sporulation of *Aspergillus niger* on the samples (**Figure 50**) varied in intensity and concentration across each sample, despite the 48 hours of conditioning. These occurrences can be attributed to the heterogeneous structure of the model paper.

None of the coated model paper samples incorporating TiO_2 NPs inhibits or slows down the growth of *A. niger,* although growth appears less pronounced on the sample with the lowest TiO_2 concentration (T0.50) (**Figure 50**)**.** While the overall ability of TiO_2 to limit *Aspergillus* growth in dark conditions is considered either weak or non-existent [9,219], several researchers also report the resistance of this fungi to the photocatalytic effects of TiO_2 [311,312].

After inoculation of the samples with *Trichoderma citrinoviride,* the growth and sporulation also resulted in varying growth patterns and sporulation on equivalent samples. **Figure 50** and **Figure 51** depict the growth of *Aspergillus niger and Trichoderma citrinoviride* on the surfaces of the samples, showing some of the most pronounced growth intensities across each sample.

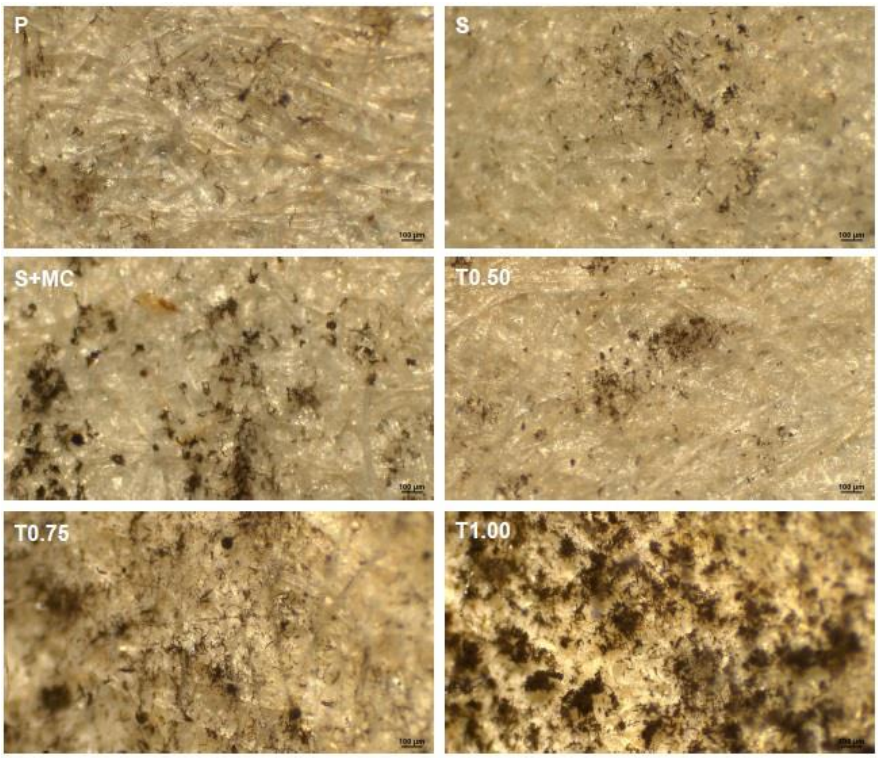

Figure 50 - *Aspergillus niger* growth expansion patterns on the samples, scale bar: 100 µm.

During both fungal inoculations (*Aspergillus niger and Trichoderma citrinoviride)*, the most intense growth and sporulation were observed on the sample coated with the bilayer coating incorporating the highest TiO_2 weight concentration (T1.00), which can be attributed to the fungal adaptation to stress conditions [141,145].

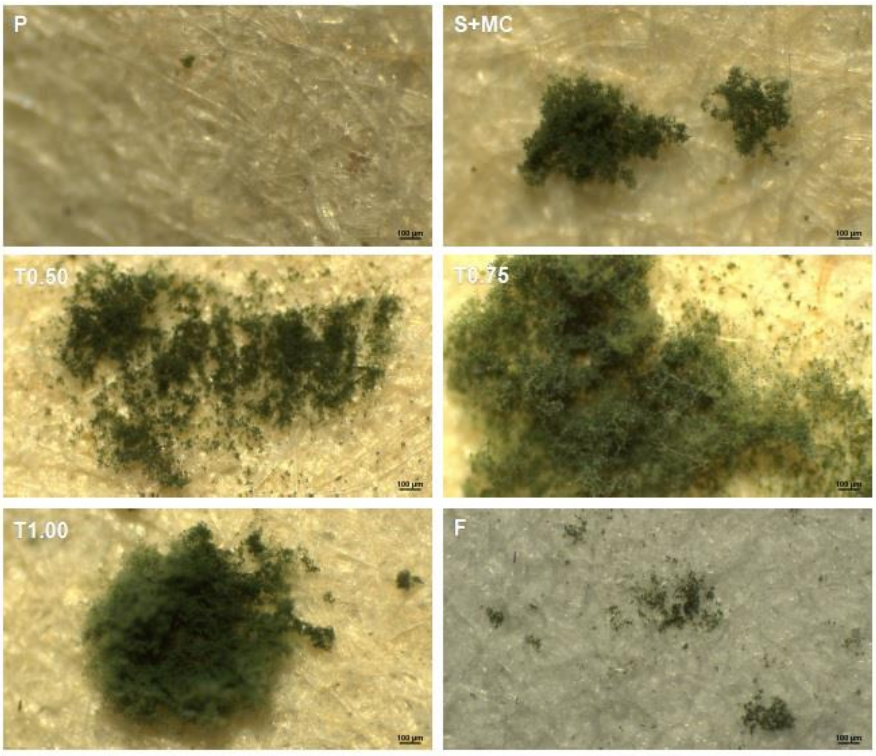

Figure 51 - *Trichoderma citrinoviride* expansion patterns on the model paper samples and on filter paper (F), scale bar: 100 μm.

Under the same testing conditions, the equivalent samples from both experiments exhibited variations in intensities of fungal growth and sporulation scattered throughout the surface of each sample. The bilayer coatings incorporating TiO_2 cannot slow down or deactivate the growth of either of the two tested fungal species. However, it seems that the highest weight concentrations of TiO_2 (T1.00 and T0.75) induce more intensive sporulation. More research is needed to investigate these occurrences, including the introduction of TiO_2 weight concentrations higher than 1% to exclude hormesis[20] [313] and the utilization of other excitation wavelengths, with all these aspects assessed in a separate experiment.

[20] The concept of hormesis is characterized by a dose-response relationship, where low doses or concentrations of a substance result in stimulation due to an adaptive response, while high doses result in inhibition.

4.11. REVERSIBILITY OF THE COATINGS

Phase III*: Evaluation of the bilayer coatings on the model paper's surface

SEM-EDS analyses were performed to assess the reversibility of the coatings in distilled water. **Figure 52**, left and right, shows the sample coated with the bilayer coating incorporating 0.75% TiO_2 *w/w* (T0.75) before and after the attempt at coating removal.

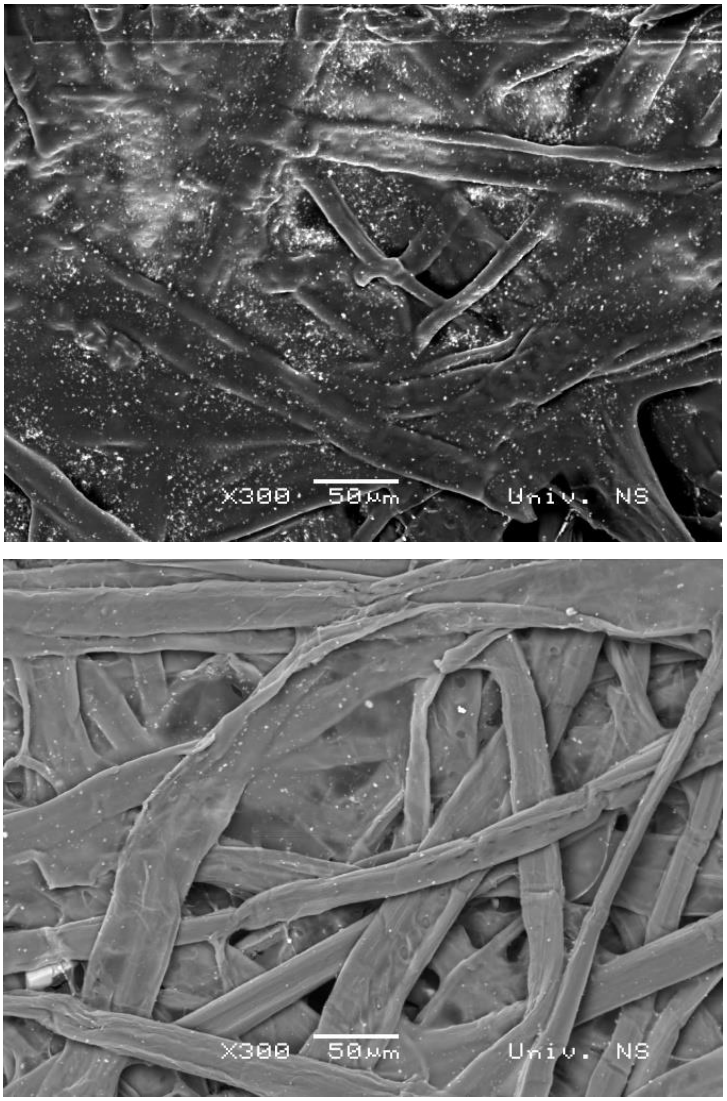

Figure 52 - SEM micrograph of the T0.75 at 300× magnification before (above) and after (below) water immersion.

EDS analysis of the immersed sample (**Figure 53** and **Figure 54)** confirms that TiO_2 NPs are removed from the top layer to a large extent compared with EDS analyses from before the immersion (**Figure 12** and **Figure 13**). The removal of the TiO_2 NPs was successful, likely

due to the water-solubility of the polymer matrix in which they were dispersed (methylcellulose). However, the underlying starch layer, employed to consolidate and strengthen the paper structure, proved challenging to remove due to its deep penetration and strong adhesion within the paper structure, as previously outlined by Lama [281]. Incomplete reversibility of starches is a common challenge faced by paper conservators [314].

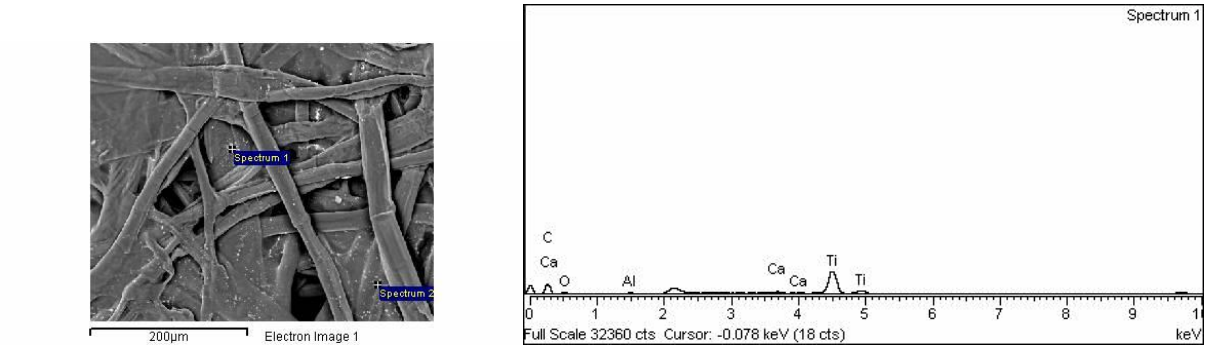

Figure 53 - SEM micrograph (left) and EDS surface elemental composition analysis of specific positions of the T0.75 after water immersion (right).

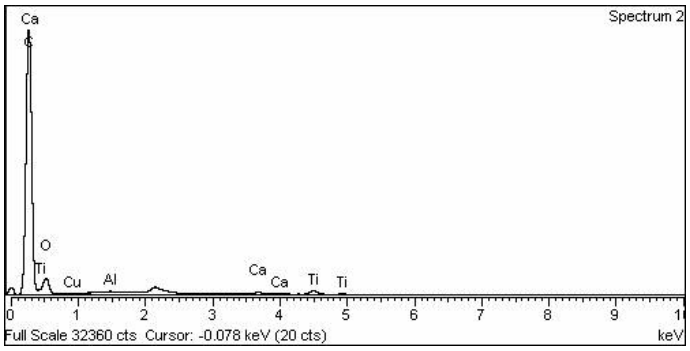

Figure 54 - EDS surface elemental composition analysis of specific positions of the T0.75 after immersion.

5. CONCLUSIONS

Phase I, Phase I*: Evaluation of the monolayer coatings on the model paper's surface

- The surface morphology and elemental composition of the model paper (Takogami B) resemble those of historic paper.
- The monolayer coatings (starch and methylcellulose) provide transparent films. The starch film covers the model paper's surface; however, the formed layer is not entirely uniform.
- The application of each coating influences the thickness and grammage of the model paper. With starch coating, most wet film thicknesses result in an excessive increase in these two physical characteristics.
- The monolayer coatings (starch and methylcellulose) can protect the model paper's colour and opacity from the effects of heat (accelerated thermal ageing).
- With starch coating, an over-application (wet film thickness of 100 μm) results in an excessive increase in gloss.
- The application of the monolayer coatings alters the surface properties of the model paper. The starch coatings decrease the contact angles of the model paper's surface. The most pronounced changes are detected at the highest wet film thickness. Methylcellulose coatings, on the other hand, increase contact angles. The water droplet absorption time is prolonged as a result of the application of both monolayer coatings, while accelerated thermal ageing prolongs water droplet absorption times even more.

These findings confirm that the amount of coating (wet film thickness) applied to the model paper strongly influences the outcomes of conservation treatments. The established advantages and disadvantages of the applications have influenced the formulation of the bilayer coatings (order of application, wet film thickness). Therefore, a more hydrophilic coating (starch) was applied as the bottom layer, while the more hydrophobic one (methylcellulose) served as the top layer. The combination of wet film thicknesses that caused the least changes in several properties of the model paper was used for application.

Phase II: Evaluation of the bilayer coatings on the printed model paper's surface

- At lower TiO_2 weight concentrations (0.2% and 0.5% TiO_2), bilayer coatings can slow down the colour change of the printed model paper induced by accelerated UV ageing.

- All coatings have reduced the model paper's water contact angle and water droplet absorption times. After ageing, these two values additionally decrease in most samples. In nano-TiO_2-modified bilayer coatings, the decrease is proportional to the increase in TiO_2 NP weight concentration. Accelerated UV ageing makes the model paper's surface coated with nano-TiO_2-modified bilayer coatings more hydrophilic.
- The incorporation of TiO_2 NPs into the coating does not cause significant changes in the IR spectra, suggesting that only physical interactions have occurred.

Phase III, Phase III*: Evaluation of the bilayer coatings on the model paper's surface

- The TiO_2 NPs are almost uniformly distributed in the nanocomposite film. The sizes and arrangements of aggregates are consistent for all three TiO_2 weight concentrations.
- The proposed nano-TiO_2-modified bilayer coatings could not deactivate the growth of two fungal species (*Aspergillus niger* and *Trichoderma citrinoviride*) on the model paper. The presence of TiO_2 in the coating also induces sporulation, which is attributed to the fungal stress response.
- At a lower TiO_2 weight concentration (0.5% TiO_2), the proposed bilayer coatings can preserve the model paper's optical properties (gloss value, total colour difference) from the effects of heat (accelerated thermal ageing). However, the monolayer coatings affect the original colour of the model paper to a lesser extent.
- The application of the coatings enhances all mechanical properties aside from bursting strength, which decreases proportionally with an increased TiO_2 weight concentration. On the other hand, the stiffness of the samples decreases as the TiO_2 weight concentration is raised.
- The nano-TiO_2-modified bilayer coatings show only partial reversibility in distilled water. While TiO_2 NPs can be removed to a significant extent from the surface of the model paper through immersion in distilled water, starch removal is incomplete.
- The bilayer coatings demonstrated higher stability to oxidation compared to the monolayer coatings and were able to effectively protect the model paper from thermal degradation.

Based on the obtained results, it was concluded that while the proposed nano-TiO_2-modified bilayer coatings offer several protective features, such as protection from UV radiation and heat, they do not provide protection against cellulolytic fungi.

The scientific contribution of this research was manifested through:

- Improvement of methodologies by establishing more reliable criteria for selecting coatings in paper conservation (i.e., determination of optimal wet film thickness).
- Development of nanocomposite coating formulations for the protection of paper from UV radiation (i.e., nano-TiO_2 modified bilayer coating). Identification of the optimal coating composition to achieve targeted effects.
- Enhanced understanding of fungi-paper interactions.

The protective bilayer coating proposed here represents an innovative formulation for the preservation of cellulosic works that are either printed or firmly bound to paper in some other way. Application of aqueous coatings is not suitable for overly water-sensitive surfaces, as it can lead to further deterioration.

6. REFERENCES

1. Walker, A. LIBER Available online: https://cool.culturalheritage.org/byform/mailing-lists/cdl/2006/1069.html (accessed on 22 January 2024).
2. Princi, E. *Handbook of Polymers in Paper Conservation*; 1st ed.; iSmithers Rapra Publishing: Shropshire, U.K., 2011;
3. Baglioni, P.; Chelazzi, D.; Giorgi, R. Deacidification of Paper, Canvas and Wood. In *Nanotechnologies in the Conservation of Cultural Heritage: A compendium of materials and techniques*; Springer Science + Business Media: Dordrecht, Netherlands, 2015; pp. 117–144.
4. Strlič, M.; Kolar, J.; Scholten, S. Paper and Durability. In *Ageing and stabilisation of paper*; Strlič, M., Kolar, J., Eds.; National and University Library: Ljubljana, Slovenia, 2005; pp. 3–8.
5. Wilson, W.K.; Parks, E.J. An Analysis of the Aging of Paper: Possible Reactions and Their Effects on Measurable Properties*. *Restaurator* **1979**, *3*, 37–61.
6. Giorgi, R. Inorganic Nanomaterials for the Deacidification of Paper. In *Nanoscience for the Conservation of Works of Art*; Baglioni, P., Chelazzi, D., Eds.; RSC Publishing: Cambridge, U.K., 2013; pp. 396–429.
7. Wang, H.; Lu, G.; Zhang, J.; Zheng, D. Multifunctional Nanocomposites for Paper Conservation. *Studies in Conservation* **2013**, *58*, 23–29, doi:10.1179/2047058412Y.0000000038.
8. Horie, C. V. *Materials for Conservation: Organic Consolidants, Adhesives and Coatings*; Rees-Jones, S.G., Linstrum, D., Eds.; 2nd ed.; Butterworth & Co Ltd.: London, U.K., 1987;
9. Gómez-Ortíz, N.; De La Rosa-García, S.; González-Gómez, W.; Soria-Castro, M.; Quintana, P.; Oskam, G.; Ortega-Morales, B. Antifungal Coatings Based on Ca(OH)2 Mixed with ZnO/TiO2 Nanomaterials for Protection of Limestone Monuments. *ACS Appl Mater Interfaces* **2013**, *5*, 1556–1565, doi:10.1021/am302783h.
10. Goffredo, G.B.; Citterio, B.; Biavasco, F.; Stazi, F.; Barcelli, S.; Munafò, P. Nanotechnology on Wood: The Effect of Photocatalytic Nanocoatings against Aspergillus Niger. *J Cult Herit* **2017**, *27*, 125–136, doi:10.1016/j.culher.2017.04.006.
11. Munafò, P.; Goffredo, G.B.; Quagliarini, E. TiO2-Based Nanocoatings for Preserving Architectural Stone Surfaces: An Overview. *Constr Build Mater* **2015**, *84*, 201–218, doi:10.1016/j.conbuildmat.2015.02.083.
12. Afsharpour, M.; Imani, S. Preventive Protection of Paper Works by Using Nanocomposite Coating of Zinc Oxide. *J Cult Herit* **2017**, *25*, 142–148, doi:10.1016/j.culher.2016.12.007.
13. Baglioni, P.; Chelazzi, D.; Giorgi, R. Innovative Nanomaterials: Principles, Availability and Scopes. In *Nanotechnologies in the Conservation of Cultural*

Heritage: A compendium of materials and techniques; Springer Science + Business Media: Dordrecht, Netherlands, 2015; pp. 1–14.

14. Ariafar, A.A.; Afsharpour, M.; Samanian, K. Use of TiO2/Chitosan Nanoparticles for Enhancing the Preservative Effects of Carboxymethyl Cellulose in Paper-Art-Works against Biodeterioration. *Int Biodeterior Biodegradation* **2018**, *131*, 67–77, doi:10.1016/j.ibiod.2017.04.025.

15. Lisuzzo, L.; Cavallaro, G.; Milioto, S.; Lazzara, G. Halloysite Nanotubes Filled with MgO for Paper Reinforcement and Deacidification. *Appl Clay Sci* **2021**, *213*, 1–9, doi:10.1016/j.clay.2021.106231.

16. Cavallaro, G.; Lazzara, G.; Milioto, S.; Parisi, F. Halloysite Nanotubes as Sustainable Nanofiller for Paper Consolidation and Protection. *J Therm Anal Calorim* **2014**, *117*, 1293–1298, doi:10.1007/s10973-014-3865-5.

17. Amornkitbamrung, L.; Bračič, D.; Bračič, M.; Hribernik, S.; Malešič, J.; Hirn, U.; Vesel, A.; Kleinschek, K.S.; Kargl, R.; Mohan, T. Comparison of Trimethylsilyl Cellulose-Stabilized Carbonate and Hydroxide Nanoparticles for Deacidification and Strengthening of Cellulose-Based Cultural Heritage. *ACS Omega* **2020**, *5*, 29243–29256, doi:10.1021/acsomega.0c03997.

18. Dei, L.; Chelazzi, D. Biomineralization, Geopolymers and Hybrid Nanocomposites. In *Nanoscience for the Conservation of Works of Art*; Baglioni, P., Chelazzi, D., Eds.; RSC Publishing: Cambridge, U.K., 2013; pp. 372–395.

19. Afsharpour, M.; Rad, F.T.; Malekian, H. New Cellulosic Titanium Dioxide Nanocomposite as a Protective Coating for Preserving Paper-Art-Works. *J Cult Herit* **2011**, *12*, 380–383, doi:10.1016/j.culher.2011.03.001.

20. Zhang, J.; Zhou, P.; Liu, J.; Yu, J. New Understanding of the Difference of Photocatalytic Activity among Anatase, Rutile and Brookite TiO2. *Physical Chemistry Chemical Physics* **2014**, *16*, 20382–20386, doi:10.1039/c4cp02201g.

21. The American Institute for Conservation AIC's Code of Ethics and Guidlines for Practice Available online: https://www.culturalheritage.org/docs/default-source/resources/governance/organizational-documents/code-of-ethics-and-guidelines-for-practice.pdf?sfvrsn=ca344aed_26 (accessed on 15 March 2023).

22. Zou, X.; Gurnagul, N.; Uesaka, T.; Bouchard, J. Accelerated Aging of Papers of Pure Cellulose: Mechanism of Cellulose Degradation and Paper Embrittlement. *Polym Degrad Stab* **1994**, *43*, 393–402.

23. European Confederation of Conservator-Restorers' Organisations E.C.C.O's Code of Ethics Available online: https://www.ecco-eu.org/wp-content/uploads/2021/03/ECCO_professional_guidelines_II.pdf (accessed on 15 March 2023).

24. IUPAC Polymer. In *Compendium of Chemical Terminology*; International Union of Pure and Applied Chemistry, 2006.

25. Jenkins, A.D.; Kratochvíl, P.; Stepto, R.F.T.; Suter, U. V Glossary of Basic Terms in Polymer Science (IUPAC Recommendations 1996). *Pure and Applied Chemistry* **1996**, *68*, 2287–2311.

26. Fried, J.R. *Polymer Science and Technology*; 2nd ed.; Prentice Hall (Pearson Education): New Jersey, U.S.A., 2003;

27. Alves, T.F.R.; Morsink, M.; Batain, F.; Chaud, M. V.; Almeida, T.; Fernandes, D.A.; da Silva, C.F.; Souto, E.B.; Severino, P. Applications of Natural, Semi-Synthetic, and Synthetic Polymers in Cosmetic Formulations. *Cosmetics* 2020, *7*.

28. Stevens, M.P. *Polymer Chemistry - An Introduction*; 3rd ed.; Oxford University Press, Inc.: Oxford, U.K., 1999;

29. Petrie, E.M. *Handbook of Adhesives and Sealants*; 1st ed.; McGraw-Hill Professional, 1999;

30. Fanconi, B. Molecular Vibrations of Polymers. *Annu Rev Phys Chem* **1980**, *31*, 265–291.

31. Team Xometry Semi-Crystalline vs Amorphous Polymers: Which One Is More Durable? Available online: https://www.xometry.com/resources/materials/semi-crystalline-vs-amorphous-polymers/ (accessed on 4 March 2024).

32. Schubert, U.S. From Polymers or Colloids to Polymers and Colloids. *Colloid Polym Sci* **2020**, *298*, 1609–1610, doi:10.1007/s00396-020-04759-5.

33. Tse, N.; Miles, A.; Roberts, A. Film Formation of Artists Acrylic Paints in Tropical Climates Using Dynamic Speckle Interferometry. In Proceedings of the Lasers in the conservation of artworks IX; Saunders, D., Strlič, M., Korenberg, C., Luxford, N., Birkholzer, K., Eds.; Archetype Publications: London, U.K., 2013; pp. 32–39.

34. Felton, L.A. Mechanisms of Polymeric Film Formation. *Int J Pharm* **2013**, *457*, 423–427, doi:10.1016/j.ijpharm.2012.12.027.

35. Al-Assaf, S. Polysaccharides: Origin, Source and Properties. In *The Radiation Chemistry of Polysaccharides*; Al-Assaf, S., Coqueret, X., Dahlan, K.Z.H.M., Sen, M., Ulanski, P., Eds.; IAEA: Vienna, Austria, 2016; pp. 5–23.

36. Blanco, A.; Monte, M.C.; Campano, C.; Balea, A.; Merayo, N.; Negro, C. Nanocellulose for Industrial Use: Cellulose Nanofibers (CNF), Cellulose Nanocrystals (CNC), and Bacterial Cellulose (BC). In *Handbook of Nanomaterials for Industrial Applications*; Elsevier, 2018; pp. 74–126 ISBN 9780128133514.

37. Han, Shaobo. Thermoelectric Polymer-Cellulose Composite Aerogels, Linköping University: Norrköping, Sweden, 2019.

38. Baumann, M.G.D.; Conner, A.H. Carbohydrate Polymers as Adhesives. In *Handbook of Adhesive Technology*; Pizzi, A., Mittal, K.L., Eds.; Marcel Dekker, Inc.: New York, U.S.A., 2003.

39. Shanks, R.A.; Pardo, I.R.M. Cellulose Solubility, Gelation, and Absorbency Compared with Designed Synthetic Polymers. In *Cellulose-Based Superabsorbent Hydrogels (in*

Polymers and Polymeric Composites: A Reference Series book series); Mondal, I.H., Ed.; Springer, 2018; pp. 1–26.

40. Zhbankov, R.G.; Firsov, S.P.; Buslov, D.K.; Nikonenko, N.A.; Marchewka, M.K.; Ratajczak, H. Structural Physico-Chemistry of Cellulose Macromolecules. Vibrational Spectra and Structure of Cellulose. *J Mol Struct* **2002**, *614*, 117–125, doi:10.1016/S0022-2860(02)00252-1.

41. Ruiz-Recasens, C.; Campo-Francés, G.; Fernandez-Vidal, I.; Oriola, M. Identification of Cellulose Ethers in Cultural Heritage by Means of MALDI-TOF-MS. *J Cult Herit* **2017**, *24*, 53–59, doi:10.1016/j.culher.2016.11.008.

42. Borges, I. da S.; Casimiro, M.H.; Macedo, M.F.; Sequeira, S.O. Adhesives Used in Paper Conservation: Chemical Stability and Fungal Bioreceptivity. *J Cult Herit* **2018**, *34*, 1–8, doi:10.1016/j.culher.2018.03.027.

43. Shokri, J.; Adibki, K. Application of Cellulose and Cellulose Derivatives in Pharmaceutical Industries. In *Cellulose - Medical, Pharmaceutical and Electronic Applications*; Van De Ven, T.G.M., Ed.; InTech, 2013; pp. 47–66.

44. Chen, C.; Xi, Y.; Weng, Y. Recent Advances in Cellulose-Based Hydrogels for Tissue Engineering Applications. *Polymers (Basel)* 2022, *14*.

45. LeCorre, D.; Bras, J.; Dufresne, A. Influence of Botanic Origin and Amylose Content on the Morphology of Starch Nanocrystals. *Journal of Nanoparticle Research* **2011**, *13*, 7193–7208, doi:10.1007/s11051-011-0634-2.

46. Zhang, Y.; Han, J.; Liu, Z. Starch-Based Edible Films. In *Environmentally Compatible Food Packaging*; Elsevier Inc., 2008; pp. 108–136 ISBN 9781845691943.

47. Henry, W.; et al Adhesives. In *Paper Conservation Catalog*; American Institute for Conservation, Book and Paper Group: Washington D.C., U.S.A., 1989.

48. Gott, B.; Barton, H.; Samuel, D.; Torrence, R. Biology of Starch. In *Ancient Starch Research*; Torrence, R., Barton, H., Eds.; Routledge: New York. U.S.A., 2006; pp. 35–45.

49. Sapper, M.; Chiralt, A. Starch-Based Coatings for Preservation of Fruits and Vegetables. *Coatings* **2018**, *8*, doi:10.3390/coatings8050152.

50. Hubbe, M.A.; Bowden, C. Handmade Paper: A Review of Its History, Craft, and Science. *Bioresources* **2009**, *4*, 1736–1792, doi:10.15376/biores.4.4.1736-1792.

51. Thakur, R.; Pristijono, P.; Scarlett, C.J.; Bowyer, M.; Singh, S.P.; Vuong, Q. V. Starch-Based Films: Major Factors Affecting Their Properties. *Int J Biol Macromol* **2019**, *132*, 1079–1089, doi:10.1016/j.ijbiomac.2019.03.190.

52. Jivan, M.J.; Yarmand, M.; Madadlou, A. Preparation of Cold Water-Soluble Potato Starch and Its Characterization. *J Food Sci Technol* **2014**, *51*, 601–605, doi:10.1007/s13197-013-1200-y.

53. Majzoobi, M.; Farahnaky, A. Granular Cold-Water Swelling Starch; Properties, Preparation and Applications, a Review. *Food Hydrocoll* **2021**, *111*, 1–11, doi:10.1016/j.foodhyd.2020.106393.

54. Bloom, J.M. Papermaking: The Historical Diffusion of an Ancient Technique. In *Mobilities of knowledge*; Jöns, H., Meusburger, P., Heffernan, M., Eds.; Springer: Cham, Switzerland, 2017; Vol. 10, pp. 51–66.

55. Dadmohamadi, K.; Achachluei, M.M.; Jafari, M.T. The Effect of Cellulose Nanofibers on Paper Documents Containing Starch and Gelatine Sizing. *Restaurator* **2022**, *43*, 181–197, doi:10.1515/res-2022-0001.

56. Chen, J.; Chen, L.; Xie, F.; Li, X. Starch. In *Drug Delivery Applications of Starch Biopolymer Derivatives*; Springer : Singapore, Singapore, 2019; pp. 29–40.

57. Hunter, D. *Papermaking: The History and Technique of an Ancient Craft*; 1st ed.; Dover Publications, Inc: New York, U.S.A., 1978;

58. Muslim Heritage The Beginning of the Paper Industry Available online: https://muslimheritage.com/paper-industry/ (accessed on 21 September 2023).

59. Henry, W.; et al Sizing/Resizing. In *Paper Conservation Catalog*; American Institute for Conservation, Book and Paper Group: Washington D.C., U.S.A., 1988.

60. Garlick, K. A Brief Review of the History of Sizing and Resizing Practices. *Book Pap Group Annu* 1986, *5*.

61. Bloom, J.M. *Paper before Print: The History and Impact of Paper in the Islamic World*; Yale University Press: New Haven, U.S.A.; London, U.K., 2001;

62. Georgia Institute of Technology Robert C. Williams Museum of Papermaking Available online: https://paper.gatech.edu/advent-paper-machine (accessed on 15 March 2024).

63. The Editors of Encyclopaedia Britannica Bryan Donkin Available online: https://www.britannica.com/biography/Bryan-Donkin (accessed on 26 February 2024).

64. Tumosa, C.S.; Erhardt, D.; Hufford, K.; Quasney, E. The Deterioration of Newsprint and Implications for Its Preservation. *WAAC Newsletter* **2008**, *30*.

65. CEPI Press Release: The Paper Value Chain Reached a 70,5% Recycling Rate in 2022 Available online: https://www.cepi.org/press-release-the-paper-value-chain-reached-a-705-recycling-rate-in-2022/ (accessed on 21 September 2023).

66. UPM Communication Papers Sustainability in the Paper Industry Available online: https://www.upmpaper.com/sustainability/sustainability-paper-industry/ (accessed on 16 December 2023).

67. Aryal, G.M.; Kandel, K.P.; Bhattarai, R.K.; Giri, B.; Adhikari, M.; Ware, A.; Han, S.; George, G.; Luo, Z.; Gautam, B.R.; et al. Material Properties of Traditional Handmade Paper Samples Fabricated from Cellulosic Fiber of Lokta Bushes. *ACS Omega* **2022**, *7*, 32717–32726, doi:10.1021/acsomega.2c04398.

68. Szczepanowska, H. *Biodeterioration of Cultural Heritage: Dynamic Interfaces between Fungi, Fungal Pigments and Paper*; MDPI: Basel, Switzerland, 2023;

69. Szczepanowska, H.M. *Conservation of Cultural Heritage: Key Principles and Approaches*; 1st ed.; Routledge: Abingdon, U.K., 2013;

70. Schweidler, M. *The Restoration of Engravings, Drawings, Books, and Other Works on Paper*; Perkinson, R., Ed.; 1st ed.; Getty Conservation Institute: Los Angeles, U.S.A., 2006;

71. Chelazzi, D.; Giorgi, R.; Baglioni, P. Inorganic Nanoparticles for the Deacidification of Waterlogged Wood. In *Nanoscience for the Conservation of Works of Art*; Baglioni, P., Chelazzi, D., Eds.; RSC : Cambridge, U.K., 2013; pp. 430–467.

72. Lu, Y.; Lu, Y.-C.; Hu, H.-Q.; Xie, F.-J.; Wei, X.-Y.; Fan, X. Structural Characterization of Lignin and Its Degradation Products with Spectroscopic Methods. *Journal of Spectroscopy* **2017**, 1–15, doi:10.1155/2017/8951658.

73. Colburn, A.; Vogler, R.J.; Patel, A.; Bezold, M.; Craven, J.; Liu, C.; Bhattacharyya, D. Composite Membranes Derived from Cellulose and Lignin Sulfonate for Selective Separations and Antifouling Aspects. *Nanomaterials* **2019**, *9*.

74. Davidson, R.S.; Choudhury, H.; Origgi, S.; Castellan, A.; Trichet, V.; Capretti, G. The Reaction of Phloroglucinol in the Presence of Acid with Lignin-Containing Materials. *J Photochem Photobiol A Chem* **1995**, *91*, 87–93.

75. TAPPI T 401 - Fiber Analysis of Paper and Paperboard 2020.

76. Sharma, B.; Dhuldhoya, N.; Merchant, S.; Merchant, U. An Overview on Pectins. *Times Food Processing Journal* **2006**, 44–51.

77. Gigac, J.; Fišerová, M.; Rosenberg, M. Improvement of Paper Strength via Surface Application of Sugar Beet Pectin. *Chemical Papers* **2008**, *62*, 509–515, doi:10.2478/s11696-008-0059-2.

78. Hummert, E. Resizing: A Brief Review of Restoration and Conservation Literature from the 17th to the 21st Century. *Restaurator* 2019, *40*, 219–237.

79. Gorassini, A.; Calvini, P.; Baldin, A. *Fourier Transform Infrared Spectroscopy (FTIR) Analysis of Historic Paper Documents as a Preliminary Step for Chemometrical Analysis*; 2008;

80. Hubbe, M.A.; Gill, R.A. Fillers for Papermaking: A Review of Their Properties, Usage Practices, and Their Mechanistic Role. *Bioresources* **2016**, *11*, 2886–2963.

81. Mousavipazhouh, H.; Azadfallah, M.; Jouybari, I.R. Encapsulation of Precipitated Calcium Carbonate Fillers Using Carboxymethyl Cellulose /Polyaluminium Chloride: Preparation and Its Influence on Mechanical and Optical Properties of Paper. *Maderas: Ciencia y Tecnologia* **2018**, *20*, 703–714, doi:10.4067/S0718-221X2018005041601.

82. WebExhibits Pigments through the Ages Available online: https://www.webexhibits.org/pigments/intro/pigments.html (accessed on 10 March 2024).

83. Benkhaya, S.; M' rabet, S.; El Harfi, A. A Review on Classifications, Recent Synthesis and Applications of Textile Dyes. *Inorg Chem Commun* **2020**, *115*, doi:10.1016/j.inoche.2020.107891.

84. IARC Monographs Working Group General Introduction to the Chemistry of Dyes. In *IARC Monographs on the Evaluation of Carcinogenic Risks to Humans. Some*

Aromatic Amines, Organic Dyes, and Related Exposures; International Agency for Research on Cancer: Lyon, France, 2010; Vol. 99.

85. Margarit, A. Oak Gall Ink Explained Available online: http://www.medievalcodes.ca/2020/01/oak-gall-ink-explained.html (accessed on 10 March 2024).

86. Fine Art Restoration Co. Soot and Sepia: The Preservation of Ink Drawings Available online: https://fineart-restoration.co.uk/news/soot-and-sepia-the-preservation-of-ink-drawings/ (accessed on 10 March 2024).

87. Werner, S. *Studying Early Printed Books 1450 - 1800: A Practical Guide*; 1st ed.; Wiley-Blackwell: Hoboken, NJ, U.S.A., 2019;

88. Neumann, S. Mechanising Handmade Paper: Traditional and Modern Paper Production in 19th-Century Europe. In *Paper Stories - Paper and Book History in Early Modern Europe*; De Gruyter, 2023; pp. 91–110 ISBN 9783111162768.

89. Art on Paper Discussion Group Imaging in Practice: Techniques for the Examination of Works of Art on Paper. *The Book and Paper Group Annual* **2020**, *39*, 176–187.

90. Brown, N.; Lichtblau, D.; Fearn, T.; Strlič, M. Characterisation of 19th and 20th Century Chinese Paper. *Herit Sci* **2017**, *5*, doi:10.1186/s40494-017-0158-x.

91. Kamarudin, Z. Integrating Scientific Analysis in the Second-Year Studio Project for Craft Product Using Handmade Paper. *South East Asia Journal of Contemporary Business, Economics and Law* **2019**, *20*, 55–64.

92. Beghello, L. Some Factors That Influence Fiber Flocculation. *Nord Pulp Paper Res J* **1998**, *13*, 274–279.

93. ARMACAD Heritage Studies Research and Study Opportunities Available online: https://armacad.info/discipline/heritage-studies (accessed on 30 October 2023).

94. Republika Hrvatska - Ministarstvo kulture i medija Kulturna Baština Available online: https://min-kulture.gov.hr/?id=349&pregled=1&datum=Wed%20Jan%2023%202019%2017:02:19%20GMT+0100%20(srednjoeuropsko%20standardno%20vrijeme) (accessed on 8 April 2023).

95. UNESCO Institute for Statistics Cultural Heritage Available online: https://uis.unesco.org/en/glossary-term/cultural-heritage (accessed on 11 March 2024).

96. UNESCO *Convention Concerning the Protection of the World Cultural and Natural Heritage*; UNESCO: Paris, France, 1972;

97. Council of Europe Most Relevant Documents of UNESCO Concerning Cultural Heritage Available online: https://www.coe.int/en/web/herein-system/unesco (accessed on 27 March 2024).

98. Canadian Conservation Institute Agents of Deterioration Available online: https://www.canada.ca/en/conservation-institute/services/agents-deterioration.html (accessed on 25 March 2023).

99. Ballestrem, A.; von Imhoff, H.C.; McMillan, E.; Perrot, P.N. The Conservator-Restorer: A Definition of the Profession. *The International Journal of Museum Management and Curatorship* **1984**, *3*, 75–78.

100. Foot, M. Preservation Policy and Planning. In *Preservation management for libraries, archives and museums*; Gorman, G.E., Shep, S.J., Eds.; Facet Publishing: London, U.K., 2006; pp. 19–41.

101. Porck, H.J.; Ligterink, F.J.; Bruin, G.; Scholten, S. Valuation Model for Paper Conservation Research. In *Preservation management for libraries, archives and museums*; Gorman, G.E., Shep, S.J., Eds.; Facet Publishing: London, U.K., 2006; pp. 83–96.

102. Feller, R.L. *Accelerated Aging: Photochemical and Thermal Aspects*; Berland, D., Ed.; Getty Conservation Institute: Los Angeles, U.S.A., 1994; ISBN 0892361255.

103. Library of Congress The Deterioration and Preservation of Paper: Some Essential Facts Available online: https://www.loc.gov/preservation/care/deterioratebrochure.html (accessed on 14 March 2024).

104. TAPPI T 509 - Hydrogen Ion Concentration (PH) of Paper Extracts (Cold Extraction Method) 2014.

105. TAPPI T 529 - Surface PH Measurement of Paper 2021.

106. Ahn, K.; Hartl, A.; Hofmann, C.; Henniges, U.; Potthast, A. Investigation of the Stabilization of Verdigris-Containing Rag Paper by Wet Chemical Treatments. *Herit Sci* **2014**, *2*, doi:10.1186/2050-7445-2-12.

107. Baranaski, A.; Lagan, J.M.; Lojewski, T. Acid-Catalysed Degradation. In *Ageing and stabilisation of paper*; Strlič, M., Kolar, J., Eds.; National and University Library: Ljubljana, Slovenia, 2005; pp. 93–109.

108. Thomson, G. *The Museum Environment*; Oddy, A., Lintrum, D., Eds.; 2nd ed.; Butterworth-Heinemann Ltd.: London, U.K., 1986;

109. Hatchfield, P.B. *Pollutants in the Museum Environment: Practical Strategies for Problem Solving in Design, Exhibition and Storage*; Archetype Publications: London, 2002;

110. Zhang, X.; Yan, Y.; Yao, J.; Jin, S.; Tang, Y. Chemistry Directs the Conservation of Paper Cultural Relics. *Polym Degrad Stab* **2023**, *207*, 110228, doi:10.1016/J.POLYMDEGRADSTAB.2022.110228.

111. Library of Congress Care, Handling, and Storage of Works on Paper Available online: https://www.loc.gov/preservation/care/paper.html (accessed on 4 November 2023).

112. Michalski, S. Agent of Deterioration: Light, Ultraviolet and Infrared Available online: https://www.canada.ca/en/conservation-institute/services/agents-deterioration/light.html (accessed on 20 March 2023).

113. Saunders, D. *Museum Lighting: A Guide for Conservators and Curators*; The Getty Conservation Institute: Los Angeles, U.S.A., 2020;

114. Haillant, O.; Fromageot, D.; Lemaire, J. Experimental Techniques in the Studies of Photo-Stability. In *Ageing and stabilisation of paper*; Strlič, M., Kolar, J., Eds.; National and University Library: Ljubljana, Slovenia, 2005; pp. 49–70.

115. Kolar, J.; Strlič, M.; Malešič, J.; Lemaire, J.; Fromageot, D. Photooxidative Degradation. In *Ageing and stabilisation of paper*; Strlič, M., Kolar, J., Eds.; National and University Library: Ljubljana, Slovenia, 2005; pp. 149–162.

116. Malešič, J.; Kolar, J.; Strlič, M.; Kočar, D.; Fromageot, D.; Lemaire, J.; Haillant, O. Photo-Induced Degradation of Cellulose. *Polym Degrad Stab* **2005**, *89*, 64–69, doi:10.1016/j.polymdegradstab.2005.01.003.

117. Jiménez-Reyes, M.; Tenorio, D.; García-Rosales, G.; Jiménez- Becerril, J.; Luna-Castro, G.E. Effects of UV Radiation on Paper: A Chromatic Study. *Brazilian Journal of Analytical Chemistry* **2021**, *8*, 34–47, doi:10.30744/BRJAC.2179-3425.AR-51-2020.

118. Gijsman, P.; Diepens, M. Photolysis and Photooxidation in Engineering Plastics. In Proceedings of the ACS Symposium Series; American Chemical Society, January 1 2009; Vol. 1004, pp. 287–306.

119. Rychlý, J.; Strlič, M. Degradation and Ageing of Polymers. In *Ageing and stabilisation of paper*; Strlič, M., Kolar, J., Eds.; National and University Library: Ljubljana, Slovenia, 2005; pp. 9–23.

120. Jablonsky, M.; Šima, J. Oxidative Degradation of Paper – A Minireview. *J Cult Herit* 2021, *48*, 269–276.

121. Bandelli, D.; Mastrangelo, R.; Poggi, G.; Chelazzi, D.; Baglioni, P. New Sustainable Polymers and Oligomers for Cultural Heritage Conservation. *Chem Sci* **2024**, doi:10.1039/D3SC03909A.

122. Strlič, M.; Kolar, J.; Pihlar, B. Methodology and Analytical Techniques in Paper Stability Studies. In *Ageing and stabilisation of paper*; Strlič, M., Kolar, J., Eds.; National and University Library: Ljubljana, Slovenia, 2005; pp. 27–47.

123. Michalski, S. Double the Life for Each Five-Degree Drop, More than Double the Life for Each Halving of Relative Humidity. In Proceedings of the 13th Triennial meeting Rio de Janeiro preprints vol.1; ICOM-CC: Rio De Janeiro, Brazil, 2002; pp. 66–72.

124. Mailhot, B.; Gardette, J.L. *Mechanism of Thermolysis, Thermooxidation and Photooxidation of Polyacrylonitrile*; 1994; Vol. 44;.

125. Van Der Reyden, D. Recent Scientific Research in Paper Conservation. *Journal of the American Institute for Conservation* **1992**, *31*, 117–138.

126. Małachowska, E.; Pawcenis, D.; Dańczak, J.; Paczkowska, J.; Przybysz, K. Paper Ageing: The Effect of Paper Chemical Composition on Hydrolysis and Oxidation. *Polymers (Basel)* **2021**, *13*, doi:10.3390/polym13071029.

127. Małachowska, E.; Dubowik, M.; Boruszewski, P.; Łojewska, J.; Przybysz, P. Influence of Lignin Content in Cellulose Pulp on Paper Durability. *Sci Rep* **2020**, *10*, doi:10.1038/s41598-020-77101-2.

128. Strlič, M.; Rychlý, J.; Haillant, O.; Kočar, D.; Kolar, J. Chemiluminiscence of Cellulose and Paper. In *Ageing and stabilisation of paper*; Strlič, M., Kolar, J., Eds.; National and University Library: Ljubljana, Slovenia, 2005.

129. White, J.R. Polymer Ageing: Physics, Chemistry or Engineering? Time to Reflect. *Comptes Rendus Chimie* **2006**, *9*, 1396–1408, doi:10.1016/j.crci.2006.07.008.

130. Savković, Ž.; Stupar, M.; Unković, N.; Knežević, A.; Vukojević, J.; Grbić, M.L. Fungal Deterioration of Cultural Heritage Objects. In *Biodegradation Technology of Organic and Inorganic Pollutants*; Mendes, K.E., Ed.; IntechOpen, 2021.

131. Ejaz, U.; Sohail, M.; Ghanemi, A. Cellulases: From Bioactivity to a Variety of Industrial Applications. *Biomimetics* 2021, *6*.

132. Pinzari, F.; Gutarowska, B. Extreme Colonizers and Rapid Profiteers: The Challenging World of Microorganisms That Attack Paper and Parchment. In *Microorganisms in the Deterioration and Preservation of Cultural Heritage*; Joseph, E., Ed.; Springer International Publishing, 2021; pp. 79–113.

133. Srivastava, A.K.; Singh, R.K.; Singh, D. Microbe-Based Bioreactor System for Bioremediation of Organic Contaminants: Present and Future Perspective. In *Microbe Mediated Remediation of Environmental Contaminants*; Kumar, A., Kumar Singh, V., Singh, P., Kumar Mishra, V., Eds.; Elsevier, 2020; pp. 241–253 ISBN 9780128211991.

134. IFLA Core Programme on Preservation and Conservation (PAC); Council on Library and Information Resources (CLIR); Adcock, E.P.; Varlamoff, M.-T.; Kremp, V. IFLA Principles for the Care and Handling of Library Material. *International Preservation Issues: No. 1*. 1998.

135. Bobu, E.; Nicu, R.; Obrocea, P.; Ardelean, E.; Dunca, S.; Bălăeş, T. Antimicrobial Properties of Coatings Based on Chitosan Derivatives for Applications in Sustainable Paper Conservation. *Cellulose Chemistry and Technology* **2016**, *50*, 689–699.

136. Mustafa, H.K.; Anwer, S.S.; Zrary, T.J. Influence of PH, Agitation Speed, and Temperature on Growth of Fungi Isolated from Koya, Iraq. *Kuwait Journal of Science* **2023**, doi:10.1016/J.KJS.2023.02.036.

137. Kasonga, T.K.; Coetzee, M.A.A.; Kamika, I.; Momba, M.N.B. Isolation and Identification of South African Indigenous Fungal Strains and Assessment of Their Ability to Degrade Diclofenac in Synthetic Wastewater. *Fungi Bio-prospects in Sustainable Agriculture, Environment and Nano-technology: Volume 2: Extremophilic Fungi and Myco-mediated Environmental Management* **2021**, 213–249, doi:10.1016/B978-0-12-821925-6.00011-3.

138. Pietikäinen, J.; Pettersson, M.; Bååth, E. Comparison of Temperature Effects on Soil Respiration and Bacterial and Fungal Growth Rates. *FEMS Microbiol Ecol* **2005**, *52*, 49–58, doi:10.1016/j.femsec.2004.10.002.

139. Hasan, A.M.; AL-Jubori, M.H. Determination of Optimal Temperature and PH for Radial Growth of Some Dermatophyte Species Isolated from Leukemia Patients. *J Sci* **2015**, *56*, 95–99.

140. Tapia, M.S.; Alzamora, S.M.; Chirife, J. Effects of Water Activity (a w) on Microbial Stability: As a Hurdle in Food Preservation. In *Water Activity in Foods: Fundamentals and Applications*; Barbosa-Cánovas, G. V, Fontana Jr, A.J., Schmidt, S.J., Labuza, T.P., Eds.; Wiley-Blackwell: Hoboken, NJ, U.S.A., 2007; pp. 239–271.

141. Hagiwara, D.; Sakamoto, K.; Abe, K.; Gomi, K. Signaling Pathways for Stress Responses and Adaptation in Aspergillus Species: Stress Biology in the Post-Genomic Era. *Biosci Biotechnol Biochem* **2016**, *80*, 1667–1680, doi:10.1080/09168451.2016.1162085.

142. Baldauf, S.L.; Palmert, J.D. Animals and Fungi Are Each Other's Closest Relatives: Congruent Evidence from Multiple Proteins. *Proc. Natl. Acad. Sci. USA* **1993**, *90*, 11558–11562.

143. Pinheiro, A.C.; Sequeira, S.O.; Macedo, M.F. Fungi in Archives, Libraries, and Museums: A Review on Paper Conservation and Human Health. *Crit Rev Microbiol* **2019**, *45*, 686–700, doi:10.1080/1040841X.2019.1690420.

144. Sanmartín, P.; Noya-Pintos, D.; Fuentes, E.; Pozo-Antonio, J.S. Cracks in Consolidants Containing TiO2 as a Habitat for Biological Colonization: A Case of Quaternary Bioreceptivity. *Materials Science and Engineering C* **2021**, *124*, doi:10.1016/j.msec.2021.112058.

145. Singaravelan, N.; Grishkan, I.; Beharav, A.; Wakamatsu, K.; Ito, S.; Nevo, E. Adaptive Melanin Response of the Soil Fungus Aspergillus Niger to UV Radiation Stress at "Evolution Canyon", Mount Carmel, Israel. *PLoS One* **2008**, *3*, doi:10.1371/journal.pone.0002993.

146. Rakotonirainy, M.S.; Bénaud, O.; Vilmont, L.B. Contribution to the Characterization of Foxing Stains on Printed Books Using Infrared Spectroscopy and Scanning Electron Microscopy Energy Dispersive Spectrometry. *Int Biodeterior Biodegradation* **2015**, *101*, 1–7, doi:10.1016/j.ibiod.2015.02.031.

147. Dufossé, L.; Fouillaud, M.; Caro, Y.; Mapari, S.A.S.; Sutthiwong, N. Filamentous Fungi Are Large-Scale Producers of Pigments and Colorants for the Food Industry. *Curr Opin Biotechnol* 2014, *26*, 56–61.

148. Gessler, N.N.; Egorova, A.S.; Belozerskaya, T.A. Melanin Pigments of Fungi under Extreme Environmental Conditions (Review). *Appl Biochem Microbiol* **2014**, *50*, 105–113, doi:10.1134/S0003683814020094.

149. Gupta, C.; Jain, P.; Kumar, D.; Dixit, A.K.; Jain, R.K. Production of Cellulase Enzyme from Isolated Fungus and Its Application as Efficient Refining Aid for Production of Security Paper. *IJAMBR* **2015**, *3*, 11–19.

150. Jayasekara, S.; Ratnayake, R. Microbial Cellulases: An Overview and Applications. In *Cellulose*; Pascual, A.R., Martin, M.E.E., Eds.; IntechOpen, 2019.

151. Mycorena The Industrial Possibilities of Fungi Available online: https://mycorena.com/mycotalks/the-industrial-possibilities-of-fungi (accessed on 7 January 2024).

152. Sequeira, S.O.; Phillips, A.J.L.; Cabrita, E.J.; Macedo, M.F. Ethanol as an Antifungal Treatment for Paper: Short-Term and Long-Term Effects. *Studies in Conservation* **2017**, *62*, 33–42, doi:10.1080/00393630.2015.1137428.

153. Menicucci, F.; Palagano, E.; Michelozzi, M.; Ienco, A. Essential Oils for the Conservation of Paper Items. *Molecules* **2023**, *28*, 5003, doi:10.3390/molecules28135003.

154. Fouda, A.; Abdel-Maksoud, G.; Saad, H.A.; Gobouri, A.A.; Mohammedsaleh, Z.M.; El-Sadany, M.A.H. The Efficacy of Silver Nitrate (AgNo3) as a Coating Agent to Protect Paper against High Deteriorating Microbes. *Catalysts* **2021**, *11*, 1–18, doi:10.3390/catal11030310.

155. Sequeira, S.; Cabrita, E.J.; Macedo, M.F. Antifungals on Paper Conservation: An Overview. *Int Biodeterior Biodegradation* **2012**, *74*, 67–86, doi:10.1016/j.ibiod.2012.07.011.

156. Michaelsen, A.; Pinzari, F.; Barbabietola, N.; Piñar, G. Monitoring the Effects of Different Conservation Treatments on Paper-Infecting Fungi. *Int Biodeterior Biodegradation* **2013**, *84*, 333–341, doi:10.1016/j.ibiod.2012.08.005.

157. Ioanid, E.G.; Frunză, ,V; Rusu, D.; Vlad, A.M.; Tanase, C.; Dunca, S. Radio-Frequency Plasma Discharge Equipment for Conservation Treatments of Paper Supports. *International Journal of Chemical and Molecular Engineering* **2015**, *9*, 760–764.

158. Hoppanová, L.; Kryštofová, S. Nonthermal Plasma Effects on Fungi: Applications, Fungal Responses, and Future Perspectives. *Int. J. Mol. Sci* **2022**, *2022*, 11592, doi:10.3390/ijms.

159. Rakotonirainy, M.; Hanus, J.; Bonassies-Termes, S.; Heraud, C.; Lavédrine, B. Detection of Fungi and Control of Disinfection by ATP-Bioluminescence Assay. *AICCM Bulletin* **2003**, *28*, 16–22, doi:10.1179/bac.2003.28.1.004.

160. ICOM-CC Terminology to Characterize the conservation of Tangible Cultural Heritage. In Proceedings of the Resolution adopted by the ICOM-CC membership at the 15th Triennial Conference, New Delhi, 22-26 September 2008; 2008.

161. Torraca, G. The Scientist's Role in Historic Preservation with Particular Reference to Stone Conservation. In *Readings in Conservation - Historical and Philosophical Issues in the Conservation of Cultural Heritage*; Price, N.S., Talley Jr, M.K., Melucco Vaccaro, A., Eds.; The Getty Conservation Institute: Los Angeles, U.S.A., 1996; pp. 439–444.

162. Mizumura, M.; Kubo, T.; Moriki, T. Japanese Paper: History, Development and Use in Western Paper Conservation. In Proceedings of the Adapt & Evolve 2015: East Asian Materials and Techniques in Western Conservation. Proceedings from the International Conference of the Icon Book & Paper Group, London 8–10 April 2015; The Institute of Conservation: London, 2017; pp. 43–59.

163. Northeast Document Conservation Center Repairing Paper Artifacts Available online: https://nsrc.org/workshops/2012/nsrc-library-senegal/raw-

attachment/wiki/References/NEDCC_Repairing_Paper_Artifacts.pdf (accessed on 25 August 2023).

164. The Conservation Unit of the Museums and Galleries Commission *The Science for Conservators Series Volume 1: An Introduction to Materials*; Ashley-Smith, J., Wilks, H., Eds.; 2nd ed.; Routledge: London, U.K., 1992; Vol. 1;.

165. De Filpo, G.; Palermo, A.M.; Tolmino, R.; Formoso, P.; Nicoletta, F.P. Gellan Gum Hybrid Hydrogels for the Cleaning of Paper Artworks Contaminated with Aspergillus Versicolor. *Cellulose* **2016**, *23*, 3265–3279, doi:10.1007/s10570-016-1021-z.

166. De Filpo, G.; Palermo, A.M.; Munno, R.; Molinaro, L.; Formoso, P.; Nicoletta, F.P. Gellan Gum/Titanium Dioxide Nanoparticle Hybrid Hydrogels for the Cleaning and Disinfection of Parchment. *Int Biodeterior Biodegradation* **2015**, *103*, 51–58, doi:10.1016/j.ibiod.2015.04.012.

167. Afsharpour, M.; Gilani, S. Guar Gum Nanocomposites: Green Corrosion Inhibitors of Iron-Gall Ink on Paper Artworks. *Starch/Staerke* **2021**, *74*, doi:10.1002/star.202100174.

168. Del Curto, D.; Turrina, A. Towards a Reasoned Glossary of Green Conservation: A Semantic Review of Green-Oriented Terms in the Field of Cultural Heritage. *Sustainability* **2023**, *15*, doi:10.3390/su151612104.

169. GoGreen Green Heritage Manifesto: The First European Manifesto for More Sustainable Museums Available online: https://gogreenconservation.eu/news/green-heritage-manifesto-the-first-european-manifesto-for-more-sustainable-museums/ (accessed on 3 March 2024).

170. Butt, M.A. Thin-Film Coating Methods: A Successful Marriage of High-Quality and Cost-Effectiveness—A Brief Exploration. *Coatings* 2022, *12*.

171. Liu, Y.; Yu, S.; Shi, Q.; Ge, X.; Wang, W. Multilayer Coatings for Tribology: A Mini Review. *Nanomaterials* **2022**, *12*, doi:10.3390/nano12091388.

172. Tabakov, V.P.; Vereschaka, A.S.; Vereschaka, A.A. Multilayer Composition Coatings for Cutting Tools: Formation and Performance Properties. *Mechanics and Industry* **2017**, *18*, 706, doi:10.1051/meca/2017063.

173. Dei, L. Conservation Treatments: Cleaning, Consolidation and Protection. In *Nanoscience for the Conservation of Works of Art*; Baglioni, P., Chelazzi, D., Eds.; RSC Publishing: Cambridge, U.K., 2013; pp. 77–92.

174. ICOM-CC Terminology for Conservation (2008) Available online: https://www.icom-cc.org/en/terminology-for-conservation (accessed on 8 April 2024).

175. Artesani, A.; Turo, F. Di; Zucchelli, M.; Traviglia, A. Recent Advances in Protective Coatings for Cultural Heritage-an Overview. *Coatings* **2020**, *10*, doi:10.3390/coatings10030217.

176. Viñas, S.M. Contemporary Theory of Conservation. *Reviews in Conservation* **2002**, *3*, 25–34, doi:10.4324/9780080476834.

177. Krella, A.K. Degradation of Protective PVD Coatings. In *Handbook of Materials Failure Analysis with Case Studies from the Chemicals, Concrete and Power Industries*; Makhlouf, A.S.H., Aliofkhazraei, M., Eds.; Butterworth-Heinemann, 2016; pp. 411–440 ISBN 9780081001257.

178. Caruso, M.R.; D'Agostino, G.; Milioto, S.; Cavallaro, G.; Lazzara, G. A Review on Biopolymer-Based Treatments for Consolidation and Surface Protection of Cultural Heritage Materials. *J Mater Sci* 2023, *58*, 12954–12975.

179. Noshy, W.; Ali Hassan, R.R.; Mohammed, N. Using Biopolymers to Strengthen the Historical Printed Paper: Mechanical and Optical Characters. *Pigment and Resin Technology* **2022**, *51*, 212–226, doi:10.1108/PRT-01-2021-0008.

180. Blaxland, C.L. Adhesives in an Historic Library - a Conservator's View. *Int J Adhes Adhes* **1994**, *14*, 123–129.

181. Brückle, I. Update: Remoistenable Lining with Methyl Cellulose Adhesive Preparation. *Book Pap Group Annu* **1996**, *15*, 25–26.

182. Operamolla, A.; Mazzuca, C.; Capodieci, L.; Di Benedetto, F.; Severini, L.; Titubante, M.; Martinelli, A.; Castelvetro, V.; Micheli, L. Toward a Reversible Consolidation of Paper Materials Using Cellulose Nanocrystals. *ACS Appl Mater Interfaces* **2021**, *13*, 44972–44982, doi:10.1021/acsami.1c15330.

183. Spagnuolo, L.; D'Orsi, R.; Operamolla, A. Nanocellulose for Paper and Textile Coating: The Importance of Surface Chemistry. *Chempluschem* 2022, *87*, e202200204.

184. Baudone, F. Funori: Natural Adhesive for the Resizing of Paper Materials. In *Works of Art on Parchment and Paper: Interdisciplinary Approaches*; Golob, N., Vodopivec Tomažič, J., Eds.; Znanstvena založba Filozofske fakultete Univerze v Ljubljani: Ljubljana, 2019; Vol. 1, pp. 227–235.

185. Barrulas, R. V.; Nunes, A.D.; Sequeira, S.O.; Casimiro, M.H.; Corvo, M.C. Cleaning Fungal Stains on Paper with Hydrogels: The Effect of PH Control. *Int Biodeterior Biodegradation* **2020**, *152*, 104996, doi:10.1016/j.ibiod.2020.104996.

186. Mazzuca, C.; Micheli, L.; Carbone, M.; Basoli, F.; Cervelli, E.; Iannuccelli, S.; Sotgiu, S.; Palleschi, A. Gellan Hydrogel as a Powerful Tool in Paper Cleaning Process: A Detailed Study. *J Colloid Interface Sci* **2014**, *416*, 205–211, doi:10.1016/j.jcis.2013.10.062.

187. Biricik, Y.; Sönmez, S.; Özden, Ö. Effects of Surface Sizing with Starch on Physical Strength Properties of Paper. *Asian Journal of Chemistry* **2011**, *23*, 3151–3154.

188. Strnadovä, J.; Durovič, M. The Cellulose Ethers in Paper Conservation. *Restaurator* **1994**, *15*, 220–241.

189. Feller, R.L.; Wilt, M. *Evaluation of Cellulose Ethers for Conservation*; The Getty Conservation Institute: Los Angeles, U.S.A., 1990;

190. Sönmez, S.; Özden, Ö. Barrier Properties of Paper and Cardboard. In *Academic Researches In Architecture, Engineering Planning And Design*; Salman S, Ed.; Gece Kitaplığı: Ankara, 2018; pp. 171–183 ISBN 9786052883945.

191. Wang, J.; Hu, D.; Xing, H.; Qi, Y.; Li, Y. Facile and Scalable Conservation of Chinese Ancient Paintings Using Water-Borne Fluoropolymer. *ACS Omega* **2020**, *5*, 33162–33169, doi:10.1021/acsomega.0c04827.

192. Scientific Laboratory Supplies Ltd. Lugol Solution (Iodine/Potassium Iodide Solution) Available online: https://www.scientificlabs.co.uk/product/haematology-and-histology-stains/32922-250ML#overview (accessed on 29 March 2024).

193. Vodopivec Tomašič, J.; Avguštin Florjančič, B.; Grkman, S.; Černič, M.; Ljuba, M.; Haraurer, D.; Kotar, M.; Planinc, L.; Petelin, N.; Rahovsky Šuligoj, T. The Dalmatin Bible - Structure and Conservation. *Vjesnik bibliotekara Hrvatske* **2015**, *58*, 67–100.

194. Fairbrass, S. Sticky Problems for Conservators of Works of Art on Paper. *Int. J. Adhesion and Adhesives* **1995**, *15*.

195. Fahad, M.; Khan, M.A.; Gilbert, M. Investigation of Thermal Gel Formation of Methylcellulose in Glycols Using DSC and XRD. *Gels* **2021**, *7*, doi:10.3390/gels7040205.

196. Byakodi, M.; Shrikrishna, N.S.; Sharma, R.; Bhansali, S.; Mishra, Y.; Kaushik, A.; Gandhi, S. Emerging 0D, 1D, 2D, and 3D Nanostructures for Efficient Point-of-Care Biosensing. *Biosens Bioelectron X* **2022**, *12*, doi:10.1016/j.biosx.2022.100284.

197. Gemmellaro, P. Titanium Dioxide Nanoparticles in the Field of Conservation of Cultural Heritage, Università degli Studi di Catania Facoltà di Scienze : Catania, Italy, 2011.

198. U.S. Environmental Protection Agency *Technical Fact Sheet – Nanomaterials*; 2017;

199. Sato, K.; Li, J.-G.; Kamiya, H.; Ishigaki, T. Ultrasonic Dispersion of TiO2 Nanoparticles in Aqueous Suspension. *Journal of the American Ceramic Society* **2008**, *91*, 2481–2487, doi:10.1111/j.1551-2916.2008.02493.x.

200. Bonini, M.; Baglioni, P.; Chelazzi, D. Inorganic Nanomaterials: Synthesis and Properties. In *Nanoscience for the Conservation of Works of Art*; Baglioni, P., Chelazzi, D., Eds.; RSC Publishing: Cambridge, U.K., 2013; pp. 315–344.

201. Tantra, R.; Jing, S.; Pichaimuthu, S.K.; Walker, N.; Noble, J.; Hackley, V.A. Dispersion Stability of Nanoparticles in Ecotoxicological Investigations: The Need for Adequate Measurement Tools. *Journal of Nanoparticle Research* **2011**, *13*, 3765–3780, doi:10.1007/s11051-011-0298-y.

202. Kotov, N.A.; Meldrum, F.C.; Fendler, J.H. Monoparticulate Layers of Titanium Dioxide Nanocrystallites with Controllable Interparticle Distances. *J Phys Chem* **1994**, *98*, 8827–8830.

203. Hielscher, T. Ultrasonic Production of Nano-Size Dispersions and Emulsions. In Proceedings of the ENS 2005; Paris, France, December 2005; pp. 138–143.

204. Tso, C.P.; Zhung, C.; Shih, Y.; Tseng, Y.-M.; Wu, S.C.; Doong, R. Stability of Metal Oxide Nanoparticles in Aqueous Solutions. *Water Science and Technology* **2010**, *61*, 127–133, doi:10.2166/wst.2010.787.

205. Bartoletti, A.; Odlyha, M.; Bozec, L. Insights from the NANOforArt Project: Application of Calcium-Based Nanoparticle Dispersions for Improved Preservation of Parchment Documents. *Restaurator* **2022**, *43*, 143–158, doi:10.1515/res-2022-0005.

206. Baglioni, P.; Chelazzi, D.; Giorgi, R. Consolidation of Wall Paintings and Stone. In *Nanotechnologies in the Conservation of Cultural Heritage: A compendium of materials and techniques*; Springer Science + Business Media: Dordrecht, Netherlands, 2015; pp. 15–59.

207. Malešič, J.; Kadivec, M.; Kunaver, M.; Skalar, T.; Kralj Cigić, I. Nano Calcium Carbonate versus Nano Calcium Hydroxide in Alcohols as a Deacidification Medium for Lignocellulosic Paper. *Herit Sci* **2019**, *7*, 1–14, doi:10.1186/s40494-019-0294-6.

208. Ditaranto, N.; Van Der Werf, I.D.; Picca, R.A.; Sportelli, M.C.; Giannossa, L.C.; Bonerba, E.; Tantillo, G.; Sabbatini, L. Characterization and Behaviour of ZnO-Based Nanocomposites Designed for the Control of Biodeterioration of Patrimonial Stoneworks. *New Journal of Chemistry* **2015**, *39*, 6836–6843, doi:10.1039/c5nj00527b.

209. Roveri, M.; Gherardi, F.; Goidanich, S.; Gulotta, D.; Castelvetro, V.; Fischer, R.; Winandy, L.; Weber, J.; Toniolo, L. Self-Cleaning and Antifouling Nanocomposites for Stone Protection: Properties and Performances of Stone-Nanomaterial Systems. In Proceedings of the IOP Conference Series: Materials Science and Engineering 364; Institute of Physics Publishing, June 18 2018; Vol. 364.

210. Aleksić, G.; Cigula, T.; Vukoje, M.; Itrić Ivanda, K. Bilayer Coating Composed of Starch and Methyl Cellulose-Nanoscale TiO2 for the Protection of Historic Paper from UV. *Coatings* **2023**, *13*, 899, doi:10.3390/coatings13050899.

211. Baty, P. *The Anatomy of Color: The Story of Heritage Paints and Pigments*; 1st ed.; Thames and Hudson Ltd.: London, U.K., 2017;

212. Smijs, T.G.; Pavel, S. Titanium Dioxide and Zinc Oxide Nanoparticles in Sunscreens: Focus on Their Safety and Effectiveness. *Nanotechnol Sci Appl* 2011, *4*, 95–112.

213. He, J.; Du, Y. en; Bai, Y.; An, J.; Cai, X.; Chen, Y.; Wang, P.; Yang, X.; Feng, Q. Facile Formation of Anatase/Rutile TiO2 Nanocomposites with Enhanced Photocatalytic Activity. *Molecules* **2019**, *24*, doi:10.3390/molecules24162996.

214. Park, B.G. Photocatalytic Activity of TiO2-Doped Fe, Ag, and Ni with N under Visible Light Irradiation. *Gels* **2022**, *8*, doi:10.3390/gels8010014.

215. Banerjee, S.; Dionysiou, D.D.; Pillai, S.C. Self-Cleaning Applications of TiO2 by Photo-Induced Hydrophilicity and Photocatalysis. *Appl Catal B* **2015**, *176–177*, 396–428, doi:10.1016/j.apcatb.2015.03.058.

216. La Russa, M.F.; Rovella, N.; Alvarez De Buergo, M.; Belfiore, C.M.; Pezzino, A.; Crisci, G.M.; Ruffolo, S.A. Nano-TiO2 Coatings for Cultural Heritage Protection: The Role of the Binder on Hydrophobic and Self-Cleaning Efficacy. *Prog Org Coat* **2016**, *91*, 1–8, doi:10.1016/j.porgcoat.2015.11.011.

217. Afsharpour, M.; Hadadi, M. Titanium Dioxide Thin Film: Environmental Control for Preservation of Paper-Art-Works. *J Cult Herit* **2014**, *15*, 569–574, doi:10.1016/j.culher.2013.10.008.

218. The European Commission Goodbye E171: The EU Bans Titanium Dioxide as a Food Additive Available online: https://ec.europa.eu/newsroom/sante/items/732079/en (accessed on 29 March 2023).

219. Franco-Castillo, I.; Hierro, L.; de la Fuente, J.M.; Seral-Ascaso, A.; Mitchell, S.G. Perspectives for Antimicrobial Nanomaterials in Cultural Heritage Conservation. *Chem* **2021**, *7*, 629–669, doi:10.1016/j.chempr.2021.01.006.

220. Kang, X.; Liu, S.; Dai, Z.; He, Y.; Song, X.; Tan, Z. Titanium Dioxide: From Engineering to Applications. *Catalysts* 2019, *9*, 1–32.

221. Veleva, L. Protective Coatings and Inorganic Anti-Corrosion Pigments. In *Paint and Coatings Testing Manual Book*; Koleske, J. V, Ed.; ASTM International, 2012; p. 282.

222. Moma, J.; Baloyi, J. Modified Titanium Dioxide for Photocatalytic Applications. In *Photocatalysts - Applications and Attributes*; Khan, S.B., Ed.; IntechOpen, 2019; pp. 37–56.

223. Mardare, L.; Benea, L. Effects of TiO2 Nanoparticles on the Corrosion Protection Ability of Polymeric Primer Coating System. *Polymers (Basel)* **2021**, *13*, 1–16, doi:10.3390/polym13040614.

224. Japico Japanese Fine Papers from 30 g/Sqm On Available online: https://japico-shop.eu/635-781-Takogami-B-43-g/sqm-in-sheets-size-68-x-98-cm-Japico-Japanese-tissues-for-restoration-/-Japanese-fine-papers-for-fine-art-and-prints-tissus-japonais-pour-la-restauration-/-papiers-fins-japonais-pour-les-beaux-arts-et-de-gravures (accessed on 2 October 2023).

225. Sprinter Flint K+E Novavit F918 Supreme Bio Available online: https://www.sprinter.com.au/flint-ke-novavit-f918-supreme-bio/ (accessed on 28 January 2024).

226. FlintGroup Novavit® F 918 SUPREME BIO Available online: flintgrp.com/media/4270/sf_process_ti_f918_e.pdf (accessed on 24 January 2024).

227. Talas Wheat Paste No. 301 Available online: https://www.talasonline.com/Wheat-Paste-No-301 (accessed on 6 April 2024).

228. Talas Methyl Cellulose Available online: https://www.talasonline.com/Methyl-Cellulose (accessed on 5 March 2023).

229. U.S. Research Nanomaterials Inc Titanium Oxide Nanopowder / Nanoparticles (TiO2, Anatase, 99.9%, 18nm) Available online: https://www.us-nano.com/inc/sdetail/269 (accessed on 6 April 2024).

230. Chen, X.; Hosseini, S.N.; van Huis, M.A. Heating-Induced Transformation of Anatase TiO2 Nanorods into Rock-Salt TiO Nanoparticles: Implications for Photocatalytic and Gas-Sensing Applications. *ACS Appl Nano Mater* **2022**, *5*, 1600–1606, doi:10.1021/acsanm.1c04346.

231. The Conservation Unit of the Museums and Galleries Commission *The Science for Conservators Series Volume 3: Adhesives and Coatings*; Ashley-Smith, J., Ed.; 2nd ed.; Routledge: London, U.K., 1992; Vol. 3;.

232. Farnsworth, D. *Sidedness: Wire and Felt Side of Handmade Paper*; Stone, N., Ed.; Magnolia Editions: Oakland, U.S.A., 2018;

233. Cappa, F.; Fruehmann, B.; Schreiner, M. Raman Spectroscopy for the Material Analysis of Medieval Manuscripts. In *Nanotechnologies and Nanomaterials for Diagnostic, Conservation and Restoration of Cultural Heritage*; Lazzara, G., Fakhrullin, R., Eds.; Elsevier: Amsterdam, Netherlands; Cambridge, MA, U.S.A., 2019; pp. 127–147 ISBN 9780128139103.

234. Carter, H.; Bégin, P.; Grattan, D. Migration of Volatile Compounds through Stacked Sheets of Paper during Accelerated Ageing Part 1: Acid Migration at 90° C. *Restaurator* **2000**, *21*, 77–84.

235. Havermans, J. Effects of Air Pollutants on the Accelerated Ageing of Cellulose-Based Materials. *Restaurator* **1995**, *16*, 209–233.

236. Caulfield, D.F.; Gunderson, D.E. Paper Testing and Strength Characteristics. In Proceedings of the TAPPI proceedings of the 1988 paper preservation symposium; October 19-21, 1988, Washington DC, U.S.A.; TAPPI Press: Washington DC, U.S.A., 1988; pp. 31–40.

237. Darwish, S.S. Evaluation of the Effectiveness of Some Consolidants Used for the Treatment of the XIXth Century Egyptian Cemetery Wall Paintings. *International journal of conservation science* **2013**, *4*, 413–422.

238. Indictor, N.; Baer, N.S.; Phelan, W.H. An Evaluation of Pastes for Use in Paper Conservation. *Restaurator* **1975**, *2*, 139–150.

239. Sappi Europe SA Paper Standards & Measurements 2007.

240. Brundle, C.R.; Evans Jr, C.A.; Wilson, S. *Encyclopedia of Materials Characterization: Surfaces, Interfaces, Thin Films*; Fitzpatrick, L.E., Ed.; Butterworth-Heinemann: Stoneham, U.S.A., 1992;

241. JEOL What Is Scanning Electron Microscopy? Available online: https://www.jeolusa.com/RESOURCES/Electron-Optics/Scanning-Electron-Microscopy-Basics.

242. Mautner, A.; Hakalahti, M.; Rissanen, V.; Tammelin, T. Crucial Interfacial Features of Nanocellulose Materials. In *Nanocellulose and Sustainability: Production, Properties, Applications and Case Studies*; Lee, K.-Y., Ed.; CRC Press: Boca Raton, 2018; pp. 87–128.

243. Vuckovac, M.; Latikka, M.; Liu, K.; Huhtamäki, T.; Ras, R.H.A. Uncertainties in Contact Angle Goniometry. *Soft Matter* **2019**, *15*, 7089–7096, doi:10.1039/c9sm01221d.

244. Caminati, G. Cultural Heritage Artefacts and Conservation: Surfaces and Interfaces. In *Nanoscience for the Conservation of Works of Art*; Baglioni, P., Chelazzi, D., Eds.; RSC Publishing: Cambridge, U.K., 2013; pp. 1–48.

245. Michigan Metrology, L. Average Roughness Basics Available online: https://michmet.com/average-roughness-basics/ (accessed on 22 October 2023).

246. Agate, S.; Williams, A.; Dougherty, J.; Velev, O.D.; Pal, L. Polymer Color Intelligence: Effect of Materials, Instruments, and Measurement Techniques - A Review. *ACS Omega* 2023, *8*, 23257–23270.

247. Mokrzycki, W.; Tatol, M. Colour Difference ΔE-A Survey. *Machine Graphics and Vision* **2011**, *20*, 383–411.

248. Instytut Fotonowy Micro Fading Tester Available online: https://www.fotonowy.pl/products/micro-fading-tester/ (accessed on 15 March 2024).

249. Sevastyanova, O.; Li, J.; Gellerstedt, G. On the Reaction Mechanism of the Thermal Yellowing of Bleached Chemical Pulps. *Nord Pulp Paper Res J* **2006**, *21*, 188–192.

250. Mosca Conte, A.; Pulci, O.; Knapik, A.; Bagniuk, J.; Del Sole, R.; Lojewska, J.; Missori, M. Role of Cellulose Oxidation in the Yellowing of Ancient Paper. *Phys Rev Lett* **2012**, *108*, doi:10.1103/PhysRevLett.108.158301.

251. Budischowsky, D.; Zwirchmayr, N.S.; Hosoya, T.; Bacher, M.; Hettegger, H.; Potthast, A.; Rosenau, T. Degradation of Cellulosic Key Chromophores by Ozone: A Mechanistic and Kinetic Study. *Cellulose* **2021**, *28*, 6051–6071, doi:10.1007/s10570-021-03909-4.

252. Farnood, R. Optical Properties of Paper: Theory and Practice. In *Advances in Pulp and Paper Research, Oxford 2009, Trans. of the XIVth Fund. Res. Symp. Oxford, 2009*; I'Anson, S.J., Ed.; FRC: Manchester, U.K., 2018; pp. 273–352.

253. Van Der Reyden, D.; Hofmann, C.; Baker, M. Effects of Aging and Solvent Treatments on Some Properties of Contemporary Tracing Papers. *JAIC* **1993**, *32*, 177–206.

254. Imbotec Group Gloss Introduction Available online: http://www.gloss-meters.com/GlossIntro2.html (accessed on 16 October 2023).

255. Marshall, J.; Johnsen, S. Fluorescence as a Means of Colour Signal Enhancement. *Phil. Trans. R. Soc. B* **2017**, *372*, 20160335, doi:10.1098/rstb.2016.0335.

256. Midwest Optical Systems, I. Fluorescence Available online: https://midopt.com/solutions/monochrome-imaging/fluorescence/.

257. Donaldson, L.A.; Radotic, K. Fluorescence Lifetime Imaging of Lignin Autofluorescence in Normal and Compression Wood. *J Microsc* **2013**, *251*, 178–187, doi:10.1111/jmi.12059.

258. Dolovski, A.M.; Ivanda, K.I.; Kulčar, R.; Preprotić, S.P. Fluorescence Spectroscopic Analysis of Biodegraded Pressure-Sensitive Labels Made from Agro-Industrial and Post-Consumer Waste. In Proceedings of the International Symposium on Graphic Engineering and Design; University of Novi Sad - Faculty of Technical Sciences, Department of Graphic Engineering and Design, 2022; pp. 777–784.

259. Kenkel, J. *Analytical Chemistry for Technicians*; 3rd ed.; CRC Press LLC: Boca Raton, U.S.A., 2003;

260. Karlovits, M.; Gregor-Svetec, D. Durability of Cellulose and Synthetic Papers Exposed to Various Methods of Accelerated Ageing. *Acta Polytechnica Hungarica* **2012**, *9*, 81–100.

261. Frank, B. Revisiting Paper Strength Measurements for Estimating Combined Board Strength. *Tappi J* **2007**, *6*, 10–17.

262. Malhotra, G. The Science Behind Bursting Strength Testing: A Comprehensive Guide Available online: https://medium.com/@testinginstrumentss/the-science-behind-bursting-strength-testing-a-comprehensive-guide-8b27e4a15751 (accessed on 18 August 2023).

263. Silverstein.R M; Webster, F.X. Infrared Spectrometry. In *Spectrometric Identification of Organic Compounds*; John Wiley & Sons, Inc: Hoboken, NJ, U.S.A., 1998.

264. Shirai, H.; Duchesne, C.; Furutani, Y.; Fuji, T. Attenuated Total Reflectance Spectroscopy with Chirped-Pulse Upconversion. *Opt Express* **2014**, *22*, 29611, doi:10.1364/oe.22.029611.

265. Chen, F.; Yang, X.; Wu, Q. Antifungal Capability of TiO2 Coated Film on Moist Wood. *Build Environ* **2009**, *44*, 1088–1093, doi:10.1016/j.buildenv.2008.07.018.

266. Bono, N.; Ponti, F.; Punta, C.; Candiani, G. Effect of UV Irradiation and TiO2-Photocatalysis on Airborne Bacteria and Viruses: An Overview. *Materials* 2021, *14*, 1–20.

267. Chandra, M.; Kalra, A.; Sharma, P.K.; Kumar, H.; Sangwan, R.S. Optimization of Cellulases Production by Trichoderma Citrinoviride on Marc of Artemisia Annua and Its Application for Bioconversion Process. *Biomass Bioenergy* **2010**, *34*, 805–811, doi:10.1016/j.biombioe.2010.01.024.

268. Bergamonti, L.; Potenza, M.; Haghighi Poshtiri, A.; Lorenzi, A.; Sanangelantoni, A.M.; Lazzarini, L.; Lottici, P.P.; Graiff, C. Ag-Functionalized Nanocrystalline Cellulose for Paper Preservation and Strengthening. *Carbohydr Polym* **2020**, *231*, 1–8, doi:10.1016/j.carbpol.2019.115773.

269. Baglioni, P.; Giorgi, R. Inorganic Nanomaterials for the Consolidation of Wall Paintings and Stones. In *Nanoscience for the Conservation of Works of Art*; Baglioni, P., Chelazzi, D., Eds.; RSC Publishing: Cambridge, U.K., 2013; pp. 345–371.

270. Daniels, V. The Reversibility of Starch Paste. In Proceedings of the Lining and backing: the support of paintings, paper and textiles : papers delivered at the UKIC Conference, 7-8 November 1995; Phenix, A., Ed.; United Kingdom Institute for Conservation of Historic and Artistic Works: London, U.K., 1995; pp. 72–76.

271. Ahmed, H.E.; Kolisis, F.N. An Investigation into the Removal of Starch Paste Adhesives from Historical Textiles by Using the Enzyme α-Amylase. *J Cult Herit* **2011**, *12*, 169–179, doi:10.1016/j.culher.2010.08.001.

272. Mazzuca, C.; Micheli, L.; Cervelli, E.; Basoli, F.; Cencetti, C.; Coviello, T.; Iannuccelli, S.; Sotgiu, S.; Palleschi, A. Cleaning of Paper Artworks: Development of an Efficient Gel-Based Material Able to Remove Starch Paste. *ACS Appl Mater Interfaces* **2014**, *6*, 16519–16528.

273. Aleksić, G.; Cigula, T.; Vukoje, M.; Itrić Ivanda, K. Influence of Wet Film Thickness on the Functional Applications of Biopolymers in Paper Conservation. *Colloids and Interfaces* **2023**, *7*, 43, doi:10.3390/colloids7020043.

274. Aleksić, G.; Cigula, T.; Pal, M.; Vukoje, M. The Influence of Nano-TiO2 Modified Bilayer Coatings on the Mechanical Properties of Paper. In Proceedings of the Book of Abstract Blaž Baromić 27th International Conference on Printing, Design and Graphic Communication 2023 (PDC 23); University of Zagreb Faculty of Graphic Arts: Zagreb, Croatia, 2023; pp. 183–189.

275. Bicchieri, M.; Biocca, P.; Colaizzi, P.; Pinzari, F. Microscopic Observations of Paper and Parchment: The Archaeology of Small Objects. *Herit Sci* **2019**, *7*, doi:10.1186/s40494-019-0291-9.

276. Bajpai, P. Paper and Its Properties. *Biermann's Handbook of Pulp and Paper* **2018**, 35–63, doi:10.1016/B978-0-12-814238-7.00002-7.

277. Fauteux, F.; Rémus-Borel, W.; Menzies, J.G.; Bélanger, R.R. Silicon and Plant Disease Resistance against Pathogenic Fungi. *FEMS Microbiol Lett* 2005, *249*, 1–6.

278. Hynninen, V.; Patrakka, J.; Nonappa Methylcellulose–Cellulose Nanocrystal Composites for Optomechanically Tunable Hydrogels and Fibers. *Materials* **2021**, *14*, doi:10.3390/ma14185137.

279. Campbell, W.B. The Mechanism of Bonding. *Tappi* **1959**, *42*, 507–509, doi:10.32964/tj42.12.999.

280. Żołek-Tryznowska, Z.; Kałuża, A. The Influence of Starch Origin on the Properties of Starch Films: Packaging Performance. *Materials* **2021**, *14*, 1–11, doi:10.3390/ma14051146.

281. Lama, E.; Veneranda, M.; Prieto-Taboada, N.; Hernando, F.L.; Rodríguez Laso, M.D.; Madariaga, J.M. A First Evaluation of the Usefulness of Kudzu Starch in Cultural Heritage Restoration. *Sci Rep* **2020**, *10*, 15598, doi:10.1038/s41598-020-72643-x.

282. Mohammed, A.A.B.A.; Hasan, Z.; Omran, A.A.B.; Elfaghi, A.M.; Khattak, M.A.; Ilyas, R.A.; Sapuan, S.M. Effect of Various Plasticizers in Different Concentrations on Physical, Thermal, Mechanical, and Structural Properties of Wheat Starch-Based Films. *Polymers (Basel)* **2023**, *15*, doi:10.3390/polym15010063.

283. Montinaro, N.; Fustaino, M.; Bellisario, D.; Quadrini, F.; Santo, L.; Pantano, A. Testing the Dispersion of Nanoparticles in a Nanocomposite with an Ultra-Low Fill Content Using a Novel Non-Destructive Evaluation Technique. *Materials* **2022**, *15*, doi:10.3390/ma15031208.

284. Li, W.; Zheng, K.; Chen, H.; Feng, S.; Wang, W.; Qin, C. Influence of Nano Titanium Dioxide and Clove Oil on Chitosan-Starch Film Characteristics. *Polymers (Basel)* **2019**, *11*, doi:10.3390/polym11091418.

285. Alcantara-Garcia, J.; Ploeger, R. Teaching Polymer Chemistry through Cultural Heritage. *J Chem Educ* **2018**, *95*, 1118–1124, doi:10.1021/acs.jchemed.7b00975.

286. Balliana, E.; Ricci, G.; Pesce, C.; Zendri, E. Assessing the Value of Green Conservation for Cultural Heritage: Positive and Critical Aspects of Already Available Methodologies. *International journal of conservation science* **2016**, *7*, 185–202.

287. Irie, H.; Tsuji, K.; Hashimoto, K. Hydrophobic Anatase TiO2-Based Thin Films Modified with Al, Cr Derivatives to Reach Reversible Wettability Control. *Physical Chemistry Chemical Physics* **2008**, *10*, 3072–3076.

288. Hegyi, A.; Grebenişan, E.; Lăzărescu, A.V.; Stoian, V.; Szilagyi, H. Influence of TiO2 Nanoparticles on the Resistance of Cementitious Composite Materials to the Action of Fungal Species. *Materials* **2021**, *14*, doi:10.3390/ma14164442.

289. Ehlert, M.; Radtke, A.; Topolski, A.; Śmigiel, J.; Piszczek, P. The Photocatalytic Activity of Titania Coatings Produced by Electrochemical and Chemical Oxidation of Ti6Al4V Substrate, Estimated According to ISO 10678:2010. *Materials* **2020**, *13*, doi:10.3390/ma13112649.

290. Irfan, F.; Tanveer, M.U.; Moiz, M.A.; Husain, S.W.; Ramzan, M. TiO2 as an Effective Photocatalyst Mechanisms, Applications, and Dopants: A Review. *European Physical Journal B* **2022**, *95*, doi:10.1140/epjb/s10051-022-00440-8.

291. Plazonić, I.; Bates, I.; Vukoje, M. Changes in Straw-Containing Laboratory Papers Caused by Accelerated Ageing. *Heritage* **2022**, *5*, 1836–1851, doi:10.3390/heritage5030095.

292. Pauler, N. *Paper Optics Optical and Colour Science Related to the Pulp and Paper Industry*; AB Lorentzen & Wettre: Stockholm, Sweden, 2012;

293. Papermaking. In *Encyclopedia of Forest Sciences*; Burley, J., Evans, J., Youngquist, J.A., Eds.; Academic Press: Oxford, U.K., 2004.

294. Diebold, M.P. Effect of TiO2 Pigment on Gloss Retention: A Two-Component Approach. *JCT CoatingsTech* **2009**, 32–39.

295. Reinosa, J.J.; Leret, P.; Álvarez-Docio, C.M.; Del Campo, A.; Fernández, J.F. Enhancement of UV Absorption Behavior in ZnO-TiO2 Composites. *Boletin de la Sociedad Espanola de Ceramica y Vidrio* **2016**, *55*, 55–62, doi:10.1016/j.bsecv.2016.01.004.

296. Vukoje, M.; Kulčar, R.; Ivanda, K.I.; Bota, J.; Cigula, T. Improvement in Thermochromic Offset Print UV Stability by Applying PCL Nanocomposite Coatings. *Polymers (Basel)* **2022**, *14*, doi:10.3390/polym14071484.

297. Jawad, M.K.; Abid, N.K. Study the Effect of TiO2 Nanoparticles on Physical Properties of Biopolymer Blend. In Proceedings of the IOP Conference Series: Materials Science and Engineering 757; Institute of Physics Publishing, April 1 2020; Vol. 757, p. 012073.

298. Lynn, R.P. Improvement of Heat Stability of Paper Made from Sulfite and Kraft Pulps. Paper Engineering Senior Theses, no. 360., Western Michigan University: Kalamazoo, U.S.A., 1966.

299. Brandberg, A.; Kulachenko, A. Compression Failure in Dense Non-Woven Fiber Networks. *Cellulose* **2020**, *27*, 6065–6082, doi:10.1007/s10570-020-03153-2.

300. Geminiani, L.; Campione, F.P.; Corti, C.; Luraschi, M.; Motella, S.; Recchia, S.; Rampazzi, L. Differentiating between Natural and Modified Cellulosic Fibres Using ATR-FTIR Spectroscopy. *Heritage* **2022**, *5*, 4114–4139, doi:10.3390/heritage5040213.

301. Tkalčec, M.M.; Bistričić, L.; Leskovac, M. Influence of Adhesive Layer on the Stability of Kozo Paper. *Cellulose* **2015**, *23*, 853–872, doi:10.1007/s10570-015-0816-7.

302. Stuart, B.H. *Infrared Spectroscopy: Fundamentals and Applications*; 1st ed.; John Wiley and Sons, Ltd.: Chichester, U.K., 2004;

303. El-Sakhawy, M.; Mohamed, S.; Salama, A.; Sarhan, H.-A. Preparation and Infrared Study of Cellulose Based Amphiphilic Materials. *Cellulose Chemistry and Technology* **2018**, *52*, 193–200.

304. Ciolacu, D.; Ciolacu, F.; Popa, V.I. Amorphous Cellulose - Structure and Characterization. *Cellulose Chem. Technol.* **2011**, *45*, 13–21.

305. Gao, L.; Zhu, T.; He, F.; Ou, Z.; Xu, J.; Ren, L. Preparation and Characterization of Functional Films Based on Chitosan and Corn Starch Incorporated Tea Polyphenols. *Coatings* **2021**, *11*, doi:10.3390/coatings11070817.

306. Łojewska, J.; Lubańska, A.; Miśkowiec, P.; Łojewski, T.; Proniewicz, L.M. FTIR in Situ Transmission Studies on the Kinetics of Paper Degradation via Hydrolytic and Oxidative Reaction Paths. *Appl Phys A Mater Sci Process* **2006**, *83*, 597–603, doi:10.1007/s00339-006-3529-9.

307. Ivanova-Petropulos, V.; Mitrev, S.; Stafilov, T.; Markova, N.; Leitner, E.; Lankmayr, E.; Siegmund, B. Characterisation of Traditional Macedonian Edible Oils by Their Fatty Acid Composition and Their Volatile Compounds. *Food Research International* **2015**, *77*, 506–514, doi:10.1016/j.foodres.2015.08.014.

308. Kulčar, R.; Vukoje, M.; Itrić Ivanda, K.; Cigula, T.; Jamnicki Hanzer, S. Understanding the Role of Paper-Ink Interactions on the Lightfastness of Thermochromic Prints. *Materials* **2023**, *16*, doi:10.3390/ma16083225.

309. Niaounakis, M. *Biopolymers: Applications and Trends*; 1st ed.; Elsevier Inc.: Amsterdam, Netherlands, 2015;

310. Ferreira, P.J.; Gamelas, J.A.; Moutinho, I.M.; Ferreira, A.G.; Gómez, N.; Molleda, C.; Figueiredo, M.M. Application of FT-IR-ATR Spectroscopy to Evaluate the Penetration of Surface Sizing Agents into the Paper Structure. *Ind Eng Chem Res* **2009**, *48*, 3867–3872, doi:10.1021/ie801765c.

311. Al Hallak, M.; Verdier, T.; Bertron, A.; Castelló Lux, K.; El Atti, O.; Fajerwerg, K.; Fau, P.; Hot, J.; Roques, C.; Bailly, J.D. Comparison of Photocatalytic Biocidal Activity of TiO2, ZnO and Au/ZnO on Escherichia Coli and on Aspergillus Niger under Light Intensity Close to Real-Life Conditions. *Catalysts* **2023**, *13*, doi:10.3390/catal13071139.

312. Yu, K.P.; Huang, Y.T.; Yang, S.C. The Antifungal Efficacy of Nano-Metals Supported TiO2 and Ozone on the Resistant Aspergillus Niger Spore. *J Hazard Mater* **2013**, *261*, 155–162, doi:10.1016/j.jhazmat.2013.07.029.

313. Gambino, M.; Ahmed, M.A.A.A.; Villa, F.; Cappitelli, F. Zinc Oxide Nanoparticles Hinder Fungal Biofilm Development in an Ancient Egyptian Tomb. *Int Biodeterior Biodegradation* **2017**, *122*, 92–99, doi:10.1016/j.ibiod.2017.05.011.

314. Udina, R. Reversibility and the Right Conservation Treatment. In Proceedings of the INTACH Conservation Insights 2020: Lectures on Paper Conservation; Indian National Trust for Art and Cultural Heritage (INTACH): New Delhi, India, 2020; pp. 201–210.

315. Polymer Science Learning Center The Tau of Tacticity Available online: https://pslc.ws/macrog/tact.htm (accessed on 29 January 2024).

316. Guillitte Bioreceptivity: A New Concept for Building Ecology Studies. *Sci Total Environ* **1995**, *167*, 215–220.

317. Koretsky, Z. Phasing out an Embedded Technology: Insights from Banning the Incandescent Light Bulb in Europe. *Energy Res Soc Sci* **2021**, *82*, doi:10.1016/j.erss.2021.102310.

318. Goldman, D. What You Need to Know about the Incandescent Light Bulb Ban Available online: https://edition.cnn.com/2023/08/01/business/incandescent-light-bulb-ban/index.html (accessed on 26 January 2024).

319. Nichols, G.; Byard, S.; Bloxham, M.J.; Botterill, J.; Dawson, N.J.; Dennis, A.; Diart, V.; North, N.C.; Sherwood, J.D. A Review of the Terms Agglomerate and Aggregate with a Recommendation for Nomenclature Used in Powder and Particle Characterization. *J Pharm Sci* **2002**, *91*, 2103–2109, doi:10.1002/jps.10191.

320. HAK, C.R.C.; FATANAH, D.N.E.; ABDULLAH, Y.; SULAIMAN, M.Y.M. The Effect of Surfactants on the Stability of TiO2 Aqueous Suspension. *International Journal of Current Research in Science, Engineering & Technology* **2018**, *1*, 172, doi:10.30967/ijcrset.1.s1.2018.172-178.

321. X-Rite What Is Meant by the Term “Observer Angle”? Available online: https://www.xrite.com/service-support/what_is_meant_by_the_term_observer_angle (accessed on 1 April 2024).

322. Cheydleur, R.; O’Connor, K. *A New Series of Measurement Conditions Defined*; X-Rite : Grand Rapids, Michigan, U.S.A., 2011;

7. LIST OF ABBREVIATIONS

B.C. - Before Christ

A.D. - Anno Domini

TiO_2 - Titanium dioxide

NPs - Nanoparticles

w/w – Weight concentration

$CaCO_3$ - Calcium carbonate

θ - Contact angle

SD - Standard deviation

ROS - Reactive oxygen species

*CIE L*a*b** - International Commission on Illumination colour space model (*L*a*b*)* theory

ΔE_{ab} - Total colour difference

SEM - Scanning electron microscopy

EDS - Energy dispersive X-ray spectroscopy

FT-IR - Fourier-transform infrared spectroscopy

MEA - Malt extract agar

ATR - Attenuated total reflection

ISO - International Organization for Standardization

RH - Relative humidity

GU - gloss units

EM - Electromagnetic spectrum

UV - Ultraviolet region

UV-Vis - Ultraviolet-visible region

IR - Infrared region

TS - Taber stiffness

TSU – Taber stiffness unit

SCT - Short-span compression

UNESCO - The United Nations Educational, Scientific and Cultural Organization

ICOM-CC - International Council of Museums Committee for Conservation

GLAM - galleries, libraries, archives, and museums

*Phase I, Phase I** - Evaluation of the monolayer coatings on the model paper's surface

Phase II - Evaluation of the bilayer coatings on the printed model paper's surface

*Phase III, Phase III** - Evaluation of the bilayer coatings on the model paper's surface

RP, *U* and *P* - Uncoated model paper in ***Phase I, Phase II*** and ***Phase III***

F - Fiter paper

MC12 - Model paper coated with methylcellulose using the wet film deposit of 12µm

MC24 - Model paper coated with methylcellulose using the wet film deposit of 24 µm

MC50 - Model paper coated with methylcellulose using the wet film deposit of 50 µm

MC100 - Model paper coated with methylcellulose using the wet film deposit of 100 µm

WSP12 - Model paper coated with starch using the wet film deposit of 12µm

WSP24 - Model paper coated with starch using the wet film deposit of 24 µm

WSP50 - Model paper coated with starch using the wet film deposit of 50 µm

WSP100 - Model paper coated with starch using the wet film deposit of 100 µm

S+MC - Model paper coated with starch and methylcellulose

S+MC+0.2TiO₂ - Model paper coated with S+MC incorporating 0.2% TiO_2 *w/w*

S+MC+0.5TiO₂ and *T0.50* - Model paper coated with S+MC incorporating 0.5% TiO_2 *w/w*

T.0.75 - Model paper coated with S+MC incorporating 0.75% TiO_2 *w/w*

S+MC+1.0TiO₂ and *T1.00* - Model paper coated with S+MC incorporating 1.0% TiO_2 *w/w*

S+MC+2.0TiO₂ - Model paper coated with S+MC incorporating 2.0% TiO_2 *w/w*

BIOGRAPHY

Gabriela Aleksić was born on February 2nd, 1981, in Zagreb. She earned a degree in graphic technology from the University of Zagreb Faculty of Graphic Arts in 2011. In 2013, she completed Additional Pedagogical-Psychological Education for Teachers, a university programme at the University of Rijeka, Faculty of Humanities and Social Sciences. From 2006 to 2010, she served as a gallery assistant (exhibition staff) at the Klovićevi Dvori Gallery in Zagreb, where she gained initial exposure to preventive conservation methods aimed at preserving cultural heritage artifacts from environmental factors of deterioration. She also worked as a freelancer on the digitalization of old cadastral maps (2009–2012), as an early-career high school teacher of bookbinding operations at school for children with intellectual and developmental difficulties (2013–2014), and as an ink and proof press specialist (2014–2015), prior to working in book and paper conservation at the National and University Library in Zagreb (2015–present day). During her time at the library, she engaged in both preventive and remedial conservation, organized national and international events (e.g., the international conference Solidarity in Culture: Heritage Protection Under Conditions of Crisis. 2021), authored an exhibition involving new media in 2022 (Our Past Bound in Books, 2022), led the Book Preservation and Binding Division, delivered lectures on paper preservation, conducted student practical workshops, and presented her work at national and international conferences. Gabriela actively participated in numerous educational activities in Croatia and abroad. In the summer of 2023, she was selected as one of the participants of the HS Academy - 2nd IPERION HS Doctoral School, held in Ljubljana, Slovenia. Her publications can be found under the ID 42995 in the CroRIS database.

LIST OF PUBLISHED SCIENTIFIC RESEARCH

I. **Aleksić, Gabriela**; Cigula, Tomislav; Pasanec Preprotić, Suzana: An analysis of targeted properties of materials used for preservation and storage of heritage collections // JGED. Journal of graphic engineering and design, 13 (2022), 1; 5-12. doi: 10.24867/JGED-2022-1-005 (international peer review, article, scholarly)

II. **Aleksić, Gabriela**; Cigula, Tomislav; Itrić Ivanda, Katarina: Influence of multilayered films containing cellulose nanocrystals on the properties of Japanese paper // Proceedings - The Eleventh International Symposium GRID 2022 / Vladić, Gojko

(ed.). Novi Sad: University of Novi Sad, Faculty of Technical Sciences, Department of Graphic Engineering and Design, 2022. str. 459-466 doi: 10.24867/GRID-2022-p50 (lecture, international peer review, full paper, scholarly)

III. Hudika, Tomislav; Cigula, Tomislav; Golub, Filip; **Aleksić, Gabriela**: Lightfastness of lithographic primary colours coated with nanocomposites composed of TiO_2 and water-based varnish // GRID 2022 / Vladić, Gojko (ed.). Novi Sad: University of Novi Sad, Faculty of technical sciences, Dept. of GRID, 2022. str. 145-152 doi: 10.24867/GRID-2022-p15 (lecture, international peer review, full paper, scholarly)

IV. Hudika, Tomislav; Rožić, Mirela; Cigula, Tomislav; **Aleksić, Gabriela**: Influence of light induced accelerated ageing on surface properties of cardboard packaging coated by TiO_2 nanocomposites // GRID 2022 / Vladić, Gojko (ed.). Novi Sad: University of Novi Sad, Faculty of technical sciences, Dept. of GRID, 2022. str. 153-161 doi: 10.24867/GRID-2022-p16 (lecture, international peer review, full paper, scholarly)

V. **Aleksić, Gabriela**; Cigula, Tomislav; Vukoje, Marina; Itrić Ivanda, Katarina *Influence of Wet Film Thickness on the Functional Applications of Biopolymers in Paper Conservation* // Colloids and interfaces, 7 (2023), 2; 43, 16. doi: 10.3390/colloids7020043 (international peer review, article, scholarly)

VI. **Aleksić, Gabriela**; Cigula, Tomislav; Vukoje, Marina; Itrić Ivanda, Katarina *Bilayer Coating Composed of Starch and Methyl Cellulose-Nanoscale TiO_2 for the Protection of Historic Paper from UV* // Coatings, 13 (2023), 899, 14. doi: 10.3390/coatings13050899 (international peer review, article, scholarly)

VII. **Aleksić, Gabriela**; Cigula, Tomislav; Pal, Magdolna; Vukoje, Marina *The influence of nano-TiO_2 modified bilayer coatings on the mechanical properties of paper* // 27th International Conference on Printing, Design and Graphic Communications - Proceedings, Zagreb: University of Zagreb Faculty of Graphic Arts, 2023 pp. 183-189 (lecture, international peer review, full paper, scholarly)

VIII. Cigula, Tomislav; Vukoje, Marina; Malenica, Ivan; Kulčar, Rahela; Itrić Ivanda, Katarina; **Aleksić, Gabriela**: Effect of ascorbic acid – methylcellulose coating on the protection of offset prints // 4th International Printing Technologies Symposium Printistanbul2023 Proceedings Book. Istanbul: Printing Industry Education Foundation (BASEV), 2023. pp. 85-91 (lecture, international peer review, full paper, scholarly)